C5.6 Applied Complex Variables

These notes were written by a number of authors, including **Jon Chapman**, **Heike Gramberg**, **Peter Howell**, **Sam Howison**, **Jim Oliver** and **Ian Hewitt**.

Please email comments and corrections to the course lecturer **Ian Hewitt** <hewitt@maths.ox.ac.uk>.

0.1 Recommended Prerequisites

The course requires Part A core complex analysis, and is devoted to extensions and applications of that material. A knowledge of the basic properties of the Fourier transform, as found for example in Part A *Integral Transforms*, will be assumed. Part A *Fluid Dynamics and Waves* is helpful but not absolutely essential: the necessary results from inviscid two-dimensional hydrodynamics will be quoted as required, and for further details the reader is referred to the Part A lecture notes. Part C *Perturbation Methods* is also helpful in the analysis of certain contour integrals.

0.2 Synopsis

Review of core complex analysis, analytic continuation, multifunctions, contour integration, conformal mapping and Fourier transforms. [3 lectures]

Riemann mapping theorem (in statement only). Schwarz–Christoffel formula. Solution of Laplace's equation by conformal mapping onto a canonical domain; applications including inviscid hydrodynamics. [2 lectures]. Free streamline flows in the hodograph plane. Unsteady flow with free boundaries in porous media. [3 lectures].

Applications of Cauchy integrals and Plemelj formulae. Solution of mixed boundary value problems motivated by thin aerofoil theory and the theory of cracks in elastic solids. Riemann-Hilbert problems. Cauchy singular integral equations. [3 lectures]. Complex Fourier transform. Contour integral solutions of ODEs. [2 lectures]. Wiener-Hopf method. [3 lectures].

0.3 Reading list

[1] G. F. Carrier, M. Krook and C. E. Pearson, *Functions of a Complex Variable* (Society for Industrial and Applied Mathematics, 2005.) ISBN 0898715954.

[2] M. J. Ablowitz and A. S. Fokas, *Complex Variables: Introduction and Applications* (2nd edition, Cambridge University Press, 2003). ISBN 0521534291.

[3] J. R. Ockendon, S. D. Howison, A. A. Lacey and A. B. Movichan, *Applied Partial Differential Equations: Revised Edition* (Oxford University Press, 2003). ISBN 0198527713.

1 Review of core complex analysis

1.1 Introduction

Here we summarise the important results and techniques of core complex analysis that are assumed for the remainder of this course. This is by no means a complete account of complex analysis. Many important details and most of the proofs will be omitted, but may be found in basic textbooks (e.g. Priestley). First we introduce some basic notation that will be used throughout this course.

Complex conjugation is denoted by an overbar: if x, $y \in \mathbb{R}$ and $z = x + \mathrm{i}y$, then $\overline{z} = x - \mathrm{i}y$. Conjugation commutes with all of the basic complex functions, that is, $\overline{z^k} \equiv \overline{z}^k$, $\overline{\mathrm{e}^z} \equiv \mathrm{e}^{\overline{z}}$, $\overline{\sin z} \equiv \sin \overline{z}$, etc.

A **region** in the complex plane, usually denoted D, is an open, path-connected subset of $\mathbb{C}$, simply-connected unless stated otherwise. Its boundary is denoted ∂D.

A **contour** Γ is a simple, piecewise continuously differentiable path in $\mathbb{C}$ with the positive (anti-clockwise) orientation (a *Jordan contour*), closed unless stated otherwise.

A **disc** in the complex plane is denoted by $D(a; R) = \{z \in \mathbb{C} : |z - a| < R\}$, i.e. the open disc centre a and radius R.

1.2 Holomorphic functions

A function $f(z)$ of the complex variable z is said to be *differentiable* at the point z if $\lim_{h\to 0}\big(f(z + h) - f(z)\big)/h$ exists, independent of how $h \to 0$. When this is true, we define the derivative

$$f'(z) = \lim_{h\to 0} \frac{f(z + h) - f(z)}{h}. \tag{1.1}$$

If $f(z)$ is differentiable at each point in a region D, then f is said to be *holomorphic* in D.

Suppose we decompose a holomorphic function into its real and imaginary parts by writing

$$f(z) = u(x, y) + \mathrm{i}v(x, y), \tag{1.2}$$

where $z = x + \mathrm{i}y$. Then, by taking h first real then imaginary in (1.1) and setting the two resulting values of $f'(z)$ equal, we find that u and v must satisfy the **Cauchy–Riemann equations**

$$\frac{\partial u}{\partial x} = \frac{\partial v}{\partial y}, \qquad \frac{\partial u}{\partial y} = -\frac{\partial v}{\partial x}. \tag{1.3}$$

The real and imaginary parts of any holomorphic function must satisfy (1.3). The reverse is not exactly true. If u and v are differentiable as functions of (x, y) *and* satisfy the Cauchy–Riemann equations (1.3), then $f = u(x, y) + \mathrm{i}v(x, y)$ is a holomorphic function of $z = x + \mathrm{i}y$.

By cross-differentiating the Cauchy–Riemann equations (1.3), we quickly find that both u and v satisfy Laplace's equation, i.e.

$$\nabla^2 u = \frac{\partial^2 u}{\partial x^2} + \frac{\partial^2 u}{\partial y^2} = 0, \qquad \nabla^2 v = 0. \tag{1.4}$$

The reverse is also true: if a function $u(x, y)$ satisfies Laplace's equation, then it is the real part of some function $f(z)$ that is holomorphic (at least locally). Therefore solving Laplace's equation in two dimensions is equivalent to finding a suitable holomorphic function of z. Many of the applications covered in this course spring from this basic fact.

If one were to think of a general (not necessarily holomorphic) complex-valued function $G(x, y)$, it could equivalently be viewed as a function $g(z, \overline{z})$ using the one-to-one correspondence between $(z, \overline{z})$ and (x, y). The chain rules relating partial derivatives with respect to the two sets of coordinates are given by

$$\frac{\partial}{\partial x} = \frac{\partial}{\partial z} + \frac{\partial}{\partial \overline{z}}, \qquad \frac{\partial}{\partial y} = \mathrm{i}\frac{\partial}{\partial z} - \mathrm{i}\frac{\partial}{\partial \overline{z}}, \tag{1.5}$$

which can easily be inverted to

$$\frac{\partial}{\partial z} = \frac{1}{2}\left(\frac{\partial}{\partial x} - \mathrm{i}\frac{\partial}{\partial y}\right), \qquad \frac{\partial}{\partial \overline{z}} = \frac{1}{2}\left(\frac{\partial}{\partial x} + \mathrm{i}\frac{\partial}{\partial y}\right). \tag{1.6}$$

From these and the Cauchy–Riemann equations (1.3), it follows (Exercise 1 of sheet 1) that if g is holomorphic, then

$$\frac{\partial g}{\partial \overline{z}} = 0. \tag{1.7}$$

This result may be interpreted as saying that a holomorphic function is one that is independent of $\overline{z}$.

Given a holomorphic function $f(z)$, we define a new function $\bar{f}(z)$ as follows:

$$\overline{f}(z) := \overline{f(\overline{z})} \tag{1.8}$$

(note the double conjugation). The Cauchy–Riemann equations can be used to show that, if $f(z)$ is holomorphic, then so is $\overline{f}(z)$. The mapping from $f(z)$ to $\overline{f}(z)$ is called *Schwarz reflection*. It is easily seen that a repetition of Schwarz reflection returns the original function f, i.e. $\overline{\overline{f}}(z) \equiv f(z)$.

1.3 Path integrals and Cauchy's Theorem

The integral of a complex valued function of z along a curve Γ (which may be open or closed) in $\mathbb{C}$, is defined as usual: if Γ is parameterised using a real-valued parameter t, i.e. $\Gamma = \{z(t) : t \in (t_0, t_1)\}$, then

$$\int_\Gamma g(z, \overline{z})\,\mathrm{d}z := \int_{t_0}^{t_1} g\big(z(t), \overline{z(t)}\big)\, z'(t)\,\mathrm{d}t. \tag{1.9}$$

Such an integral can easily be bounded using

$$\left|\int_\Gamma f(z)\,\mathrm{d}z\right| \leq \text{length}(\Gamma) \times \sup_{z\in\Gamma} |f(z)|\,. \tag{1.10}$$

Cauchy's Theorem: *If a function $f(z)$ is holomorphic within a simple closed contour Γ, and continuous on Γ, then*

$$\int_\Gamma f(z)\,\mathrm{d}z = 0. \tag{1.11}$$

At first glance, Cauchy's theorem might not appear very mysterious. If we write $f = u + \mathrm{i}v$ and then use Green's Theorem, then Cauchy's Theorem follows directly from the Cauchy–Riemann equations (1.3). However, this "proof" assumes that u and v have continuous partial derivatives on and inside Γ. A much more technical proof, due to Goursat, assumes only that $f'(z)$ exists everywhere inside Γ. This is significant because, as we shall see, one can then *prove* that $f'(z)$ is continuous, rather than assuming so.

It is an immediate consequence of Cauchy's theorem that if Γ_1 and Γ_2 are two curves joining the point z_0 to another point z_1, as illustrated in Figure 1.1, and if $f(z)$ is holomorphic in a region containing Γ_1, Γ_2 and the region between them, then

$$\int_{\Gamma_1} f(z)\,\mathrm{d}z = \int_{\Gamma_2} f(z)\,\mathrm{d}z, \tag{1.12}$$

so that the integral is path-independent. This is often stated as the **deformation theorem**: if one contour Γ_1 can be deformed smoothly into another one Γ_2 while crossing only points at which $f(z)$ is holomorphic, then the integral of $f(z)$ along Γ_1 is equal to the integral along Γ_2. It also allows us to define an anti-derivative of $f(z)$ by the prescription

$$F(z) = \int_{z_0}^{z} f(t)\,\mathrm{d}t, \tag{1.13}$$

provided that we do so in a simply connected region within which $f(z)$ is holomorphic, as the contour of integration is immaterial.

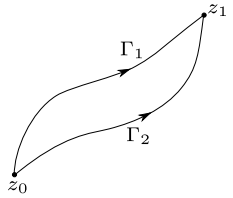

Figure 1.1: Two paths from z_0 to z_1.

A partial inverse of Cauchy's Theorem is:

Morera's Theorem. *If $f(z)$ is continuous in D and $\oint_\Gamma f(z)\mathrm{d}z = 0$ for all simple closed Γ in D, then $f(z)$ is holomorphic in D.*

1.4 Cauchy's integral formula

Take a simple closed contour Γ, and let $f(z)$ be holomorphic on Γ and inside it. Then values of $f(z)$ on Γ determine its values at all points within Γ as well, via **Cauchy's integral formula**: for all z within Γ,

$$f(z) = \frac{1}{2\pi\mathrm{i}} \oint_\Gamma \frac{f(\zeta)}{\zeta - z}\,\mathrm{d}\zeta. \tag{1.14}$$

The proof is simple, by deforming the contour to a small circle surrounding z, as shown in Figure 1.2, and adding and subtracting $f(z)$:

$$\oint_\Gamma \frac{f(\zeta)}{\zeta - z}\,\mathrm{d}\zeta = \oint_{|\zeta - z| = \epsilon} \frac{f(\zeta)}{\zeta - z}\,\mathrm{d}\zeta = \oint_{|\zeta - z| = \epsilon} \frac{f(z)}{\zeta - z}\,\mathrm{d}\zeta + \oint_{|\zeta - z| = \epsilon} \frac{f(\zeta) - f(z)}{\zeta - z}\,\mathrm{d}\zeta; \qquad (1.15)$$

the first integral on the right is equal to $2\pi\mathrm{i}f(z)$ and the second vanishes as $\epsilon \to 0$ by continuity of f.

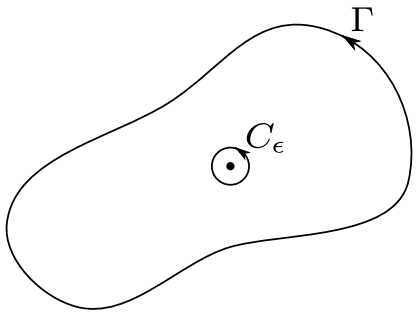

Figure 1.2: Deformation of Γ to $C_\epsilon = \{z : |\zeta - z| = \epsilon\}$.

With $f(z)$ given by Cauchy's integral formula (1.14), it is tempting to differentiate with respect to z under the integral sign to find

$$f'(z) = \frac{1}{2\pi\mathrm{i}} \oint_\Gamma \frac{f(\zeta)}{(\zeta - z)^2}\,\mathrm{d}\zeta, \qquad (1.16)$$

and indeed the formal justification of this step is not difficult. Thus the value of $f'(z)$ at any point inside Γ may be expressed solely in terms of the values taken by $f(z)$ on Γ. But then, we can differentiate again (with essentially the same justification), to find an analogous formula for $f''(z)$, namely

$$f''(z) = \frac{1}{\pi\mathrm{i}} \oint_\Gamma \frac{f(\zeta)}{(\zeta - z)^3}\,\mathrm{d}\zeta. \qquad (1.17)$$

Recall we have assumed only that $f(z)$ is holomorphic. Therefore we have established that, given only that $f'(z)$ exists (not even that it is continuous), it follows that $f''(z)$ also exists. By iterating on this process, we obtain **Cauchy's formula for derivatives:**

$$f^{(n)}(z) = \frac{n!}{2\pi\mathrm{i}} \oint_\Gamma \frac{f(\zeta)}{(\zeta - z)^{n+1}}\,\mathrm{d}\zeta. \qquad (1.18)$$

Hence, a holomorphic function is infinitely differentiable, in marked contrast with real-valued functions.

A function is called *entire* if it is holomorphic in the whole complex plane (e.g. z, e^z). Such a function must have a singularity at infinity, because of:

Liouville's Theorem: *Any bounded entire function $f(z)$ is constant.*

That is, if $|f(z)| < M$ for some M and for all z, then f is a constant. Liouville's Theorem may be proved by looking at Cauchy's integral formula (1.16) for $f'(z)$ and taking Γ to be a large circle; letting the radius of the circle tend to infinity, we deduce that $f'(z) = 0$.

There are various generalisations of Liouville's Theorem which apply when the modulus of an entire function is bounded in some specified way (not just by a constant) as $z \to \infty$. The simplest generalisation is

Corollary: *If $f(z)$ is entire and $f(z) = O(z^n)$ as $z \to \infty$ for $n \in \mathbb{N}$, then $f(z)$ is a polynomial of degree n.*

This result is easily proved by applying Liouville's Theorem to $f^{(n)}(z)$.

1.5 Taylor's Theorem and analytic continuation

Knowing that a holomorphic function has derivatives of all orders, we expect it to have power series representation.

Taylor's theorem. *If $f(z)$ is holomorphic in a disc $D(a;R)$, then there is a series representation*

$$f(z) = \sum_{n=0}^{\infty} c_n (z-a)^n, \qquad \text{where} \quad c_n = \frac{f^{(n)}(a)}{n!}, \tag{1.19}$$

and the series converges to $f(z)$ for all $0 \le |z-a| < R$.

The proof of Taylor's Theorem involves expanding the integrand in Cauchy's integral formula (1.14) using the Binomial Theorem and then integrating term by term (which is justified by uniform convergence).

Taylor's Theorem tells us that a holomorphic function is *analytic*: it can be represented by a convergent Taylor series. The *radius of convergence* of the series (1.19) is the largest possible value of R such that the series converges, i.e. the largest value of R such that $f(z)$ is holomorphic in $D(a;R)$. In other words, the radius of convergence is the distance from $z=a$ to the nearest singular point of $f(z)$. The power series (1.19) diverges for $|z-a| > R$, while on the *circle of convergence* $|z-a| = R$ it may converge at some points, but must diverge at at least one.

A simple example is the function $1/(1-z)$, which is holomorphic except at the point $z=1$. Therefore it is holomorphic on the disc $D(0;1)$ and has a Taylor expansion about $z=0$, namely

$$f(z) = \sum_{n=0}^{\infty} z^n, \tag{1.20}$$

which converges for $|z|<1$. But if we *define* a function $f(z)$ by the power series (1.20), then the series *diverges*, so that $f(z)$ does not even exist, for $|z|>1$. The function $f(z)$ defined by the power series (1.20) can be *analytically continued* onto a set outside its disc of convergence by defining a new function as follows:

$$\tilde{f}(z) = \begin{cases} \displaystyle\sum_{n=0}^{\infty} z^n & |z|<1, \\ \dfrac{1}{1-z} & |z| \ge 1,\ z \ne 1. \end{cases} \tag{1.21}$$

The resulting function $\tilde{f}(z)$ is holomorphic on the extended set $z \in \mathbb{C} \setminus \{1\}$. The **Identity Theorem** below tells us that this continuation of $f(z)$ outside its disc of convergence is unique.

In the above example (1.21), we knew the precise location of the singularity in $\tilde{f}(z)$ and indeed had an exact formula for the analytic continution into $|z| > 1$. More generally, to get outside the circle of convergence one has to form another series centred at a point near the boundary of the original circle, and hope that the new series converges in a disc containing points outside the original circle of convergence. The process is then repeated with a new circle, and so on, as illustrated in Figure 1.3. By repeating this process we hope to analytically continue the original function into an ever larger region of the complex plane.

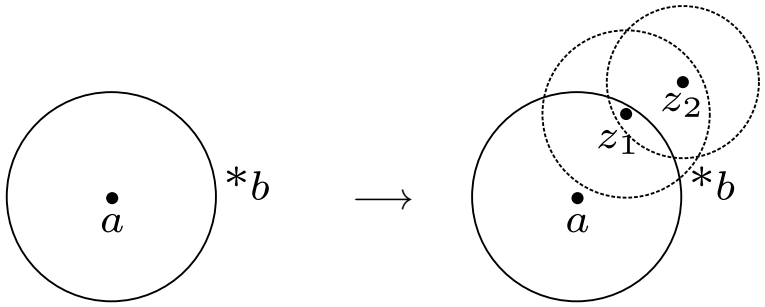

Figure 1.3: Analytic continuation of $f(z)$ out of its original circle of convergence. The radius of convergence is the distance from $z = a$ to $z = b$, the nearest singular point of $f(z)$.

However, it should not be thought that analytic continuation is automatically possible. For example, the function

$$f(z) = \sum_{n=0}^{\infty} z^{n!} \tag{1.22}$$

is holomorphic for $|z| < 1$, by comparison with the geometric series, but the sum diverges at all points $z = \mathrm{e}^{\mathrm{i}\theta}$ for which θ is a rational multiple of 2π. Thus the series has a dense set of singularities on the unit circle, and the unit circle is said to be a *natural boundary*, across which it is impossible to analytically continue the function (1.22).

The following theorem guarantees that, if an analytic continuation of a function can be found, then it is unique, locally at least.

Identity theorem. *Suppose $f_1(z)$ and $f_2(z)$ are both holomorphic in D. If there is a sequence of points $z_n \in D$, having an accumulation point which also lies in D, such that $f_1(z_n) = f_2(z_n)$, then $f_1(z) \equiv f_2(z)$ in D.*

An alternative version of the theorem is that if f_1 and f_2 agree on a dense set, then they agree everywhere. Note that it is important that the accumulation point is also in D.

A consequence of the identity theorem is that the zeroes of a non-constant function $f(z)$ holomorphic in D are isolated, in that they cannot have an accumulation point in D; if they did, then $f(z)$ would be zero by the identity theorem.

The Identity Theorem implies that functions generated by analytic continuation are locally unique. Globally, if we analytically continue a function out of an initial circle of convergence using two different chains of circles, to arrive at the same exterior point by two different

routes, the continued value is the same provided that the function is holomorphic in the region between the two chains, a result called the *Monodromy Theorem*, illustrated in Figure 1.4. If not, we may end up generating branches of a multi-function such as $\log z$.

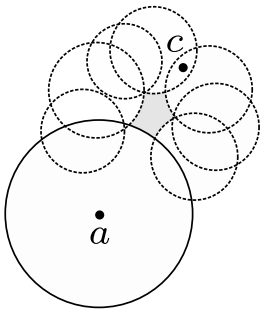

Figure 1.4: *Monodromy Theorem*: $f(z)$ is single-valued at $z = c$ provided $f(z)$ is holomorphic in the shaded area.

1.6 Laurent's Theorem and isolated singularities

Laurent's theorem. *If $f(z)$ is holomorphic in the annulus $S < |z - a| < R$, then in that annulus it has a series representation*

$$f(z) = \sum_{n=-\infty}^{\infty} c_n (z-a)^n, \qquad \text{where} \quad c_n = \frac{1}{2\pi \mathrm{i}} \oint_\Gamma \frac{f(\zeta)}{(\zeta - a)^{n+1}} \, \mathrm{d}\zeta. \tag{1.23}$$

The integration contour Γ is any simple closed path that encloses $z = a$ and lies entirely in the annulus $S < |z - a| < R$.

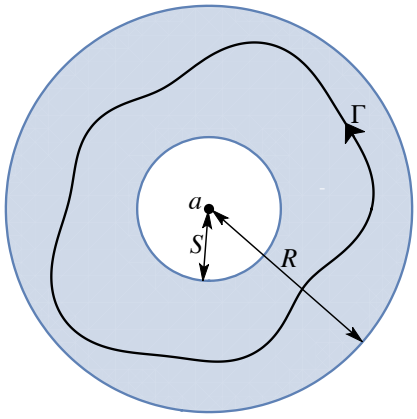

Figure 1.5: The integration contour Γ in Laurent's Theorem.

The integration contour Γ is illustrated in Figure 1.5. The part of the sum (1.23) containing negative powers of z, i.e. $\sum_{n=-\infty}^{-1} c_n (z-a)^n$, is called the *principal part* of $f(z)$ at $z = a$,

and it is holomorphic for $S < |z-a| < \infty$. The part $\sum_{n=0}^{\infty} c_n(z-a)^n$ containing non-negative powers is holomorphic for $0 \leq |z-a| < R$. Therefore these two parts of the series are both holomorphic on the *overlap region* $S < |z-a| < R$.

Classification of singularities

Suppose that $S = 0$ in Laurent's theorem, so that $f(z)$ is holomorphic on the *punctured disc* $D'(a;R) = \{z \in \mathbb{C} : 0 < |z-a| < R\}$ (where it may happen that $R = \infty$). Then $f(z)$ has an *isolated singularity* at $z = a$. These singularities can be classified into three categories, as follows.

1. If all the negative coefficients in the Laurent expansion vanish, $c_n = 0$ for all $n < 0$, then $f(z)$ can be made holomorphic at $z = a$ by setting $f(a) = c_0 = \lim_{z\to a} f(z)$. Such a singularity is termed *removable*.

2. If there is an integer $m > 0$ such that $c_{-m} \neq 0$ but $c_n = 0$ for $n < -m$, then $f(z)$ has a *pole of order* m at $z = a$. In this case $(z-a)^m f(z)$ is holomorphic at $z = a$. A function whose only singularities are poles is called *meromorphic*.

3. If neither of the above holds, then there are infinitely many nonzero negative Laurent coefficients: the principal part goes on for ever. In this case $f(z)$ has an *isolated essential singularity* at $z = a$.

The prototypical example of the third case is the function $\mathrm{e}^{1/z}$, which has an essential singularity at $z = 0$. The behaviour of $f(z)$ near a pole of order m may be singular, but the singularity is relatively tame because $(z-a)^m f(z)$ is locally holomorphic. However, the behaviour near an isolated essential singularity is truly pathalogical, as demonstrated by:

Picard's Theorem: *Suppose $f(z)$ has an isolated singularity at $z = a$ and let D_ϵ be a small neighbourhood of $z = a$ such that $f(z)$ is holomorphic in $D_\epsilon \setminus \{a\}$. Then, for every $\zeta \in \mathbb{C}$, with at most one exception (the so-called lacunary value), the equation $f(z) = \zeta$ has infinitely many roots z in D_ϵ.*

That is, the image of D_ϵ under $f(z)$ covers the *whole* complex plane (except for at most one point) *infinitely often*! For the particular example $f(z) = \mathrm{e}^{1/z}$, it is quite easy to see why this is true, and that the lacunary value in this case is zero.

The behaviour of $f(z)$ at infinity is classified according to the behaviour of $f(1/z)$ near $z = 0$; thus, for example, z has a pole of order 1 at infinity, while e^z has an essential singularity at infinity.

1.7 Cauchy's Residue Theorem

If $f(z)$ has an isolated singularity at $z = a$ and is otherwise holomorphic inside and on a contour Γ enclosing a, then (by uniform convergence)

$$\begin{aligned}\oint_\Gamma f(z)\,\mathrm{d}z &= \oint_\Gamma \sum_{n=-\infty}^{\infty} c_n (z-a)^n\,\mathrm{d}z \\ &= \sum_{n=-\infty}^{\infty} c_n \oint_\Gamma (z-a)^n\,\mathrm{d}z \\ &= 2\pi\mathrm{i}c_{-1},\end{aligned} \tag{1.24}$$

as all the other integrals vanish. The coefficient

$$c_{-1} = \mathrm{res}[f(z); a] \tag{1.25}$$

is the called *residue* of $f(z)$ at $z = a$.

The result is easily generalised to the case when $f(z)$ has several isolated singularities inside Γ, and is known as:

Cauchy's Residue Theorem: *If $f(z)$ is holomorphic inside and on Γ with the exception of a finite number of isolated singularities at $z = a_j$ inside Γ, then*

$$\oint_\Gamma f(z)\,\mathrm{d}z = 2\pi\mathrm{i}\sum_j \mathrm{res}[f(z); a_j]. \tag{1.26}$$

Calculation of residues relies on a few variations on the theme of calculating local expansions. Apart from functions such as $\mathrm{e}^{1/z}$ for which we just calculate the power series, we may often have functions with poles, in the form

$$f(z) = \frac{g(z)}{h(z)} \tag{1.27}$$

where both $g(z)$ and $h(z)$ are holomorphic at $z = a$ and $h(a) = 0$, $g(a) \neq 0$. The order of the pole then depends on the order of the zero of $h(z)$ at $z = a$. If $h(z) = z-a$ the pole is a simple one and the residue is $g(a)$, and if $h(z) = (z-a)^n$, the Taylor expansion of $g(z)$ shows that the residue is $g^{(n-1)}(a)/(n-1)!$. If $h(a) = 0$ but $h'(a) \neq 0$, expanding $h(z) = (z-a)h'(a) + \cdots$ shows that the residue is $g(a)/h'(a)$; and so on.

1.8 Multifunctions

A function $f(z)$ has a *branch point* at $z = a$ if, on taking a circuit round a, the final value of $f(z)$ is not equal to the original one. It is possible for a branch point to be at infinity: we say that $f(z)$ has a branch point at infinity if $f(1/z)$ has a branch point at the origin.

The most basic example is $\log z$, defined as

$$\log z = \log|z| + \mathrm{i}\arg z = \log r + \mathrm{i}\theta, \tag{1.28}$$

where $|z| = r$ and $\arg z = \theta$ are the *modulus* and *argument* of z, defined such that

$$z = r\mathrm{e}^{\mathrm{i}\theta}. \tag{1.29}$$

It is clear that (1.29) only defines θ up to an arbitrary integer multiple of 2π, and it is this ambiguity that leads to the multivaluedness of $\log z$. If we perform a circuit of the origin by setting $z = \epsilon \mathrm{e}^{\mathrm{i}t}$ and then letting t increase from 0 to 2π, then the value of $\log z$ does not return to its initial value $\log \epsilon$ but increases by $2\pi\mathrm{i}$. Thus there is a branch point at $z = 0$. There is also a branch point at infinity, since $\log(1/z)$ has a branch point at $z = 0$.

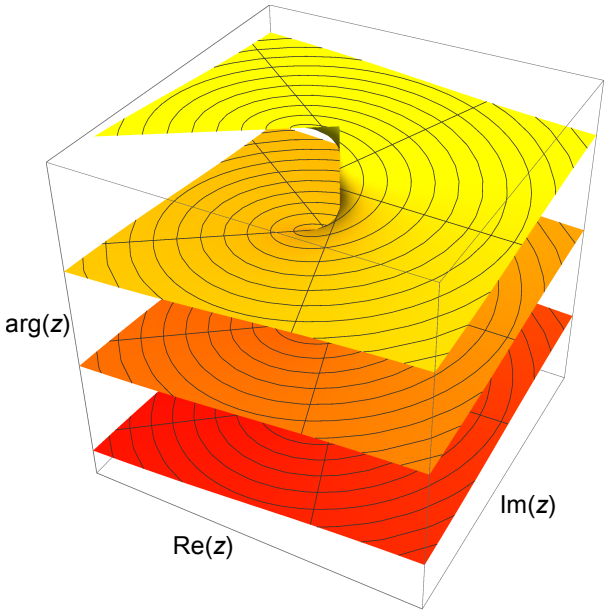

Figure 1.6: The Riemann surface for $\arg z$.

There are two solutions to this difficulty. One is to construct a *Riemann surface*, consisting of all possible values of the multifunction at each point of $\mathbb{C}$. For example, given $z \neq 0$, the argument θ of z takes a countably infinite set of values (all differing by integer multiples of 2π), resulting in the surface shown in Figure 1.6. Thus the Riemann surface for $\log z$ defined in this way resembles a multi-storey carpark. At each point on this surface, apart from the branch point $z = 0$ itself, $\log z$ defines a locally holomorphic function, but because of the mutiple layers of the surface, the value of $\log z$ for a given value of z is ambiguous.

The second solution is to restrict the domain of definition of the function so that the problematic circuits are forbidden. This is achieved by introducing *branch cuts*, joining the branch points, across which contours may not pass. Then it is possible to define single-valued *branches* of the multifunction. For example, we can define a single-valued branch of $\log z$ by drawing a branch cut that connects the branch points $z = 0$ and $z = \infty$. Obviously there is no unique way of doing so, but the most popular choice is to place the branch cut along the negative real axis, as shown in Figure 1.7. Thus we define a countable set of branches of $\log z$ corresponding to each integer k, with

$$\log z = \log r + \mathrm{i}\theta + 2\pi k\mathrm{i}, \tag{1.30}$$

and θ now restricted to lie in the range $-\pi < \theta \leq \pi$ (so that the cut cannot be crossed). Each choice of k results in a single-valued function which is holomorphic on the cut plane.

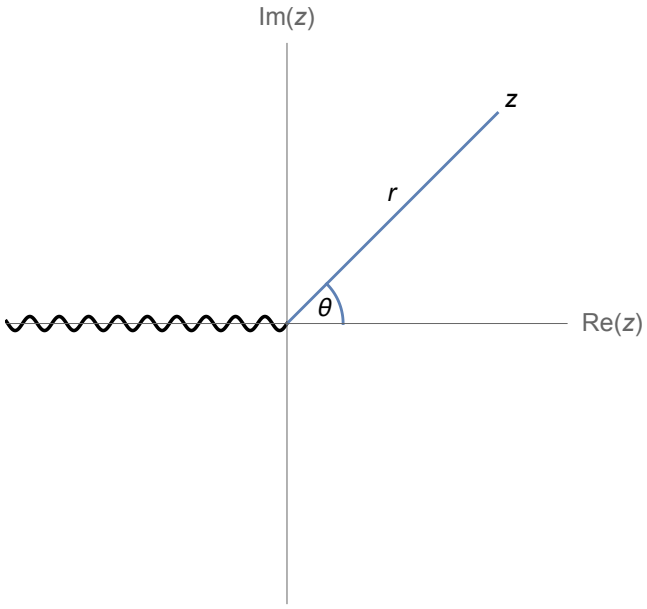

Figure 1.7: The complex plane with a branch cut along the negative real axis.

The price we pay is that the resulting function is discontinuous across the branch cut. The particular branch with $k = 0$ is often called the *principal branch* of $\log z$, and denoted by $\operatorname{Log} z$; the corresponding principal branch of $\arg z = \theta \in (-\pi, \pi]$ is denoted by $\operatorname{Arg} z$.

One other instructive example is the multifunction $\left(z^2-1\right)^{1/2}$, which can be defined by

$$\begin{aligned}\left(z^2-1\right)^{1/2} &= (z-1)^{1/2}(z+1)^{1/2} \\ &= (r_1 r_2)^{1/2} \mathrm{e}^{\mathrm{i}(\theta_1+\theta_2)/2},\end{aligned} \tag{1.31}$$

where

$$r_1 = |z-1|, \qquad r_2 = |z+1|, \qquad \theta_1 = \arg(z-1), \qquad \theta_2 = \arg(z+1). \tag{1.32}$$

One can easily check that $\left(z^2-1\right)^{1/2}$ has branch points at $z = \pm 1$. Choosing a particular branch of the multifunction corresponds to uniquely defining the two angles θ_1 and θ_2, and there are two canonical choices, the branch cuts for which are illustrated in Figure 1.8.

First suppose we define θ_1 and θ_2 such that

$$-\pi < \theta_1 \leq \pi, \qquad\qquad -\pi < \theta_2 \leq \pi. \tag{1.33}$$

The corresponding function defined by (1.31) has a branch cut that connects $z = -1$ to $z = 1$ along the line segment $[-1, 1]$ on the real axis. Just above the cut, we have $\theta_1 = \pi$, $\theta_2 = 0$ and therefore $\left(z^2-1\right)^{1/2} = \mathrm{i}\left|z^2-1\right|$. Just below the cut, we have $\theta_1 = -\pi$, $\theta_2 = 0$ and therefore $\left(z^2-1\right)^{1/2} = -\mathrm{i}\left|z^2-1\right|$. Thus the function is discontinuous and changes sign across the branch cut. Across the negative real axis with $\operatorname{Re}(z) < -1$, both θ_1 and θ_2 jump by 2π, so that the argument $(\theta_1+\theta_2)/2$ jumps by 2π, returning the same value of $\left(z^2-1\right)^{1/2}$. This explains why there is no discontinuity across the negative real axis where $\operatorname{Re}(z) < -1$.

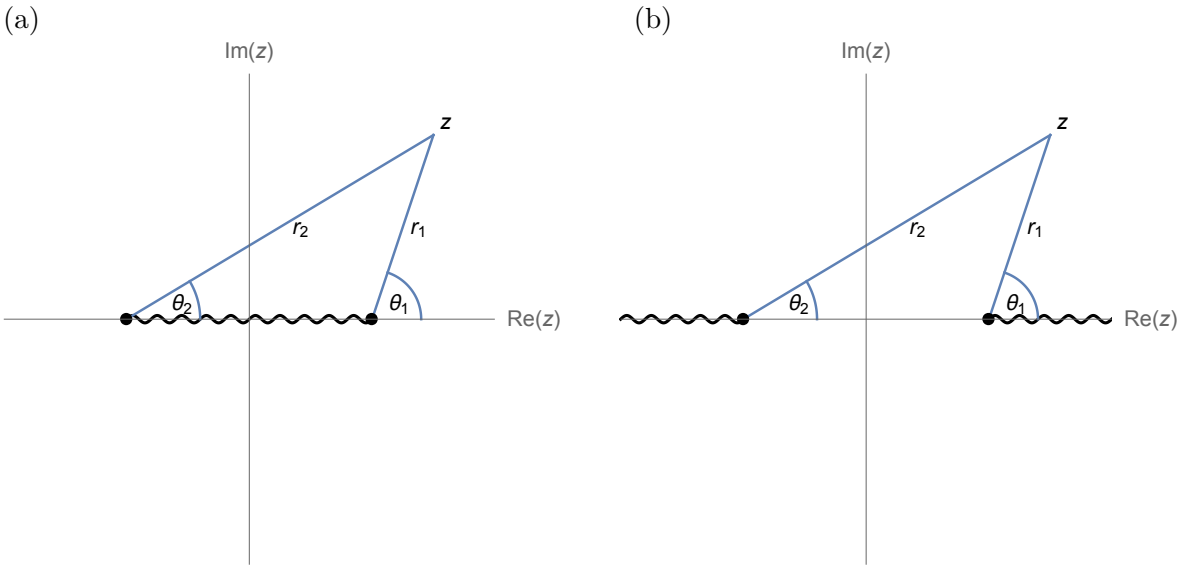

Figure 1.8: Two possible branch cuts for the multifunction $\left(z^2-1\right)^{1/2}$.

The second popular definition of $\left(z^2-1\right)^{1/2}$ occurs when we choose θ_1 and θ_2 in the ranges

$$-\pi < \theta_1 \leq \pi, \qquad\qquad 0 < \theta_2 \leq 2\pi. \tag{1.34}$$

In this case, the branch cut extends along the real axis on the intervals $(-\infty,-1]$ and $[1,\infty)$. There is not a branch point at infinity, so we should not really think of there being two branch cuts that extend to infinity, but of a single cut that connects -1 to 1 through infinity.

1.9 Evaluation of integrals

There is a collection of standard contours which are used to evaluate standard integrals. Cauchy's integral theorems apply to integration around closed contours. Often this involves closing a contour on a suitable return path and then proving that the additional contribution to the integral tends to zero as the return path tends to infinity.

Example 1

The substitution $\mathrm{e}^{\mathrm{i}\theta} = z$ transforms integrals of rational functions of $\sin\theta$, $\cos\theta$ to integrals of rational functions of z. For example, for the integral

$$\int_0^{2\pi} \frac{\mathrm{d}\theta}{a+b\sin\theta},$$

with $0<b<a$, the substitution $\mathrm{e}^{\mathrm{i}\theta} = z$ results in an integral around the unit circle, namely

$$\int_0^{2\pi} \frac{\mathrm{d}\theta}{a+b\sin\theta} = \oint_{|z|=1} \frac{2\,\mathrm{d}z}{bz^2+2\mathrm{i}az-b}. \tag{1.35}$$

The integrand has poles on the negative imaginary axis, only one of which is inside the unit disc, as illustrated in Figure 1.9, and the result is easily found using Cauchy's Residue Theorem.

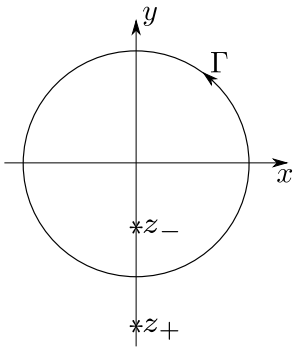

Figure 1.9: The integrand of the integral (1.35) has two simple poles at $z = z_{\pm}$.

Example 2

Consider the integral of a rational function of x, of the form

$$\int_{-\infty}^{\infty} \frac{P(x)}{Q(x)}\,\mathrm{d}x,$$

where $P(x)$ and $Q(x)$ are polynomials with $\deg(Q) \geq \deg(P) + 2$ and where Q has no real roots. Here we first take the integral from $x = -R$ to $x = R$ and close with a large semicircle in the upper half-plane, then let $R \to \infty$, as shown in Figure 1.10. Our assumption about the degrees of P and Q ensures that the contribution from the semicircle tends to zero as $R \to \infty$. Then we just need to apply Cauchy's Residue Theorem and sum up the contributions from all the residues in the upper half-plane. (Closing the contour in the lower half-plane would give the same answer, but we would have to remember an extra minus sign because Γ is then taken clockwise.)

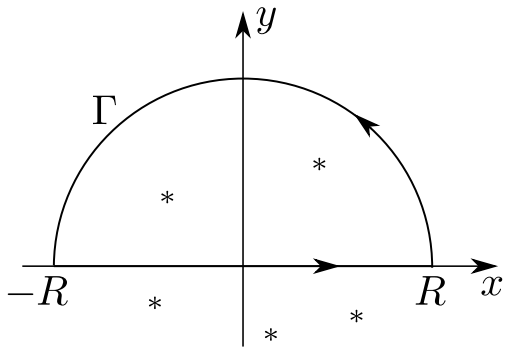

Figure 1.10: Closing the contour in the upper half-plane.

Example 3

For integrals of the form

$$\int_{-\infty}^{\infty} \frac{P(x)\cos x}{Q(x)}\,\mathrm{d}x \qquad \text{or} \qquad \int_{-\infty}^{\infty} \frac{P(x)\sin x}{Q(x)}\,\mathrm{d}x$$

we integrate

$$\frac{\mathrm{e}^{\mathrm{i}z}P(z)}{Q(z)}$$

round a semicircular contour closed in the *upper* half-plane. We must use the upper half-plane to ensure that there is no contribution from the semicircle, because

$$\mathrm{e}^{\mathrm{i}z} = \mathrm{e}^{\mathrm{i}x-y}$$

decays as $y \to +\infty$ but blows up as $y \to -\infty$. In this case, the integral exists provided $\deg(Q) \geq \deg(P) + 1$. For the limiting case where $\deg(Q) = \deg(P) + 1$, the contribution from the semicircle can be bounded by using **Jordan's result** that

$$\int_0^{\pi/2} \mathrm{e}^{-R\sin\theta}\,\mathrm{d}\theta \to 0 \quad \text{as } R \to \infty. \tag{1.36}$$

Example 4

Sometimes it is possible to construct a contour Γ such that the integral along one segment of Γ is a constant multiple of the integral along another (together with vanishing contributions from the remaining segments). For example, to evaluate

$$\int_0^\infty \frac{\mathrm{d}x}{1+x^{2n}},$$

take Γ to run from 0 or R along the real axis, then via a circular arc to return along the ray $\arg z = \pi/n$ (on which $1 + z^{2n}$ is the same as on the real axis), picking up the residue from the pole at $z = \mathrm{e}^{\mathrm{i}\pi/2n}$, as shown in Figure 1.11 (left).

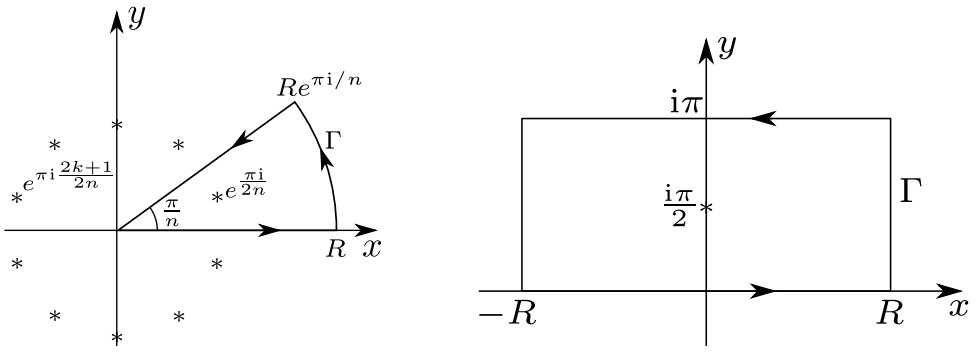

Figure 1.11: Closed contours for $f(z) = 1/(1+z^{2n})$ (left) and $f(z) = \cos(z)/\cosh(z)$ (right).

Or, to evaluate

$$\int_{-\infty}^{\infty} \frac{\cos x}{\cosh x}\,\mathrm{d}x,$$

integrate $\cos z/\cosh z$ round a rectangular contour with corners at $\pm R$, $\pm R + \mathrm{i}\pi$, as shown in Figure 1.11 (right), enclosing the pole at $z = \mathrm{i}\pi/2$.

Example 5

Integrals such as

$$\int_0^\infty \frac{\sin x}{x}\,\mathrm{d}x,$$

can be evaluated by integrating $\mathrm{e}^{\mathrm{i}z}/z$ round a contour consisting of the real axis with a small semicircular indentation at the origin, above the real axis, plus a large semicircle, as shown in Figure 1.12. The small indentation is necessary to avoid the singularity at $z = 0$, and contributes $-\pi\mathrm{i}$ times the residue at the origin. The minus sign is because the semicircle is taken clockwise, and the factor of $\pi\mathrm{i}$ instead of $2\pi\mathrm{i}$ comes from having only half a circle, so we only pick up half the residue.

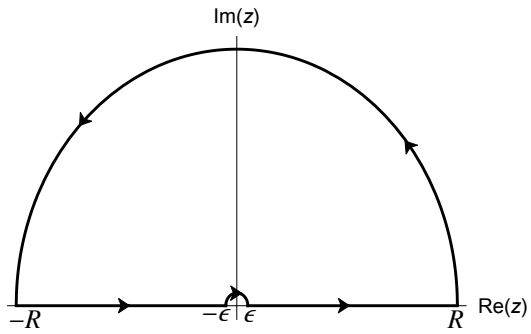

Figure 1.12: Integration contour for the integrand $\mathrm{e}^{\mathrm{i}z}/z$.

Example 6

A 'keyhole' contour is necessary for integrals involving branch cuts, for example

$$I_1 = \int_0^\infty \frac{\log x\,\mathrm{d}x}{(x+a)(x+b)} \quad (a, b > 0) \qquad \text{or} \quad I_2 = \int_0^\infty \frac{\log^2 x\,\mathrm{d}x}{1+x^2}. \tag{1.37}$$

For I_1, integrate $(\log z - \pi\mathrm{i})^2/(z+a)(z+b)$ (with the branch cut chosen along the positive real axis) round the contour shown in Figure 1.13 and exploit the different values of the log on either side of the cut. The same contour also works for I_2 but with the integrand $(\log z - \pi\mathrm{i})^3/(1+z^2)$.

1.10 Fourier and Laplace transforms

The **Fourier transform** of a real function $f(x)$ is defined by

$$\bar{f}(k) \equiv \mathcal{F}[f] = \int_{-\infty}^{\infty} f(x)\mathrm{e}^{\mathrm{i}kx}\,\mathrm{d}x, \tag{1.38}$$

and the inverse is

$$f(x) \equiv \mathcal{F}^{-1}\left[\bar{f}\right] = \frac{1}{2\pi}\int_{-\infty}^{\infty} \bar{f}(k)\mathrm{e}^{-\mathrm{i}kx}\,\mathrm{d}k. \tag{1.39}$$

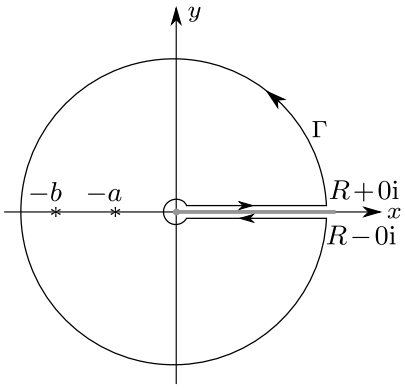

Figure 1.13: Closed contour for the integrals in Example 6. The branch cut is marked as a grey line; note that $\log z - \pi\mathrm{i} = \log(x) \mp \pi\mathrm{i}$ for $z = x \pm 0\mathrm{i}$, $x > 0$.

Note that there are various different conventions in defining the Fourier transform, but this is the version that will be used in this course. In practice, inversion is usually accomplished by contour integration in the complex k-plane.

Integration by parts shows that

$$\mathcal{F}\left[\frac{\mathrm{d}f}{\mathrm{d}x}\right] = -\mathrm{i}k\hat{f}(k), \tag{1.40}$$

so that the Fourier transform converts differential operators into algebraic operators. On the other hand, differentiation under the integral sign leads to

$$\mathcal{F}[xf(x)] = -\mathrm{i}\frac{\mathrm{d}\bar{f}}{\mathrm{d}k}. \tag{1.41}$$

The **Laplace transform** operates on functions defined on the positive real axis:

$$\hat{f}(p) \equiv \mathcal{L}[f] = \int_0^\infty f(x)\mathrm{e}^{-px}\,\mathrm{d}x. \tag{1.42}$$

If $f(x)\mathrm{e}^{-\gamma x}$ is integrable (so that $|f(x)|$ grows no faster than $\mathrm{e}^{\gamma x}$ as $x \to \infty$), then $\hat{f}(p)$ exists for $\mathrm{Re}\,p \geq \gamma$ and is holomorphic in p for $\mathrm{Re}\,p > \gamma$. It can usually be analytically continued into the rest of the complex p-plane, although singularities inevitably occur. The Laplace inversion formula is

$$f(x) \equiv \mathcal{L}^{-1}\left[\hat{f}\right] = \frac{1}{2\pi\mathrm{i}}\int_{\gamma-\mathrm{i}\infty}^{\gamma+\mathrm{i}\infty} \hat{f}(p)\mathrm{e}^{px}\,\mathrm{d}p. \tag{1.43}$$

The contour is usually (but not always) completed in the left-hand half-plane and in many problems the solution is given by a sum of residues from the interior of the completed contour. If a branch cut is present in $\hat{f}(p)$ then some kind of keyhole contour is required.

1.11 Conformal mapping

We can view a holomorphic function $f(z)$ as a mapping from a point z in the complex plane to a new point $\zeta = f(z)$. We then ask the question: given a domain in the z-plane, what is the image of that domain in the ζ-plane under the mapping $z \mapsto \zeta = f(z)$?

Basic properties

Suppose $f(z)$ is holomorphic at $z = a$. Then, by Taylor's theorem, for z near a we have

$$\zeta = f(z) = f(a) + f'(a)(z - a) + \cdots . \tag{1.44}$$

If $f'(a) \neq 0$, this shows that a small neighbourhood of $z = a$ is translated, with $z = a$ going to the point $\zeta = f(a)$, and then rotated (by an angle $\arg f'(a)$) and scaled (by a factor $|f'(a)|$), as illustrated in Figure 1.14.

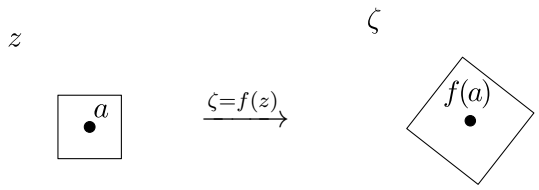

Figure 1.14: A small region of the z-plane is translated, rotated and scaled under the mapping $z \mapsto \zeta = f(z)$. (Here and henceforth, the z- and ζ-planes are just labelled "z" and "ζ".)

If two curves meet at $z = a$ and the angle between them is α, it follows from the local linearity that the angle between their images is also α (and has the same sense), as shown in Figure 1.15. Maps with this property are called *conformal*, and we have shown that a holomorphic function is a conformal map at all points where its derivative does not vanish.

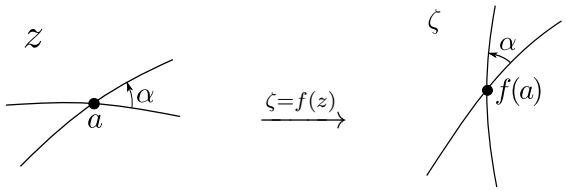

Figure 1.15: The angle (including sense) between two curves is preserved by the mapping $z \mapsto \zeta = f(z)$.

A conformal map is *locally* one-to-one, being a small perturbation of a linear map, but this is only a local statement. When we look at the image of a domain D under $f(z)$, the map may not be *globally* one-to-one, even if $f'(z)$ does not vanish in D. Figure 1.16 illustrates the kind of problem that may arise.

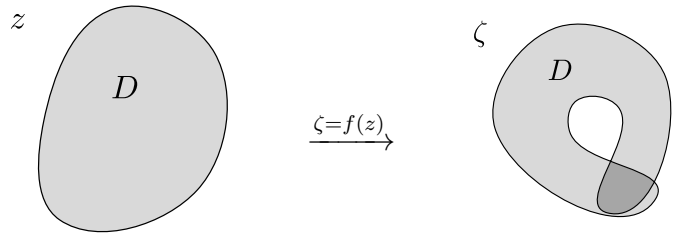

Figure 1.16: A conformal map need not be globally one-to-one.

The composition of two conformal maps is itself conformal. We can use this in building up complicated maps from simple ones.

Behaviour near a critical point

We have shown that the mapping $z \mapsto \zeta = f(z)$ is conformal provided $f'(z) \neq 0$. However, many useful mapping functions have isolated *critical points* where f' is zero. Consider a point a such that $f'(a) = 0$ and $f''(a) \neq 0$. If we write $z = a + re^{i\theta}$, then

$$\begin{aligned} f(z) &= f(a) + \frac{1}{2} f''(a)(z-a)^2 + O\left((z-a)^3\right) \\ &= f(a) + \frac{1}{2} f''(a) r^2 e^{2i\theta} + O(r^3). \end{aligned} \tag{1.45}$$

The image of a small neighbourhood of $z = a$ now covers a small neighbourhood of $f(a)$ *twice*, as shown in Figure 1.17, and the angle between two curves meeting at a is doubled.

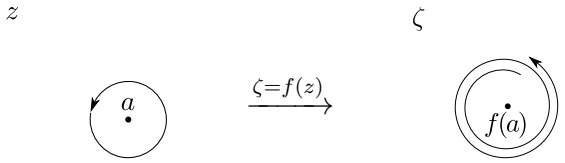

Figure 1.17: If $f'(0) = 0$ and $f''(a) \neq 0$ then angles are locally doubled.

We see that if a map $f(z)$ has a critical point at a point $z = a$ in a region D, it is neither conformal at that point, nor locally one-to-one near it. The only hope of constructing a one-to-one map using $f(z)$ is if a lies on the boundary of D. A very simple example is $f(z) = z^2$ acting on the right-hand half-plane $\mathrm{Re}\, z > 0$. The image of an interior point $z = re^{i\theta}$, where $-\pi/2 < \theta < \pi/2$, is $\zeta = r^2 e^{2i\theta}$, and we see that $-\pi < \arg\zeta < \pi$, so the map is one-to-one (as predicted by the doubling of the angles). The image of the half-plane $\mathrm{Re}\, z > 0$ is the entire ζ-plane, minus a slit along the negative real axis, as shown in Figure 1.18.

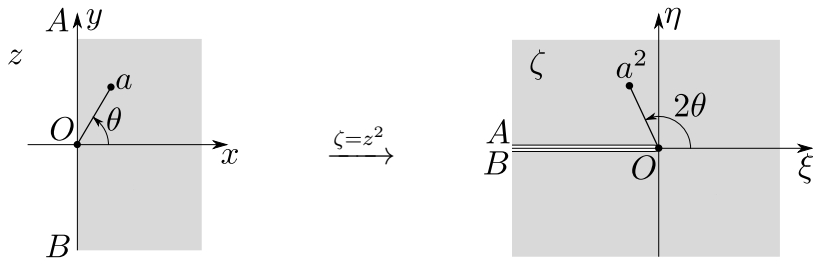

Figure 1.18: The mapping $z \mapsto \zeta = z^2$ maps the half-plane $\mathrm{Re}\, z > 0$ to the entire ζ-plane, minus a slit along the negative real axis

The Riemann mapping theorem

It is natural to ask what domains we can map to what. The answer is that virtually any simply-connected region of the complex plane can be mapped to virtually any other such region, because of:

The Riemann Mapping Theorem. *Any simply connected domain D, with the sole exception of $\mathbb{C}$ itself, can be mapped conformally onto the unit disc $|\zeta| < 1$. There are three free real parameters in the map.*

We omit the proof, which is very technical and not constructive, and instead just make some comments on the theorem.

1. The reason that there is no map from $\mathbb{C}$ itself to the unit disc is that if there were one, the mapping function would be entire and its modulus would be bounded by 1; by Liouville's theorem, the function would have to be constant (and hence not conformal).

2. The three real degrees of freedom might look mysterious. As we shall see, they arise because there is precisely a three-parameter family of maps from the unit disc to itself.

3. If D is bounded by a simple closed curve (which may pass through the point at infinity), we may use the three degrees of freedom to specify the images of three boundary points, and the map is then uniquely determined. Alternatively, we may specify the image of one interior point of D, and the image of a direction at that point.

4. It is conventional to map to the unit disc. However, any other 'canonical domain' would do, since we can map the disc onto it and then use the composition of maps. The upper half-plane is also often used as a canonical domain, and then the three boundary points in Riemann's theorem are usually taken to be 0, 1 and ∞.

5. The theorem says that the map is conformal in the interior of D (so its inverse is conformal in $|\zeta| < 1$), but it might not be conformal on the boundary of D, where singularities are needed to smooth out corners and cusps.

6. Because conformal maps preserve angles, including their orientation, if we go round ∂D in a particular sense (say, anticlockwise), then the image of ∂D is traversed in the same sense, as illustrated in Figure 1.19.

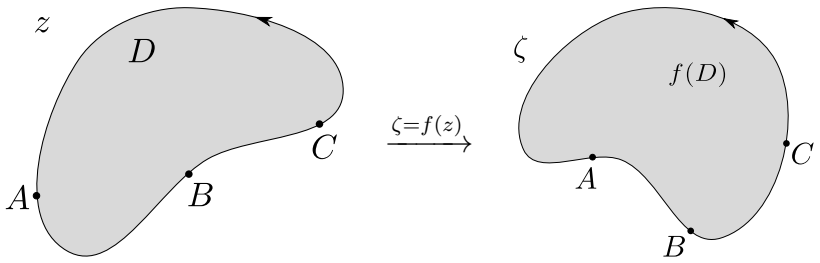

Figure 1.19: The orientation of the boundary is preserved by a conformal mapping, so that the images of the points A, B, C occur in the same order.

Standard maps

Let us look at some standard maps. In the accompanying examples, we see how to construct complicated maps from these building blocks.

Bilinear (Möbius) maps

The Möbius transformation is

$$\zeta = f(z) = \frac{az+b}{cz+d}, \qquad a, b, c, d \in \mathbb{C}, \tag{1.46}$$

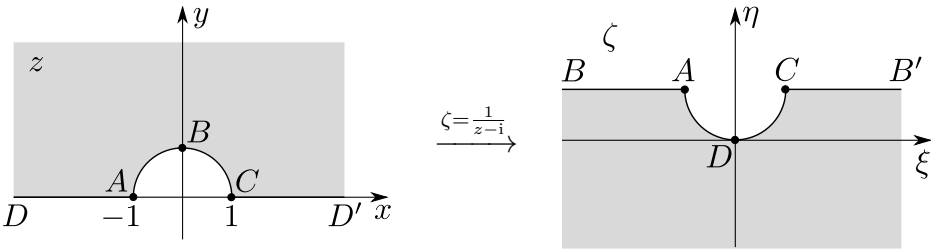

Figure 1.20: The effect of the Möbius mapping $z \mapsto \zeta = 1/(z - \mathrm{i})$ on a half-plane with a semi-circle removed.

where $ad - bc \neq 0$ (otherwise, the map is constant) and, to avoid trivial translations, rotations and scalings, $c \neq 0$. The Möbius transformation is conformal at all points except the location of its pole, and is a one-to-one map from the *extended complex plane* $\tilde{\mathbb{C}} = \mathbb{C} \cup \{\infty\}$ to itself.

It is a well known fact that Möbius transformations take circles and straight lines into circles and straight lines. (The jargon "circlines" is sometimes used for circles and straight lines; a straight line can be viewed as a circle with its centre at infinity.) It is not usually necessary to do detailed calculations when using Möbius maps on a domain bounded by straight lines and circles; it is enough to know that the boundary maps to a combination of straight lines and circles, and to know the angles where they meet, since these are also preserved by the map.

Example. The domain D consists of the upper half-plane $y > 0$ with its intersection with the closed unit disc removed (thus, it has a semicircular indentation centred on the origin). Find the image of the domain under the map $\zeta = 1/(z - \mathrm{i})$, indicating the images of significant boundary points.

Solution. The image boundary is made up of straight lines and circles. The points $z = \pm 1$ map to $\zeta = 1/(\pm 1 - \mathrm{i}) = (\pm 1 + \mathrm{i})/2$, respectively, $z = \infty$ maps to $\zeta = 0$, and $z = \mathrm{i}$ maps to $\zeta = \infty$. Therefore, the unit circle is mapped to the line $\eta = 1/2$ and the x-axis is mapped to the circle $|\zeta - \mathrm{i}/2| = 1/2$.

The image of the upper half-plane with the closed unit disc removed is then the lower half-plane $\eta < 1/2$ with the closed disc $|\zeta - \mathrm{i}/2| \leq 1$ removed, as shown in Figure 1.20. Note the order of the points marked A, B, C, D is preserved by the mapping, and that the shaded region remains on the left-hand side as we follow the boundary in the order $A \to B \to C \to D$.

Example. Find a map from the domain of the previous example to the quarter plane $\xi > 0$, $\eta > 0$.

Solution. Start by looking at the angles. We have two right angles at $z = \pm 1$, which will be preserved by a Möbius transformation. We shift one right-angle to $\zeta = 0$ and the other to $\zeta = \infty$ with the mapping

$$\zeta = \frac{z - 1}{z + 1}. \tag{1.47}$$

Then $z = 1$ is mapped to $\zeta = 0$, $z = \infty$ is mapped to $\zeta = 1$, $z = -1$ is mapped to $\zeta = \infty$, and $z = \mathrm{i}$ is mapped to $\zeta = \mathrm{i}$. This is enough information to deduce that the boundary gets mapped to the coordinate axes, as shown in Figure 1.21.

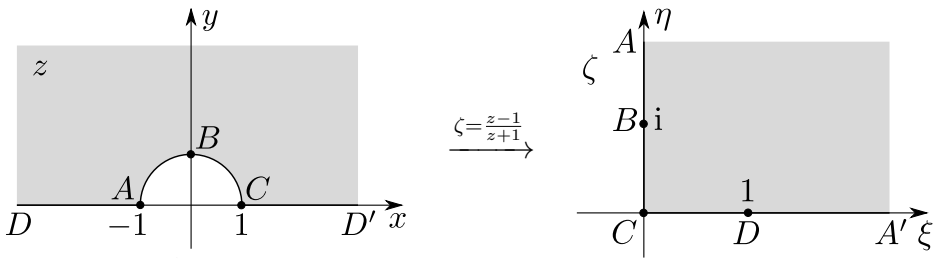

Figure 1.21: Mapping from a half-plane with a semi-circle removed to a quarter-plane.

Example. Map the upper half-plane $y > 0$ to the unit disc $|\zeta| < 1$.

Solution. The upper half-plane is described by the inequality

$$\left|\frac{z-\mathrm{i}}{z+\mathrm{i}}\right| < 1, \tag{1.48}$$

i.e. the set of points closer to i than to $-\mathrm{i}$. This is exactly what we need: if

$$\zeta = \frac{z-\mathrm{i}}{z+\mathrm{i}}, \tag{1.49}$$

then the upper half-plane is mapped to $|\zeta| < 1$.

Example. If $|w| < 1$ and $\theta \in \mathbb{R}$, show that the map

$$\zeta = \mathrm{e}^{\mathrm{i}\theta}\,\frac{z-w}{1-\overline{w}z} \tag{1.50}$$

maps the unit disc one-to-one to itself.

Solution. The map (1.50) is a Möbius transformation, with its pole at $z = 1/\overline{w}$ outside the unit disc, so is automatically one-to-one. A direct calculation reveals that

$$1-|\zeta|^2 \equiv \left[\frac{1-|w|^2}{|1-\overline{w}z|^2}\right]\left(1-|z|^2\right). \tag{1.51}$$

Since $|w| < 1$, the term in square brackets is strictly positive, and it follows that $|\zeta|^2 < 1$ if and only if $|z|^2 < 1$.

It can be shown that Möbius maps of the form (1.50) are the *only* one-to-one maps of the unit disc to itself. The two real parameters needed to define w, and the single real angle of rotation θ, are the three free parameters in the Riemann mapping theorem: having mapped a domain onto the unit disc, we can subsequently apply any map of the form (1.50) while preserving the image as the unit disc.

Example. Map the upper half plane to itself, permuting the points 0, 1 and ∞.

Solution. Because the map preserves the orientation of the interior of the domain vis a vis its boundary, only the even permutations, in which $(0, 1, \infty)$ are mapped to $(1, \infty, 0)$ or $(\infty, 0, 1)$ are possible. We need a Möbius map with real coefficients, so that the real axis maps to itself. First take $(0, 1, \infty)$ to $(1, \infty, 0)$. This means that the map has its pole at $z = 1$, so the denominator is $z-1$ (or a multiple thereof); infinity maps to zero, so the numerator must be a constant (so the map looks like constant$/z$ at infinity; finally, the remaining constant is fixed by the requirement that 0 maps to 1, and we have

$$\zeta = \frac{1}{1-z}. \tag{1.52}$$

The map taking $(0, 1, \infty)$ to $(\infty, 0, 1)$ is likewise found to be

$$\zeta = \frac{z-1}{z}; \tag{1.53}$$

it sends $z = 0$ to infinity, $z = 1$ to 0, and is asymptotic to 1 at infinity, as required.

Powers of z

The powers of z are of most interest when the boundary of D contains a corner at the origin. If D is a sector $0 < \arg z < \alpha$, then the image of this wedge under the map $\zeta = z^n$ is the sector $0 < \arg \zeta < n\alpha$, as shown in Figure 1.22, provided $n\alpha < 2\pi$ so that the map is conformal. This multiplying of angles by n is often useful in getting rid of corners in ∂D, as the next two examples show. Note that there is no need for n to be an integer; if we want to multiply an angle by $3/2$ we choose $n = 3/2$, and if we want to halve an angle we choose $n = 1/2$, and so on.

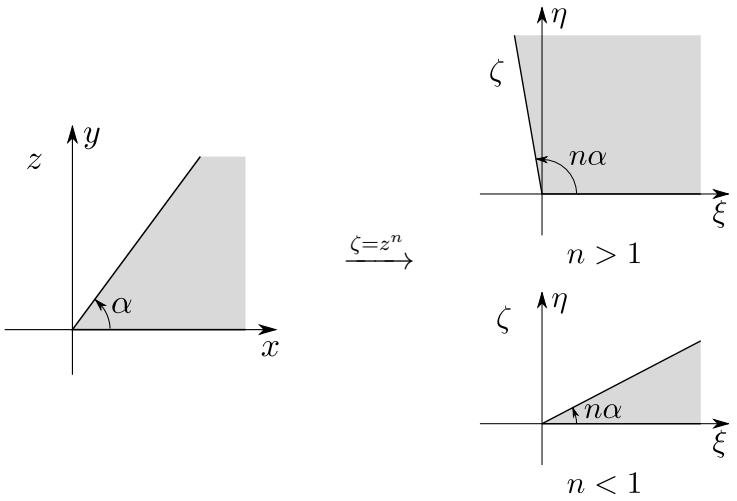

Figure 1.22: The action of the mapping $\zeta = z^n$ on a sector.

Example. The domain D consists of the sector $-\pi/6 < \arg z < \pi/6$ of the unit disc (a slice of pizza). Map it to a semicircle of radius 2.

Solution. We need to get rid of the angle of $\pi/3$ at the origin. The map $\zeta_1 = z^3$ does exactly this; however it takes the unit circle to the unit circle. Hence the required map is $\zeta = 2\zeta_1 = 2z^3$, as shown in Figure 1.23.

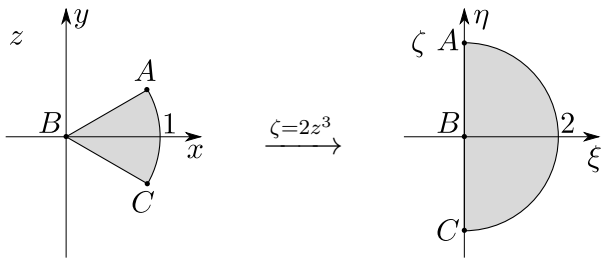

Figure 1.23: Mapping a slice of pizza to a semi-circle of radius 2.

Example. The domain D consists of the unit disc with the sector $\frac{5\pi}{6} < \arg z < \frac{7\pi}{6}$ removed, so it looks like a partly eaten pizza. Find a map from D to the upper half-plane.

Solution. The boundary of D has three corners, with angle $5\pi/3$ at the origin, and two angles of $\pi/2$ on the unit circle. We need to get rid of all of these. We do the mapping in 3 stages.

1. First put
$$\zeta_1 = z^{3/5}. \tag{1.54a}$$
This gets us to a semicircle $-\pi/2 < \arg\zeta_1 < \pi/2$, $0 < |\zeta_1| < 1$.

2. Map the semi-circle in the ζ_1-plane to a quarter plane in the ζ_2-plane using a Möbius transformation. We have two right angles at $\zeta_1 = \pm\mathrm{i}$. We choose the mapping such that $\zeta_1 = -\mathrm{i}$ is mapped to $\zeta_2 = 0$ and $\zeta_1 = \mathrm{i}$ is mapped to $\zeta_2 = \infty$, so ζ_2 is a multiple of $(\zeta_1 + \mathrm{i})/(\zeta_1 - \mathrm{i})$. If we also specify that the image of $\zeta_1 = 0$ is $\zeta_2 = 1$ we find
$$\zeta_2 = -\frac{\zeta_1 + \mathrm{i}}{\zeta_1 - \mathrm{i}}. \tag{1.54b}$$
which maps the semi-circle to the fourth quadrant in the ζ_2-plane.

3. The map
$$\zeta = -\zeta_2^2 \tag{1.54c}$$
will map the quarter plane $-\pi/2 < \arg\zeta_2 < 0$ to the upper half-plane $\eta > 0$.

The combined map is
$$\zeta = -\zeta_2^2 = -\left(-\frac{\zeta_1 + \mathrm{i}}{\zeta_1 - \mathrm{i}}\right)^2 = -\left(\frac{z^{3/5} + \mathrm{i}}{z^{3/5} - \mathrm{i}}\right)^2, \tag{1.55}$$
and the sequence of transformations is depicted in Figure 1.24.

Example. Map the semicircle $|z| < 1$, $0 < \arg z < \pi$, to the upper half-plane.

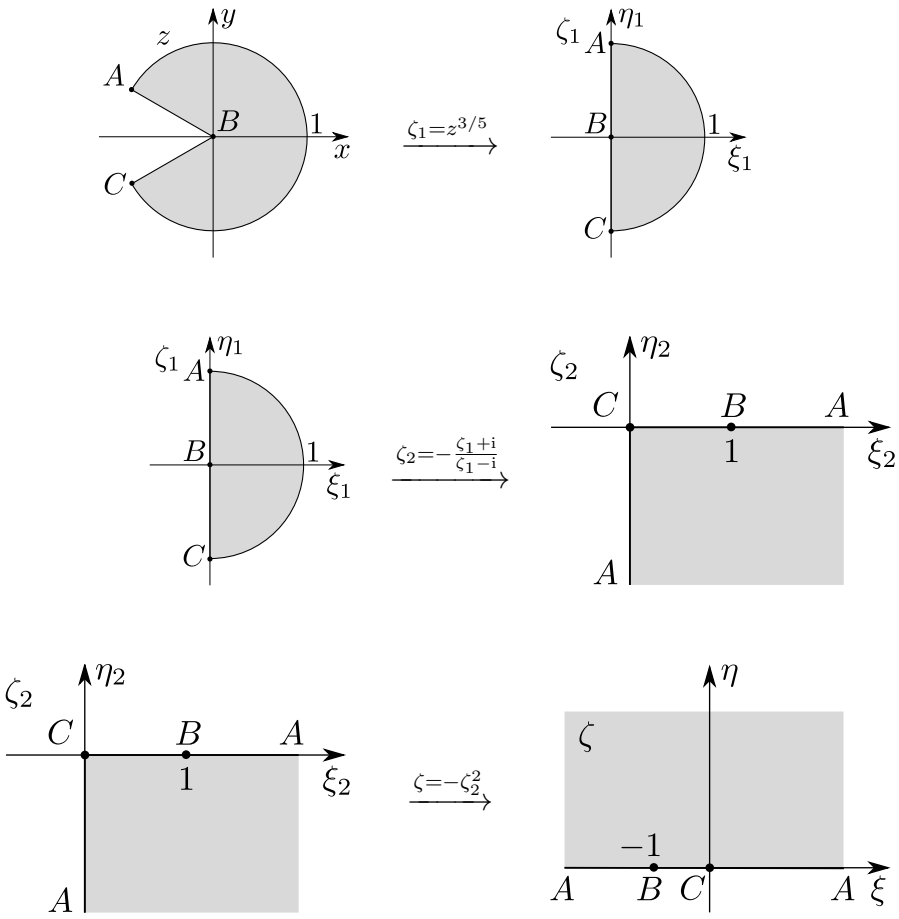

Figure 1.24: The sequence of maps from a pacman shape to the upper half-plane.

Solution. First we get rid of the semicircle by setting

$$\zeta_1 = \frac{1}{z+1}. \tag{1.56}$$

This inversion with respect to the left-hand corner point takes the semicircle to the quarter plane $\xi_1 > 1/2$, $\eta_1 < 0$. The quarter plane is mapped to the upper half plane by the transformation

$$\zeta = -(2\zeta_1 - 1)^2 = -\left(\frac{z-1}{z+1}\right)^2. \tag{1.57}$$

The succession of maps is depicted in Figure 1.25. Note that we could have made this a bit slicker by starting with the map

$$\zeta_1 = \frac{z-1}{z+1}, \tag{1.58}$$

which sends the corners of the semicircle to 0 and ∞, making the subsequent squaring easier.

Exponential and logarithm

Now consider the exponential function and its inverse, the logarithm. As $\mathrm{e}^{z+2\pi\mathrm{i}} \equiv \mathrm{e}^z$, the image of any horizontal strip of width 2π is repeated infinitely often, once for each of the

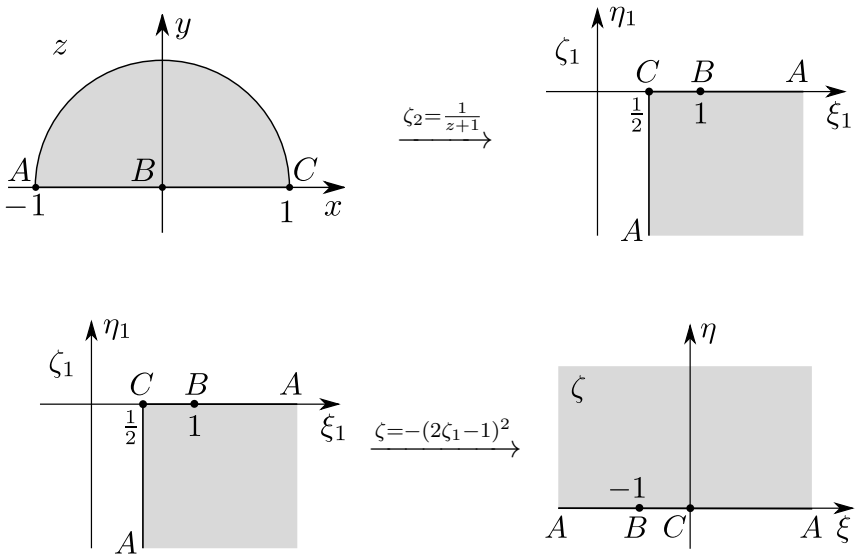

Figure 1.25: Mapping a semicircle to the upper half-plane.

strips obtained by shifting the original one vertically by 2π. Furthermore, as

$$\zeta = \mathrm{e}^z = \mathrm{e}^x \mathrm{e}^{\mathrm{i}y} \tag{1.59}$$

when $z = x + \mathrm{i}y$, the image of the 'baseline' strip $-\pi < y < \pi$, $-\infty < x < \infty$ is the whole plane with the negative real (ξ) axis removed. If we include the image of the line $y = -\pi$ as well, then the image of the strip $-\pi \leq y < \pi$ is $\mathbb{C}\backslash\{0\}$; thus the image of the whole complex plane is the whole plane (minus the origin) covered infinitely often. This is an example of Picard's theorem in action: the function e^z has an essential singularity at infinity, and its lacunary value is 0.

Horizontal lines $y =$ constant map onto rays $\arg\zeta = y$, while vertical line segments $x =$ constant, $-\pi \leq y < \pi$ map to circles of radius e^x. In particular, the imaginary axis is mapped to the unit circle. Thus the exponential map generates plane polar coordinates from a rectangular Cartesian grid.

The inverse map, the logarithm, is defined on the whole plane minus a cut from infinity to the origin. It takes the cut plane to a strip parallel to the ξ axis and of width 2π; if the cut is along $\arg z = \alpha$, then the strip is $\alpha - 2\pi < \eta < \alpha$, $-\infty < \xi < \infty$. Since

$$\zeta = \xi + \mathrm{i}\eta = \log z = \log|z| + \mathrm{i}\arg z, \tag{1.60}$$

circles $|z| =$ constant map to lines $\xi =$ constant, and rays $\arg z =$ constant map to lines $\eta =$ constant.

The effects of the exponential and logarithmic maps are illustrated in Figure 1.26. The exponential map is useful to open out a strip or half strip, and the log does the reverse. Note that neither exp nor log has a vanishing derivative.

Example. Map the half-strip $-\pi/2 < y < \pi/2$, $0 < x < \infty$ onto the interior of a semicircle, with the point at infinity mapping to the origin and the short side of the strip to the semicircle.

Solution. If we try to use the exponential function directly, we shall send the point at infinity to infinity. Instead, put $\zeta = \mathrm{e}^{-z}$; the result is illustrated in Figure 1.27.

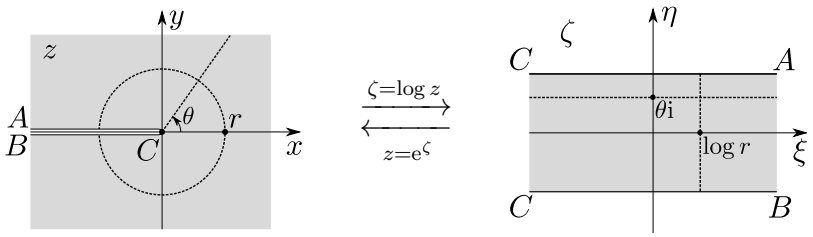

Figure 1.26: The effects of the exponential and logarithmic maps.

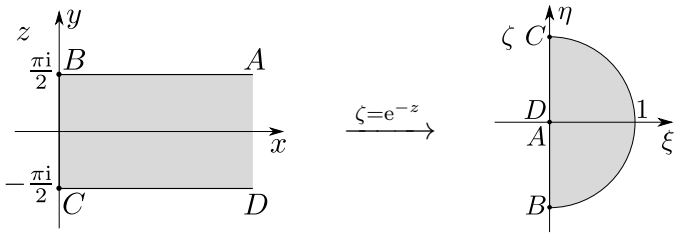

Figure 1.27: Mapping a half-strip to a semi-circle.

Example. The domain D consists of the upper half-plane with the upper half of the closed unit disc removed, as shown in the left-hand diagram in Figure 1.20. Map it to a half-strip.

Solution. We'll use the logarithmic map $\zeta = \log z$. The boundary of D consists of segments of rays and a segment of a circle centred at the origin. The rays map to horizontal lines and the semicircle to a segment of the imaginary axis. The image of D under $\zeta = \log z$ is thus the half-strip $0 < \xi < \infty$, $0 < \eta < \pi$, as shown in Figure 1.28.

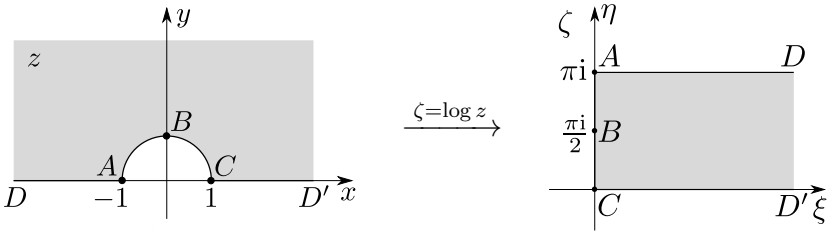

Figure 1.28: The logarithmic map transforms a half-plane with a semi-circle removed to a half-strip.

Trigonometric maps

Like the exponential, the sine and cosine functions are periodic and have essential singularities. Unlike the exponential, they have derivatives that vanish. Hence these functions can combine the properties of opening out (doubling) angles on the boundary of D with the useful strip-mapping properties of the exponential. Their inverses have similar uses to the logarithm.

Example. Investigate the effect of the mapping $\zeta = \cos z$ on the half-strip $0 < y < \infty$, $0 < x < \pi$. Calculate the image of the lines $y =$ constant.

Solution. The critical points where the derivative vamishes are at $z = 0, \pi$. Hence the internal angles of ∂D are doubled there. Note that

$$\cos z = \cos x \cosh y - \mathrm{i} \sin x \sinh y. \tag{1.61}$$

When z is real, $\cos z$ runs from 1 at $z = 0$ to -1 at $z = \pi$. Thus the line segment $z \in (0, 1)$ maps to the interval $-1 < \xi < 1$ of the ξ axis, and the image of D is below this line. The line $x = 0$, $y > 0$ maps to $\zeta = \cos \mathrm{i}y = \cosh y$, which traces the ξ axis from 1 to $+\infty$ The line $x = \pi$, $y > 0$ maps to the segment $-\infty < \xi = -\cosh y < -1$ of the ξ axis. Thus $\zeta = \cos z$ maps the half-strip to the lower half-plane, with the two critical points mapping to $\zeta = \pm 1$.

A line $y =$ constant, maps to the curve given parametrically by

$$\xi = \cos x \cosh y, \qquad \eta = -\sin x \sinh y, \qquad x \in (0, \pi), \tag{1.62}$$

namely the lower half of the ellipse

$$\frac{\xi^2}{\cosh^2 y} + \frac{\eta^2}{\sinh^2 y} = 1. \tag{1.63}$$

Similarly, the lines $x =$ constant map to the hyperbolae

$$\frac{\xi^2}{\cos^2 x} - \frac{\eta^2}{\sin^2 x} = 1, \tag{1.64}$$

which are orthogonal to the ellipses (1.63), as shown in Figure 1.29.

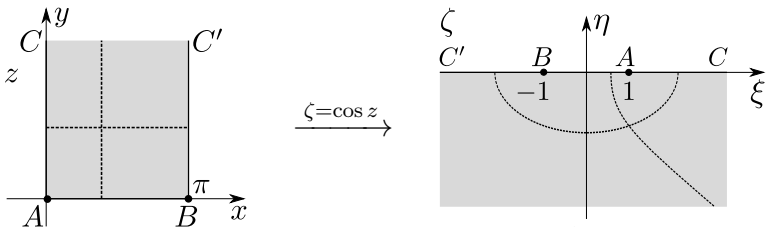

Figure 1.29: The map $\zeta = \cos z$ maps lines $x =$ constant and $y =$ constant are to orthogonal families of hyperbolae and ellipses.

Example: the tangent function. Show that the mapping $\zeta = \tan z$ maps the strip $-\pi/4 < x < \pi/4$, $-\infty < y < \infty$ to the unit disc.

Solution. It would be a mistake to think of $\tan z$ as the ratio $\sin z / \cos z$: the product of two conformal mappings has no natural geometric meaning. However, by writing

$$\tan z = \frac{\sin z}{\cos z} = -\mathrm{i} \frac{\mathrm{e}^{2\mathrm{i}z} - 1}{\mathrm{e}^{2\mathrm{i}z} + 1}, \tag{1.65}$$

we can view the tangent map as a composition between exponential and Möbius transformations, via the sequence

$$\zeta_1 = \mathrm{e}^{2\mathrm{i}z}, \qquad \zeta = -\mathrm{i} \, \frac{\zeta_1 - 1}{\zeta_1 + 1}, \tag{1.66}$$

as illustrated in Figure 1.30.

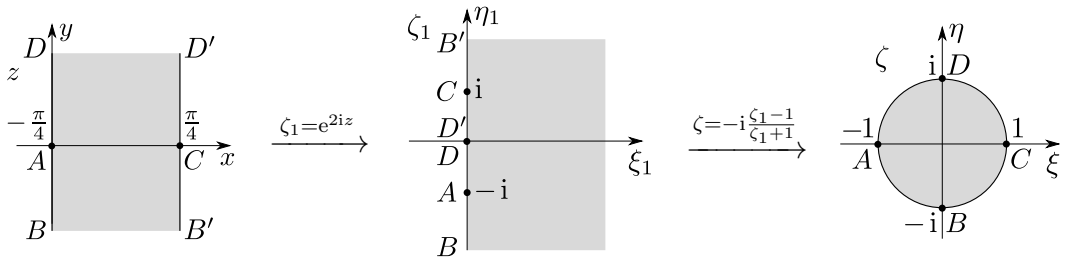

Figure 1.30: The tangent mapping viewed as the composition of an exponential with a Möbius transformation.

The Joukowski map

Our final example is the map called the *Joukowski map*,

$$\zeta = \frac{1}{2}\left(z + \frac{1}{z}\right). \tag{1.67}$$

The Joukowski map has derivative equal to zero at two critical points $z = \pm 1$. The image of the unit circle $|z| = 1$ is the slit $-1 < \xi < 1$ of the real axis, as when $z = \mathrm{e}^{\mathrm{i}\theta}$, $\zeta = \cos\theta$. The exterior of the unit circle is mapped to the whole plane exterior to this slit (which is a branch cut for the inverse mapping). Similarly the interior of the unit circle is mapped to the whole plane exterior to the same slit. A circle $|z| = \rho > 1$ is mapped to an ellipse, and a ray $\arg z =$ constant to a member of the orthogonal family of hyperbolae, as shown in Figure 1.31.

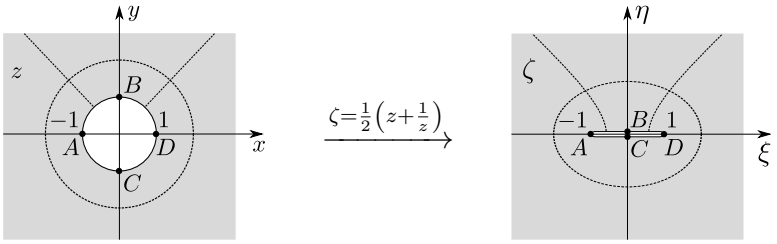

Figure 1.31: The effects of the Joukowski mapping on the region outside the unit circle.

2 Further conformal mapping

2.1 Introduction

Here we extend the ideas on conformal mapping introduced in the previous section. The Riemann Mapping Theorem guarantees that any simply connected domain D can be mapped onto the unit disc (for example). However, there is no general method to construct the required map for any given domain. One exception occurs if D is a polygon. The *Schwarz–Christoffel formula* in principle gives the conformal map from the upper half-plane to any given polygonal region. We will also show how conformal mapping can be used in practice in the solution of Laplace's equation.

2.2 Schwarz–Christoffel mapping

A (rare) constructive method for finding conformal maps (as opposed to cataloguing them) is the Schwarz–Christoffel formula. This lets us map a half-plane to a polygon (and there is an extension to circular polygons), and hence the inverse maps a polygon to a half-plane.

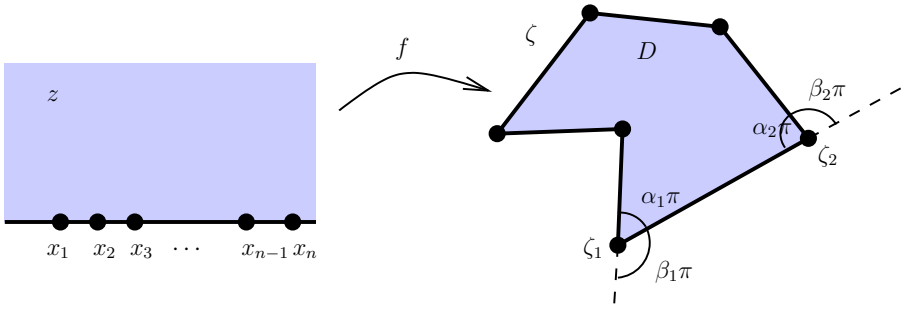

Figure 2.1: We seek a conformal map $z \mapsto \zeta = f(z)$ from the upper half-plane to a polygon with interior angles $\alpha_n\pi$ and corresponding exterior angles $\beta_n\pi$.

Our target domain is a polygon D with interior angles $\alpha_1\pi$,$\alpha_2\pi$, … , $\alpha_n\pi$, at the vertices $\zeta = \zeta_1, \zeta_2, \ldots, \zeta_n$, as shown in Figure 2.1. These vertices are ordered so that increasing n means travelling round the polygon in the anticlockwise sense. We define

$$\beta_j\pi = \pi - \alpha_j\pi, \tag{2.1}$$

so that $\beta_j\pi$ is the exterior angle. Generally, $\beta_j > 0$ at a corner where we turn *left* and $\beta_j < 0$ at a corner where we turn *right*. Then the conditions

$$\sum_{j=1}^{n} \beta_j = 2, \qquad -2 \le \beta_j \le 2 \tag{2.2}$$

are necessary for the polygon to close. Now our aim is to find a mapping $\zeta = f(z)$ which maps the upper half-plane $y > 0$ onto D with the real axis mapping to ∂D and x_1, x_2, … , x_n mapping to the vertices ζ_1, ζ_2, … , ζ_n.

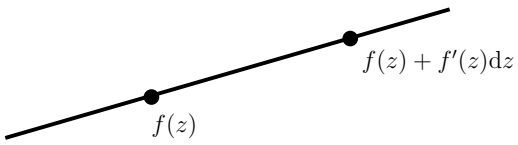

Figure 2.2: The direction of the tangent to ∂D is given by $\arg f'(z)$.

As shown schematically in Figure 2.2, the tangent to ∂D has direction angle $\arg f'(z)$, since $\mathrm{d}z = \mathrm{d}x$ is real on ∂D. This angle is supposed to be constant on each edge of the polygon ∂D. At x_j, the preimage of vertex j, the tangent angle increases by $\beta_j \pi$ and therefore we must have

$$\left[\arg f'(x)\right]_{x_j^-}^{x_j^+} = \beta_j \pi. \tag{2.3}$$

First consider the case of a single vertex, with pre-image at $z = x_j$. A function $f_j(z)$ such that

$$f_j'(z) = (z - x_j)^{-\beta_j} \tag{2.4}$$

(with a suitable branch defined) has the properties that

$$\arg f_j'(x) = \begin{cases} 0 & x > x_j, \\ -\beta_j \pi & x < x_j, \end{cases} \tag{2.5}$$

and therefore satisfies the jump condition (2.3). In addition, $f_j'(z) \neq 0$ for $z \neq x_j$, and therefore the resulting map is conformal away from the vertex.

When there are several vertices, the jump condition (2.3) is satisfied at each vertex by a *product* of functions of the form (2.4). If we try

$$f'(z) = C \prod_{j=1}^{n} f_j'(z), \tag{2.6}$$

where C is some constant, then

$$\arg f'(z) = \arg C + \sum_j \arg f_j'(z) \tag{2.7}$$

has exactly the right properties. Therefore a map from the upper-half plane to D is $\zeta = f(z)$, where

$$\frac{\mathrm{d}f}{\mathrm{d}z} = C \prod_{j=1}^{n} (z - x_j)^{-\beta_j}. \tag{2.8}$$

Hence

$$\zeta = f(z) = A + C \int^z \prod_{j=1}^{n} (t - x_j)^{-\beta_j} \, \mathrm{d}t, \tag{2.9}$$

where A and C fix the location and rotation/scaling of the polygon.

Notes

1. It can be shown that (2.9) is a one-to-one map from $\operatorname{Im} z > 0$ to D.

2. We are allowed by the Riemann Mapping Theorem to fix the pre-images of 3 boundary points, i.e. 3 of the x_j. Any more have to be found as part of the solution (by solving $f(x_j) = \zeta_j$).

3. We can choose one of the x_j to be at infinity. If (without loss of generality) $x_n = \infty$, then
$$f(z) = A + C \int^z \prod_{j=1}^{n-1} (t - x_j)^{-\beta_j} \, \mathrm{d}t. \tag{2.10}$$

4. The definition of a polygon is elastic: it includes those with vertices at ∞ and those with interior angles of 2π. Some examples are shown in Figure 2.3.

5. Most tractable examples are degenerate (*e.g.* they have a vertex at ∞) and use symmetry to simplify the integration.

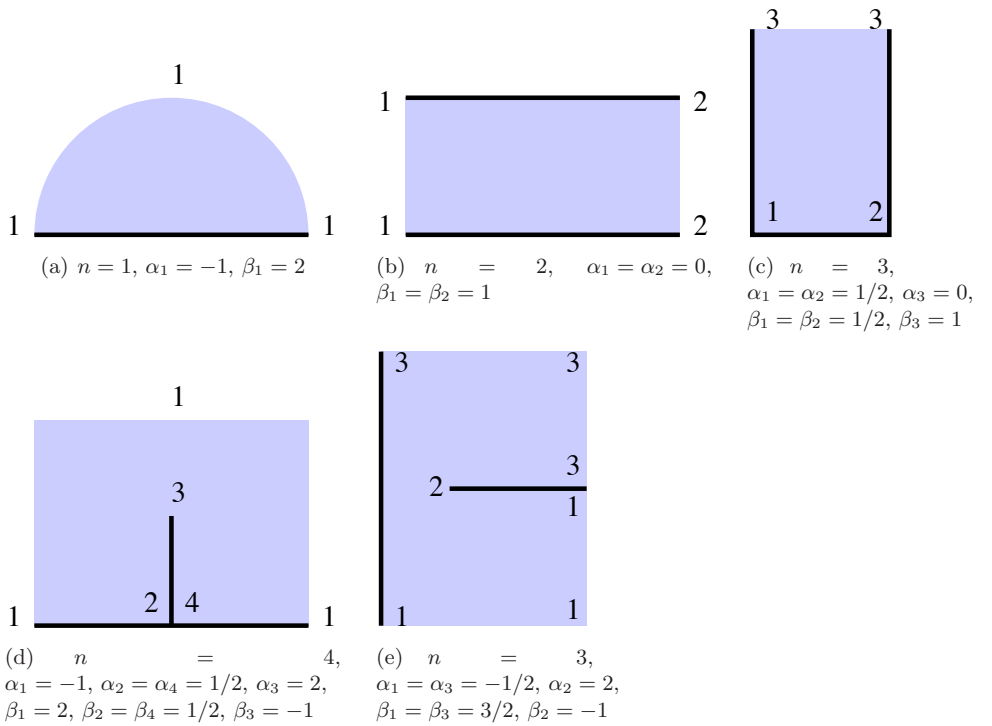

(a) $n = 1$, $\alpha_1 = -1$, $\beta_1 = 2$

(b) $n = 2$, $\alpha_1 = \alpha_2 = 0$, $\beta_1 = \beta_2 = 1$

(c) $n = 3$, $\alpha_1 = \alpha_2 = 1/2$, $\alpha_3 = 0$, $\beta_1 = \beta_2 = 1/2$, $\beta_3 = 1$

(d) $n = 4$, $\alpha_1 = -1$, $\alpha_2 = \alpha_4 = 1/2$, $\alpha_3 = 2$, $\beta_1 = 2$, $\beta_2 = \beta_4 = 1/2$, $\beta_3 = -1$

(e) $n = 3$, $\alpha_1 = \alpha_3 = -1/2$, $\alpha_2 = 2$, $\beta_1 = \beta_3 = 3/2$, $\beta_2 = -1$

Figure 2.3: Examples of polygonal regions and the corresponding values of the normalised interior angles α_j and exterior angles β_j. Note that in each case the exterior angles β_j sum to 2.

Example. Map a half-plane to a strip with the vertices corresponding to $z = 0$ and $z = \infty$.

Solution. Here ζ_1 and ζ_2 are both at ∞, with $\beta_1 = \beta_2 = 1$. We choose $x_1 = 0$ and $x_2 = \infty$ and thus the Schwarz–Christoffel formula (2.10) gives

$$\zeta = A + C \int^z \frac{\mathrm{d}t}{t} = A + C \log z. \tag{2.11}$$

If instead we wanted to map general points $z = x_1$ and $z = x_2$ on the real axis to the ends of the strip we would have

$$\zeta = A + C \int^z \frac{\mathrm{d}t}{(t - x_1)(t - x_2)} = A + \tilde{C} \log \left(\frac{z - x_1}{z - x_2} \right). \tag{2.12}$$

The values of A and C set the location, orientation, and width of the strip.

Example. Map a half-plane to a half-strip.

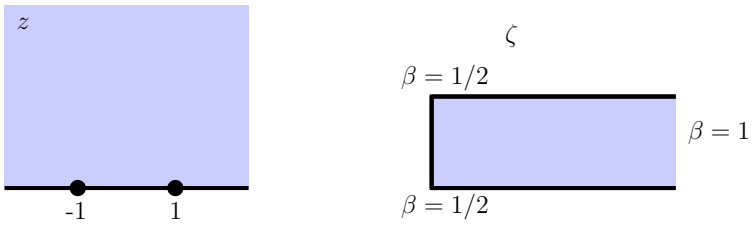

Solution. Here $n = 3$, $\beta_1 = \beta_2 = 1/2$, $\beta_3 = 1$. It is convenient to take $x_1 = -1$, $x_2 = 1$, $x_3 = \infty$, to give

$$\zeta = A + C \int^z \frac{\mathrm{d}t}{\sqrt{t^2 - 1}} = A + C \cosh^{-1} z. \tag{2.13}$$

Example. Map the upper half-plane to the slit domain shown.

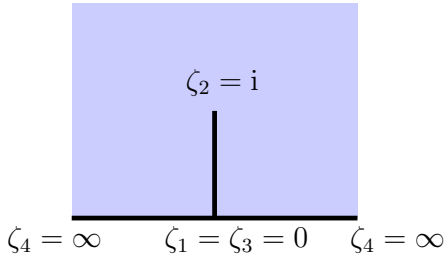

Solution. Here we have *four* vertices, with $\beta_1 = 1/2$, $\beta_2 = -1$, $\beta_3 = 1/2$, $\beta_4 = 2$. In general we can only choose three locations for the x_j, but here symmetry allows us to take $x_1 = -1$, $x_2 = 0$, $x_3 = 1$, $x_4 = \infty$. Thus

$$\zeta = A + C\int^z \frac{t}{\sqrt{t^2-1}}\,\mathrm{d}t = A + C\sqrt{z^2-1}. \tag{2.14}$$

To fix the values of the constants A and C, we must ensure that the vertices end up in the right places:

$$\zeta_1 = \zeta_3 = 0 \quad \Rightarrow \quad \zeta = 0 \text{ when } z = \pm 1 \quad \Rightarrow \quad A = 0, \tag{2.15a}$$

$$\zeta_2 = \mathrm{i} \quad \Rightarrow \quad \zeta = \mathrm{i} \text{ when } z = 0 \quad \Rightarrow \quad C = 1. \tag{2.15b}$$

Thus the required map is

$$\zeta = \sqrt{z^2-1}. \tag{2.16}$$

Although this example has 4 vertices, symmetry gives an exact solution.

2.3 Solving Laplace's equation by conformal maps

Models leading to Laplace's equation

Laplace's equation crops up in a wide variety of practically motivated models. Here are three examples.

Example 1: Steady heat flow

Fourier's law of heat conduction states that the heat flux in a homogeneous isotropic medium D of constant thermal conductivity k is

$$\boldsymbol{q} = -k\boldsymbol{\nabla} u, \tag{2.17}$$

where u is the temperature. When the temperature is time-independent, conservation of energy imples that $\boldsymbol{\nabla}\cdot\boldsymbol{q} = 0$, and hence u satisfies Laplace's equation:

$$\nabla^2 u = 0 \qquad \text{in } D. \tag{2.18}$$

At a boundary typically either the temperature u or the heat flux $\boldsymbol{q}\cdot\boldsymbol{n}$ is known. The former case leads to a *Dirichlet* boundary condition, where u is specified on the boundary. The latter case corresponds to the *Neumann* boundary condition, where $\partial u/\partial n$ is specified on the boundary. In particular, $\partial u/\partial n = 0$ at an insulated boundary.

Example 2: Electrostatics

In a steady state, the electric field $\boldsymbol{E}$ satisfies $\boldsymbol{\nabla}\times\boldsymbol{E} = \boldsymbol{0}$, and may therefore be written in terms of an *electric potential* ϕ such that

$$\boldsymbol{E} = -\boldsymbol{\nabla}\phi. \tag{2.19}$$

Moreover, in the absence of any space charge, Gauss's Law implies that $\boldsymbol{\nabla} \cdot \boldsymbol{E} = 0$, and therefore ϕ satisfies Laplace's equation

$$\nabla^2 \phi = 0. \tag{2.20}$$

The potential ϕ is the usual voltage we talk about in the context of batteries, mains electricity, lightning etc.

A common and useful boundary condition for ϕ is that it is constant on a good conductor like a metal. Thus a canonical problem is to determine the potential between two perfect conductors each of which is held at a given constant potential (for example in a *capacitor*).

Example 3: Inviscid fluid flow

The simplest model for a fluid is that it is *inviscid*, *incompressible* and *irrotational*. Fortunately this is a remarkably accurate model in many circumstances. In an incompressible fluid, the velocity field $\boldsymbol{u}$ satisfies $\boldsymbol{\nabla} \cdot \boldsymbol{u} = 0$, while an irrotational flow satisfies $\boldsymbol{\nabla} \times \boldsymbol{u} = \boldsymbol{0}$. In two dimensions, with $\boldsymbol{u} = \big(u(x,y), v(x,y)\big)$, the velocity components u and v satisfy the equations

$$\frac{\partial u}{\partial x} + \frac{\partial v}{\partial y} = 0, \qquad\qquad \frac{\partial u}{\partial y} - \frac{\partial v}{\partial x} = 0, \tag{2.21}$$

in an incompressible, irrotational flow. Finally, the pressure p may be found using *Bernoulli's Theorem*, which states that

$$p + \frac{1}{2}\rho |\boldsymbol{u}|^2 = \text{constant} \tag{2.22}$$

in a steady incompressible, irrotational flow, where ρ is the density of the fluid.

From equation (2.21a), we deduce the existence of a potential function $\psi(x,y)$, called the *streamfunction*, such that

$$u = \frac{\partial \psi}{\partial y}, \qquad\qquad v = -\frac{\partial \psi}{\partial x}. \tag{2.23}$$

Similarly, equation (2.21b) implies the existence of a *velocity potential* $\phi(x,y)$, such that

$$u = \frac{\partial \phi}{\partial x}, \qquad\qquad v = \frac{\partial \phi}{\partial y}. \tag{2.24}$$

Thus $\boldsymbol{\nabla}\phi$ is everywhere tangent to the flow, while $\boldsymbol{\nabla}\psi$ is everyhere normal to the velocity. It follows that the contours of ψ are *streamlines* for the flow, i.e. curves everywhere parallel to the velocity. Moreover, the change in the value of ψ on two neighbouring streamlines is equal to the flux of fluid between them. To see this, calculate the net flow across a curve C connecting two streamlines, as shown in Figure 2.4:

$$\begin{aligned} \text{flux} &= \int_C \boldsymbol{u} \cdot \boldsymbol{n} \, \mathrm{d}s \\ &= \int_c \left(\frac{\partial \psi}{\partial y}, -\frac{\partial \psi}{\partial x} \right) \cdot (\mathrm{d}y, -\mathrm{d}x) \\ &= \int_c \left(\frac{\partial \psi}{\partial x} \, \mathrm{d}x + \frac{\partial \psi}{\partial y} \, \mathrm{d}y \right) \\ &= [\psi]_C = \psi_2 - \psi_1, \end{aligned} \tag{2.25}$$

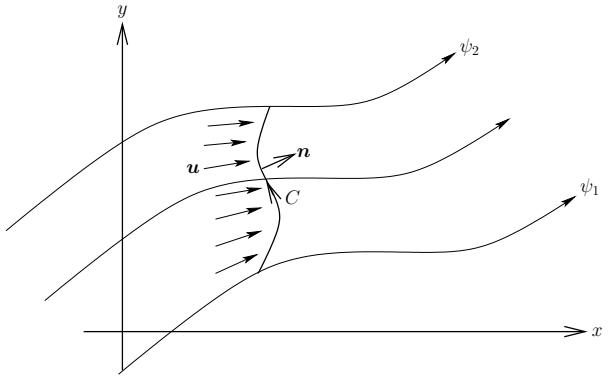

Figure 2.4: Schematic of a curve C joining two streamlines on which $\psi = \psi_1$ and $\psi = \psi_2$.

where ψ_1 and ψ_2 are the constant values of ψ on the two streamlines.

Elimination between (2.23) and (2.24) shows that both ϕ and ψ satisfy Laplace's equation. Alternatively, by combining (2.23) and (2.24), we see that ϕ and ψ satisfy the *Cauchy–Riemann equations*

$$\frac{\partial \phi}{\partial x} = \frac{\partial \psi}{\partial y}, \qquad \frac{\partial \phi}{\partial y} = -\frac{\partial \psi}{\partial x}. \tag{2.26}$$

Therefore $\phi + \mathrm{i}\psi$ is a holomorphic function of $z = x + \mathrm{i}y$:

$$\phi + \mathrm{i}\psi = w(z), \tag{2.27}$$

where w is called the *complex potential*. The velocity components can be recovered from w using

$$\frac{\mathrm{d}w}{\mathrm{d}z} = u - \mathrm{i}v. \tag{2.28}$$

At a fixed impenetrable boundary, the normal component of $\boldsymbol{u}$ must be zero. In terms of the velocity potential and streamfunction, this is equivalent to

$$\frac{\partial \phi}{\partial n} = 0, \qquad \psi = \text{constant}, \tag{2.29}$$

and therefore, in terms of the complex potential,

$$\operatorname{Im} w(z) = \text{constant} \qquad \text{at a fixed impenetrable boundary.} \tag{2.30}$$

Solution by conformal mapping

In all the above examples, we end up having to find a harmonic function u (or ϕ or ψ) in some region D subject to given boundary conditions on ∂D. The general idea is to write u as the real or imaginary part of a holomorphic function $w(z) = u(x, y) + \mathrm{i}v(x, y)$ and then map D onto a simpler domain $f(D)$ by a conformal map

$$\zeta = f(z), \tag{2.31}$$

in the hope that we can more easily find the corresponding function in the ζ-plane, i.e.

$$W(\zeta) = U(\xi, \eta) + \mathrm{i}V(\xi, \eta). \tag{2.32}$$

Because a composition of holomorphic functions is holomorphic, $W(\zeta)$ is holomorphic, and its real and imaginary parts satisfy Laplace's equation in $f(D)$. We then recover the solution in the original domain D by reversing the conformal mapping:

$$w(z) = W\big(f(z)\big). \tag{2.33}$$

Example. Find the temperature u in a domain D exterior to the circles $|z-\mathrm{i}| = 1$, $|z+\mathrm{i}| = 1$ with $u = \pm 1$ on $|z \mp \mathrm{i}| = 1$ and $u \to 0$ at ∞, as depicted in Figure 2.5.

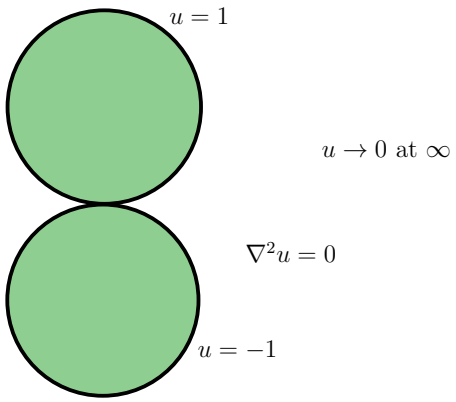

Figure 2.5: Steady heat flow in the region outside two touching circles.

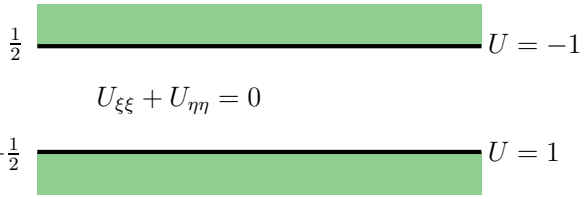

Figure 2.6: The image of the problem from Figure 2.5 under the mapping $\zeta = 1/z$.

Solution. The map $\zeta = 1/z$ takes D onto the strip $-1/2 < \operatorname{Im}\zeta < 1/2$, so the corresponding problem in the ζ-plane is as shown in Figure 2.6. By inspection, the solution is

$$U = -2\eta = 2\operatorname{Re}(\mathrm{i}\zeta), \tag{2.34}$$

and hence

$$u = 2\operatorname{Re}(\mathrm{i}/z) = \frac{2y}{x^2 + y^2}. \tag{2.35}$$

Note that u is bounded in all of D, since $|y| \lesssim x^2/2$ as $(x, y) \to (0, 0)$.

Example. Calculate the complex potential for flow past the unit circle with uniform velocity $(U_\infty, 0)$ at ∞.

Solution. The complex potential is $w = \phi + \mathrm{i}\psi$ and we can take $\psi = 0$ on the x-axis and unit circle. Also $w \sim U_\infty z$ at ∞. Under the Jowkowski map

$$\zeta = \frac{1}{2}\left(z + \frac{1}{z}\right) \tag{2.36}$$

the exterior of the unit circle maps to the ζ-plane cut from -1 to 1, as shown in Figure 2.7.

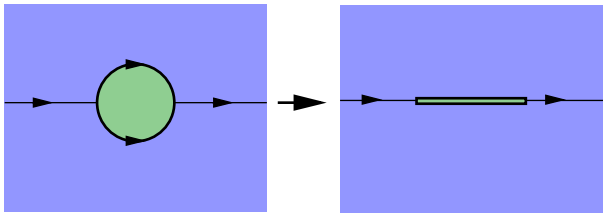

Figure 2.7: Uniform flow past a circle transformed by the Joukowski map.

In the ζ-plane we need a function $W(\zeta)$ which is real on the ξ axis and at ∞ looks like $U_\infty z \sim 2U_\infty \zeta$. The solution is just

$$W(\zeta) = 2U_\infty \zeta \qquad \Rightarrow \qquad w(z) = U_\infty\left(z + \frac{1}{z}\right). \tag{2.37}$$

Example. Find the complex potential for flow over a step of height 1, from $y = 1$, $x < 0$ to $y = 0$, $x > 0$, with velocity $(U_\infty, 0)$ at ∞.

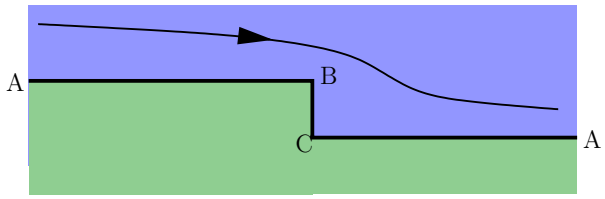

Figure 2.8: Flow over a step.

Solution. The flow is depicted in Figure 2.8. We map the half-plane $\operatorname{Im} Z > 0$ onto D by Schwarz–Christoffel (using Z not ζ because the roles are reversed). The exterior angles at the marked vertices are given by

$$\beta_A = 2, \qquad \beta_B = -\frac{1}{2}, \qquad \beta_B = \frac{1}{2}. \tag{2.38}$$

Since there are just three vertices, we can choose to map

$$Z = -1 \text{ to } B, \qquad Z = +1 \text{ to } C, \qquad Z = \infty \text{ to } A. \tag{2.39}$$

Then the Schwarz–Christoffel formula (2.10) gives

$$z = A + C\int^Z \left(\frac{t+1}{t-1}\right)^{1/2} \mathrm{d}t = A + C\left((Z^2-1)^{1/2} + \cosh^{-1} Z\right). \tag{2.40}$$

From the conditions (2.39) we find $A = 0$ and $C = 1/\pi$, so the required mapping function is given by

$$z = \frac{1}{\pi}\left((Z^2-1)^{1/2} + \cosh^{-1} Z\right). \tag{2.41}$$

At infinity $z \sim Z/\pi$, so the specified uniform flow at infinity implies that

$$w(z) \sim U_\infty z \text{ at } \infty \qquad \Rightarrow \qquad W(Z) = w(z(Z)) \sim \frac{U_\infty Z}{\pi} \text{ at } \infty. \tag{2.42}$$

Thus the flow in the Z plane is given by

$$W(Z) = \frac{U_\infty Z}{\pi}, \tag{2.43}$$

so that $w(z)$ is given implicitly by

$$z = \frac{1}{\pi}\left(\left(\frac{\pi^2 w^2}{U_\infty^2} - 1\right)^{1/2} + \cosh^{-1}\frac{\pi w}{U_\infty}\right). \tag{2.44}$$

Note that the velocity components may be found using

$$\begin{aligned} u - \mathrm{i}v &= \frac{\mathrm{d}w}{\mathrm{d}z} \\ &= \frac{\mathrm{d}W/\mathrm{d}Z}{\mathrm{d}z/\mathrm{d}Z} \\ &= U_\infty\left(\frac{Z-1}{Z+1}\right)^{1/2}. \end{aligned} \tag{2.45}$$

Therefore the velocity is zero at C ($Z = 1$) and infinite at B ($Z = -1$). In general, at a corner with interior angle γ, the complex potential locally is of the form $w \sim \text{constant} \times z^{\pi/\gamma}$ and therefore $u - \mathrm{i}v \sim \text{constant} \times z^{\pi/\gamma - 1}$, which implies that:

$$\begin{aligned} &\textit{The velocity is } \text{zero } \textit{at a corner with interior angle} < \pi \\ &\qquad\qquad \textit{and } \text{infinite } \textit{at a corner with interior angle} > \pi. \end{aligned} \tag{2.46}$$

Example. A lightning conductor is modelled by the boundary-value problem illustrated in Figure 2.9. The potential u is equal to zero at $x = 0$ and satisfies Laplace's equation in the half-space $x > 0$, except on the line $y = 0$, $x > 1$, where $u = 1$. We also require u to be bounded at infinity.

Solution. The domain D is the image of the strip $0 < X < \pi/2$, $-\infty < Y < \infty$ under the map $z = \sin Z$. In the Z-plane we have $\nabla^2 U = 0$ with $U = 0$ at $X = 0$ and $U = 1$ at $X = \pi/2$, as shown in Figure 2.10. The solution in the Z-plane is $U = \mathrm{Re}\, W = \mathrm{Re}(2Z/\pi)$, and therefore

$$u = \frac{2}{\pi}\,\mathrm{Re}\left(\sin^{-1} z\right). \tag{2.47}$$

Note that

$$\frac{\mathrm{d}}{\mathrm{d}z}\left(\frac{2}{\pi}\sin^{-1} z\right) = \frac{2}{\pi}\,\frac{1}{\sqrt{1-z^2}}, \tag{2.48}$$

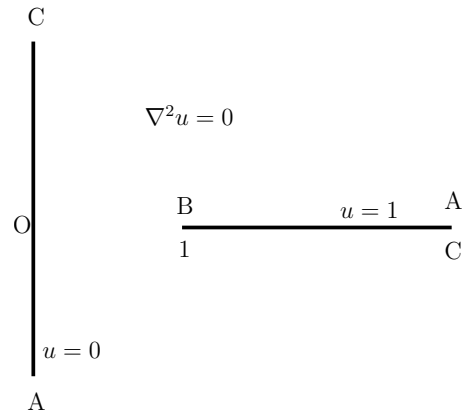

Figure 2.9: A model for a lightning conductor.

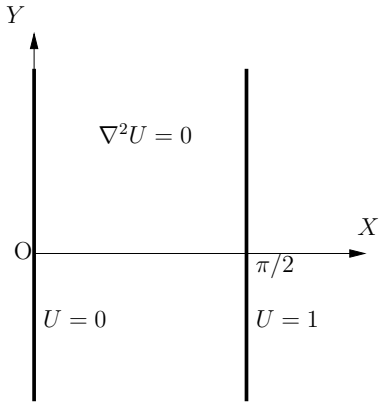

Figure 2.10: The problem from Figure 2.9 transformed by the map $Z = \sin^{-1} z$.

and it follows that $|\boldsymbol{\nabla} u| \to \infty$ as $z \to 1$, i.e. at the tip of the spike.

This example could also have been solved by using a Schwarz–Christoffel mapping to map the upper half Z-plane to D. The vertices marked A, B, C in Figure 2.9 have the exterior angles

$$\beta_A = \frac{3}{2}, \qquad \beta_B = -1, \qquad \beta_C = \frac{3}{2}. \tag{2.49}$$

We can choose to map

$$Z = -1 \text{ to } A, \qquad Z = 0 \text{ to } B, \qquad Z = 1 \text{ to } C, \tag{2.50}$$

and, because of symmetry, we are also free to map $Z = \infty$ to $z = 0$. Then the Schwarz–Christoffel formula gives

$$z = \frac{1}{\sqrt{1 - Z^2}}. \tag{2.51}$$

The problem in the Z plane is shown in Figure 2.11. The solution bounded at $Z = \pm 1$ is simply

$$U = \frac{1}{\pi}\big(\arg(Z+1) - \arg(Z-1)\big) = \operatorname{Im}\left[\frac{1}{\pi}\log\left(\frac{Z-1}{Z+1}\right)\right], \tag{2.52}$$

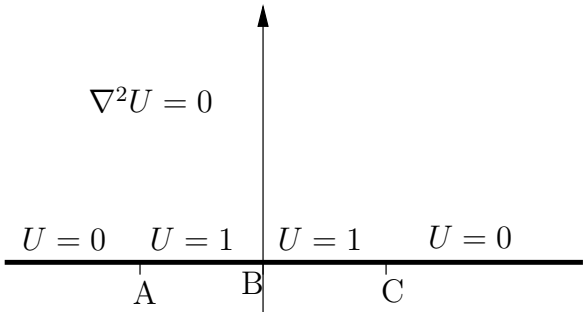

Figure 2.11: The problem from Figure 2.9 transformed by the map $z = 1/\sqrt{1 - Z^2}$.

and by inverting the conformal map we find

$$u = \frac{1}{\pi} \operatorname{Im} \left[\log \left(\frac{\sqrt{z^2 - 1} - z}{\sqrt{z^2 - 1} + z} \right) \right], \tag{2.53}$$

which is equivalent to (2.47).

3 Free surface flows

3.1 Introduction

We now move on to discuss potential flow with free surfaces. With only fixed (and known) boundaries we can find the potential whenever we can find the relevant conformal map. However, if there are *free* surfaces, these are unknown and we have to find them as part of the solution. We will discuss two scenarios where complex analysis and conformal mapping allows us to find analytic solutions.

3.2 Steady inviscid free surface flow

We now show how conformal mapping allows us to obtain steady, inviscid, incompressible, irrotational flows bounded by a combination of rigid walls and free surfaces. We recall that such flows may be described by a complex potential

$$w(z) = \phi + \mathrm{i}\psi, \tag{3.1}$$

where ϕ and ψ are the velocity potential and streamfunction, and the velocity components are then given by

$$u - \mathrm{i}v = \frac{\mathrm{d}w}{\mathrm{d}z}. \tag{3.2}$$

Any given fixed walls must be streamlines for the flow, so that $\psi = \operatorname{Im} w = \text{constant}$ there, and the velocity must be tangential to any such boundaries.

Any steady free surface must likewise be a streamline for the flow (this is the *kinematic* boundary condition). However, this is not enough information, because the location of the free surface is not known in advance. The additional condition to be imposed (the *dynamic* boundary condition) is that the external atmospheric pressure is assumed to be a known constant. (This condition must be generalised if surface tension is significant.) From Bernoulli's Theorem for a steady flow we have

$$p + \frac{1}{2}\rho|\boldsymbol{u}|^2 = p + \frac{1}{2}\rho\left|\frac{\mathrm{d}w}{\mathrm{d}z}\right|^2 = \text{constant} \tag{3.3}$$

and therefore, if p is constant, it follows that $|\mathrm{d}w/\mathrm{d}z|$ is constant, and this provides the additional information to locate the free surface.

The general solution technique will be demonstrated via an example.

Example: Teapot flow. A fluid layer of thickness h flows horizontally at speed U_∞ over a thin plate lying along the negative x-axis, before turning the corner at $x = 0$ and flowing back along the underside of the plate, as shown in Figure 3.1.

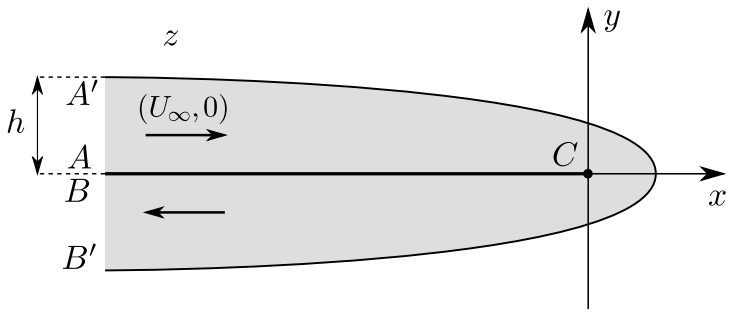

Figure 3.1: A model for flow round the spout of a teapot.

Solution. The plate ACB and the free surface $A'B'$ are both streamlines. The net flux is $U_\infty h$ so without loss of generality we set

$$\psi = 0 \text{ on } ACB, \qquad \psi = U_\infty h \text{ on } A'B'. \tag{3.4}$$

On the free surface we also have by Bernoulli's Theorem

$$|\boldsymbol{u}| = \text{constant} = U_\infty \text{ on } A'B'. \tag{3.5}$$

It is helpful to nondimensionalise by scaling z with h and w with $U_\infty h$. The resulting normalised problem is sketched in Figure 3.2, where we have also marked the "nose" N of the fluid.

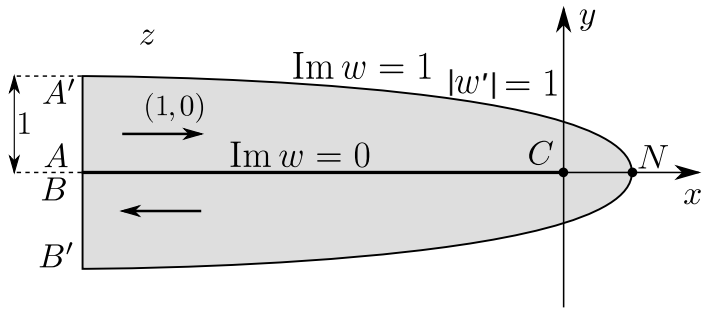

Figure 3.2: A normalised model for flow round the spout of a teapot.

Now we can view the complex potential as a conformal map $z \mapsto w(z)$ from the physical plane to the *potential plane*, and our first step is to examine what the image of the shaded fluid domain is in the w-plane. Recall that $w = \phi + \mathrm{i}\psi$. The fluid domain is bounded by curves on which $\psi = 0$ and $\psi = 1$, which are horizontal straight lines in the potential plane. At AA' we have $w \sim z$ and hence $\phi \sim x \to -\infty$. Similarly, at BB' we have $w \sim -z$ and hence $\phi \sim -x \to +\infty$. Finally, without loss of generality we can choose the origin for ϕ such that $w = 0$ at C. Then, since by symmetry $u = 0$ on CN, it follows that ϕ is constant on CN and therefore $\phi = 0$ at N. Therefore the fluid domain in the potential plane is as sketched in Figure 3.3, where $w = \mathrm{i}$ is the image of N.

Next we do the same for the *hodograph plane*, which is the image of the fluid domain under the mapping

$$z \mapsto w'(z) = \frac{\mathrm{d}w}{\mathrm{d}z} = u - \mathrm{i}v. \tag{3.6}$$

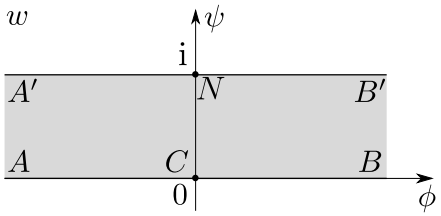

Figure 3.3: The potential plane for the teapot flow.

On the plate, the normal velocity must be zero, i.e. $v = 0$ on $y = 0$, so the streamline ACB is mapped to the u-axis. At C, the fluid turns through an angle $2\pi > \pi$, so the velocity will be infinite at the corner. Therefore u increases from 1 at A to $+\infty$ at C, then on the underside of the plate increases from $-\infty$ at C to -1 at B. Since $|w'| = 1$ on the free surface, the curve $A'B'$ is mapped to a portion of the unit circle in the hodograph plane. We infer from Figure 3.2 that $v < 0$ everywhere, with $v \to 0$ at A and A', while $v = -1$ and $u = 0$ at the nose N. Therefore the flow in the hodograph plane is as shown in Figure 3.4.

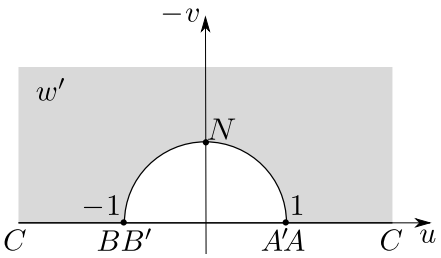

Figure 3.4: The hodograph plane for the teapot flow.

Now we map both the potential and the hodograph planes to *the same region* in an auxillary ζ plane. Note that

$$\zeta = \mathrm{e}^{\pi w} \tag{3.7}$$

maps the strip $0 < \operatorname{Im} w < 1$ to the upper half ζ-plane, while $A \mapsto 0$, $B \mapsto \infty$, $C \mapsto 1$ and $N \mapsto -1$, as shown in Figure 3.5.

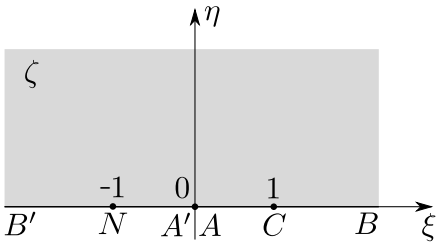

Figure 3.5: The potential plane for the teapot flow is mapped to the upper half-plane by the mapping $\zeta = \mathrm{e}^{\pi w}$.

Now, the mapping

$$\zeta = \left(\frac{w' - 1}{w' + 1)} \right)^2 \tag{3.8}$$

maps the hodograph plane onto the upper half ζ-plane, *and maps the points A, B, C, N to the same points on the real ζ-axis.* Once the locations of three points on the boundary have been fixed, the conformal map from any domain onto the upper half-plane is unique. Therefore, the complex potential and its derivative must satisfy the relation

$$e^{\pi w} = \zeta = \left(\frac{w'-1}{w'+1}\right)^2, \tag{3.9}$$

i.e. we get a differential equation for $w(z)$!

By rearranging (3.9) we get a separable differential equation

$$w' = \frac{1+e^{\pi w/2}}{1-e^{\pi w/2}} = -\coth\left(\frac{\pi w}{4}\right), \tag{3.10}$$

and integration leads to

$$\frac{4}{\pi}\log\cosh\left(\frac{\pi w}{4}\right) = -z, \tag{3.11}$$

where we have applied the boundary condition $w = 0$ when $z = 0$. Thus the complex potential $w(z)$ is given by

$$\cosh\left(\frac{\pi w}{4}\right) = \mathrm{e}^{-\pi z/4}, \tag{3.12}$$

or (by squaring both sides)

$$1 + \cosh\left(\frac{\pi w}{2}\right) = 2\mathrm{e}^{-\pi z/2}. \tag{3.13}$$

The free streamline is given by $\psi = 1$, i.e $w = \phi + \mathrm{i}$ with $\phi \in (-\infty, \infty)$, so that

$$2\mathrm{e}^{-\pi z/2} = 1 + \cosh\left(\frac{\pi\phi}{2} + \frac{\mathrm{i}\pi}{2}\right) = 1 + \mathrm{i}\sinh\left(\frac{\pi\phi}{2}\right). \tag{3.14}$$

By taking the real part of both sides, we deduce that the position of the free surface is given by the equation

$$\mathrm{e}^{-\pi x/2}\cos\left(\frac{\pi y}{2}\right) = \frac{1}{2}. \tag{3.15}$$

In particular, the film thickness at the nose $y = 0$ is given by $x = (2\log 2)/\pi \approx 0.441$: this is known as the *thinning factor*.

Example: Flow out of a slot. Fluid occupies the upper half-plane $y > 0$ above a wall at $y = 0$. There is a gap in the wall in the interval $x \in (-a, a)$, through which the fluid flows into $y < 0$ as a jet between two free surfaces. The free surfaces detach tangentially from the edges $x = \pm a$ of the slot (this *Kutta condition* ensures that the velocity is finite at these points). The jet thickness far downstream is $2Qa$, where the *contraction ratio* Q is to be found. The set-up is sketched in Figure 3.6.

If $p \to p_\infty$ and $\boldsymbol{u} \to \mathbf{0}$ as $y \to \infty$, then by Bernoulli's equation we have

$$p + \frac{1}{2}\rho|\mathbf{u}|^2 = p_\infty. \tag{3.16}$$

On the other hand, on the free surfaces BC and DC' we have $p = p_{\mathrm{atm}}$, the atmospheric pressure. Therefore on the free surface we have $|\boldsymbol{u}| = U_\infty$, where U_∞ is the speed of the uniform flow at CC' and is given by

$$\frac{1}{2}\rho U_\infty^2 = p_\infty - p_{\mathrm{atm}}. \tag{3.17}$$

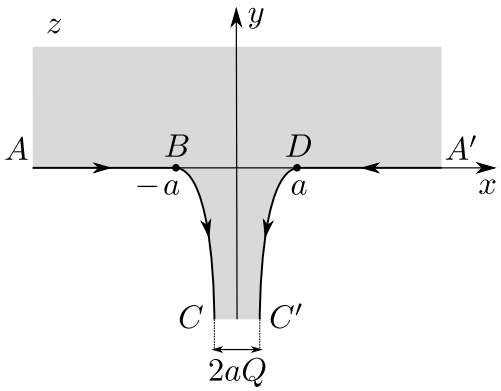

Figure 3.6: Flow out of a slot.

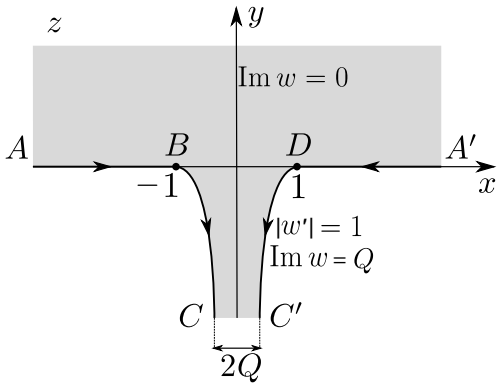

Figure 3.7: Normalised problem for flow out of a slot.

We nondimensionalise the problem by scaling z with a and w with $U_\infty a$; the resulting normalised problem is sketched in Figure 3.7. By symmetry, the y-axis is a streamline, which we choose to be $\psi = 0$. Then, given that the net flux in the jet is $2Q$, we have $\psi = Q$ on the streamline $A'DC'$ and $\psi = -Q$ on ABC. At infinity in the upper half-plane $\psi \sim Q - 2Q\theta/\pi$, where $\theta = \arg z$, which corresponds to

$$w(z) \sim -\frac{2Q}{\pi} \log z + Q \quad \text{as } z \to \infty \text{ with } \operatorname{Im} z > 0. \tag{3.18}$$

This is the complex potential due to a *point sink* of strength $4Q$, and implies that $\phi \to -\infty$ as $z \to \infty$ in the upper half-plane. At CC' we have $\phi \sim -U_\infty y$ and therefore $\phi \to \infty$ there. The potential plane is therefore as shown in Figure 3.8.

For the hodograph plane, note that the velocity tends to zero at infinity in the upper half-plane, so $w' \to 0$ at AA'. The free surfaces BC and DC' are mapped to arcs of the unit circle, with $\{u = 1, v = 0\}$ at B, $\{u = 0, v = -1\}$ at CC' and $\{u = -1, v = 0\}$ at D. The walls AB and $A'D$ are mapped to the straight lines $v = 0$, with $u \to 0$ at A and A', $u = 1$ at B and $u = -1$ at D. Therefore the hodograph plane is as shown in Figure 3.9.

The map

$$\zeta = -\left(\frac{1 - w'}{1 + w'}\right)^2 \tag{3.19}$$

takes the hodograph plane to the upper half-plane shown in Figure 3.10.

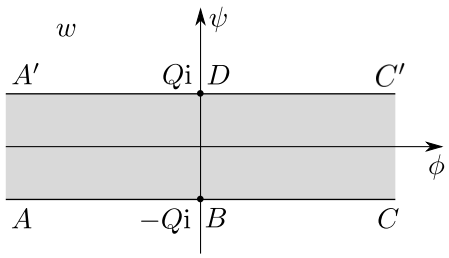

Figure 3.8: The potential plane for flow out of a slot.

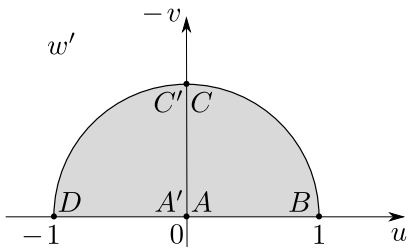

Figure 3.9: Hodograph plane for flow out of a slot.

The map

$$\zeta_1 = \mathrm{i}\,\mathrm{e}^{\pi w/2Q} \tag{3.20}$$

maps the potential plane to the upper half-plane shown in Figure 3.11, but the points along the real axis are in the wrong order! We can rearrange the points and thus map the ζ_1-plane onto the ζ-plane with the Möbius mapping

$$\zeta = \frac{\zeta_1 - 1}{\zeta_1 + 1} \tag{3.21}$$

to give

$$\left(\frac{1-w'}{1+w'}\right)^2 = \frac{1-\mathrm{i}\,\mathrm{e}^{\pi w/2Q}}{1+\mathrm{i}\,\mathrm{e}^{\pi w/2Q}}. \tag{3.22}$$

This is possible, but complicated, to solve.

If we just want the free surface shape there is a short cut to a parametric form. On the free surface we know that $|w'| = 1$ and therefore we can write

$$w' = \mathrm{e}^{-\mathrm{i}\theta}, \tag{3.23}$$

where θ is the angle the surface makes with the x-axis; $-\theta$ is the polar angle in the $(u, -v)$ hodograph plane. On BC we have $-\pi/2 < \theta < 0$, while on $C'D$ we have $-\pi < \theta < -\pi/2$, as can be seen in Figure 3.9.

Substituting (3.23) into (3.22), we find

$$\frac{1-\mathrm{i}\,\mathrm{e}^{\pi w/2Q}}{1+\mathrm{i}\,\mathrm{e}^{\pi w/2Q}} = \left(\frac{1-\mathrm{e}^{-\mathrm{i}\theta}}{1+\mathrm{e}^{-\mathrm{i}\theta}}\right)^2 = -\tan^2(\theta/2)\,, \tag{3.24}$$

which we invert to get

$$\mathrm{i}\,\mathrm{e}^{\pi w/2Q} = \frac{1+\tan^2(\theta/2)}{1-\tan^2(\theta/2)} = \sec\theta. \tag{3.25}$$

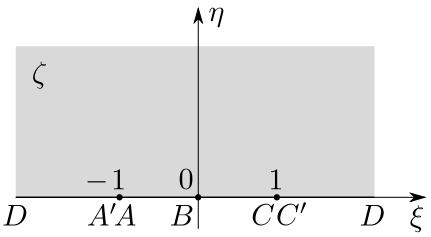

Figure 3.10: The hodograph plane for flow out of a slot is mapped to this upper half-plane by the mapping (3.19).

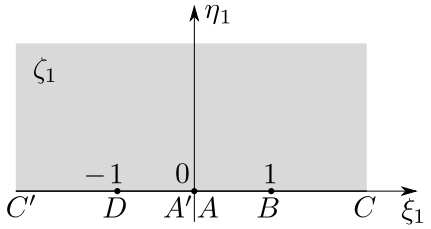

Figure 3.11: The potential plane for flow out of a slot is mapped to this upper half-plane by the mapping $\zeta_1 = \mathrm{i}\,\mathrm{e}^{\pi w/2Q}$.

Now differentiate both sides with respect to θ,

$$\frac{\mathrm{i}\pi}{2Q}\,\mathrm{e}^{\pi w/2Q}\,\frac{\mathrm{d}w}{\mathrm{d}z}\,\frac{\mathrm{d}z}{\mathrm{d}\theta} = \sec\theta\tan\theta, \tag{3.26}$$

and substitute w' and $\mathrm{e}^{\pi w/2Q}$ from (3.23) and (3.25) to find that

$$\frac{\mathrm{d}z}{\mathrm{d}\theta} = \frac{2Q}{\pi}\,\mathrm{e}^{\mathrm{i}\theta}\tan\theta. \tag{3.27}$$

Integration of this ODE gives a parametric equation $z(\theta)$ for the position of the free surface.

Taking real and imaginary parts, we get

$$\frac{\mathrm{d}x}{\mathrm{d}\theta} = \frac{2Q}{\pi}\,\sin\theta, \qquad\qquad \frac{\mathrm{d}y}{\mathrm{d}\theta} = \frac{2Q}{\pi}\,\sin\theta\tan\theta, \tag{3.28}$$

and integration with respect to θ gives

$$x = \text{const} - \frac{2Q}{\pi}\,\cos\theta, \qquad y = \text{const} + \frac{2Q}{\pi}\big(\log|\sec\theta + \tan\theta| - \sin\theta\big). \tag{3.29}$$

Considering the free surface BC, for example, we fix the constants by setting $x = -1$ and $y = 0$ at $\theta = 0$, resulting in

$$x = -1 + \frac{2Q}{\pi}\big(1 - \cos\theta\big), \qquad y = \frac{2Q}{\pi}\big(\log|\sec\theta + \tan\theta| - \sin\theta\big). \tag{3.30}$$

At C we have $\theta \to -\pi/2$, which gives $y \to -\infty$ and

$$x \to -1 + \frac{2Q}{\pi} = -Q. \tag{3.31}$$

Hence we can solve for the contraction ratio:

$$Q = \frac{\pi}{\pi + 2} \approx 0.611, \tag{3.32}$$

which agrees with experiments. The resulting jet shape is plotted in Figure 3.12.

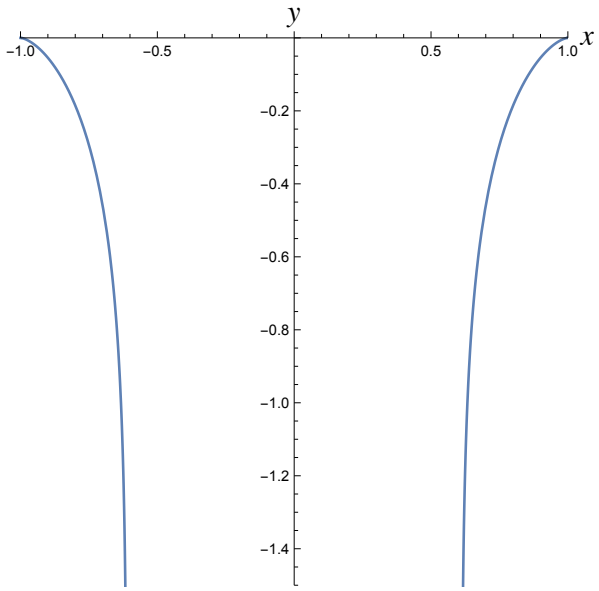

Figure 3.12: The jet shape given parametrically by (3.30) and (3.32).

3.3 Flow in porous media

Background

Darcy's Law was formulated by nineteenth-century French hydraulic engineer Henry Darcy to describe the flow of a viscous liquid through a porous medium, e.g. the flow of groundwater through rock or the flow of air through a filter. Darcy's Law relates the fluid velocity $\boldsymbol{u}$ to the pressure p through the relation

$$\boldsymbol{u} = -\frac{k}{\mu}\,\boldsymbol{\nabla} p, \tag{3.33}$$

where μ is the *viscosity* of the fluid and k is the *permeability* of the porous matrix. If the fluid is incompressible, then we also have $\boldsymbol{\nabla}\cdot\boldsymbol{u} = 0$ and thus, provided the medium is uniform (so that μ and k are constant), the pressure satisfies *Laplace's equation*

$$\nabla^2 p = 0. \tag{3.34}$$

The same equations also arise in *Hele-Shaw flow*, in which a viscous fluid is forced between two parallel plates, as shown in Figure 3.13. In this case, the permeability is given by $k = h^2/12$, where h is the thicknesss of the gap between the two plates.

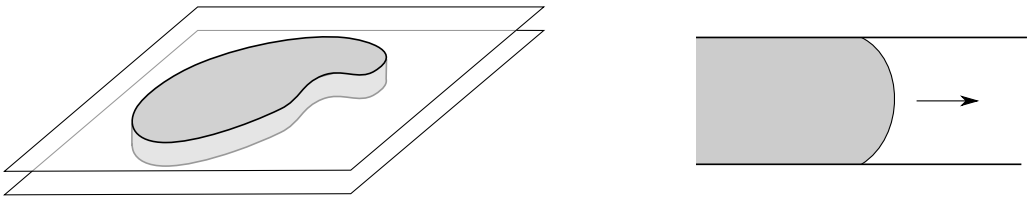

Figure 3.13: Hele-Shaw flow between two parallel plates; the right-hand diagram shows the cross-section.

Hele-Shaw flow (or two-dimensional porous medium flow) therefore provides an analogue of two-dimensional inviscid irrotational flow. However, if there are any free boundaries, then the boundary conditions there are different: a constant pressure is equivalent to $\phi =$ constant (where ϕ is the velocity potential) which is not at all similar to the Bernoulli condition relevant to inviscid flow.

We henceforth take $k/\mu = 1$ (via nondimensionalisation) and focus on two-dimensional flow, so that

$$\boldsymbol{u} = (u, v) = -\boldsymbol{\nabla} p = \boldsymbol{\nabla}\phi \tag{3.35}$$

in the fluid, where $\phi = p_{\text{atm}} - p$ is the velocity potential. At any free surface we have $p = p_{\text{atm}}$, the external atmospheric pressure, and hence

$$\phi = 0 \quad \text{at free boundary.} \tag{3.36}$$

We also have the *kinematic* boundary condition that the normal velocity $\boldsymbol{u}\cdot\boldsymbol{n}$ of the fluid must equal the normal velocity v_n of the boundary, i.e.

$$\frac{\partial\phi}{\partial n} = -\frac{\partial p}{\partial n} = v_n \quad \text{at free boundary.} \tag{3.37}$$

A convenient way to write this is to note that $p(x, y, t) = 0$ on the interface, and hence by differentiating with respect to t:

$$\frac{\mathrm{d}p}{\mathrm{d}t} = \frac{\partial p}{\partial t} + \boldsymbol{u}\cdot\boldsymbol{\nabla} p = \frac{\partial p}{\partial t} - \boldsymbol{\nabla} p\cdot\boldsymbol{\nabla} p = 0. \tag{3.38}$$

Thus the free boundary conditions are

$$\phi = 0, \quad \frac{\partial\phi}{\partial t} + |\boldsymbol{\nabla}\phi|^2 = 0 \quad \text{at free boundary.} \tag{3.39}$$

Again we note that these are quite different from the conditions at a free boundary in inviscid potential flow.

Canonical injection problem

A canonical problem is injection or suction from a point source/sink into a two-dimensional porous medium or Hele-Shaw cell, as shown in Figure 3.14. Given the strength Q of the

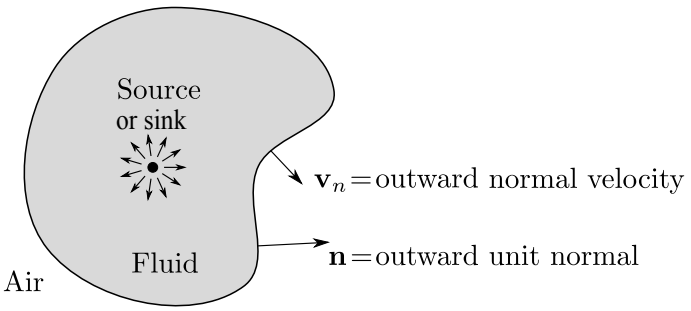

Figure 3.14: Schematic of injection into a Hele-Shaw cell.

source/sink and the initial shape $D(0)$ of the fluid domain at time $t = 0$, our aim is to

determine how the fluid domain $D(t)$ evolves as t increases. Without loss of generality, we can assume that the source/sink is at the origin. Then the required singularity is

$$\phi \sim \frac{Q}{2\pi} \log|z| \quad \text{as } z \to 0, \tag{3.40}$$

where $Q > 0$ is a source and $Q < 0$ is a sink. The conditions on the free boundary are given by equation (3.39), and the whole problem for ϕ is sketched in Figure 3.15.

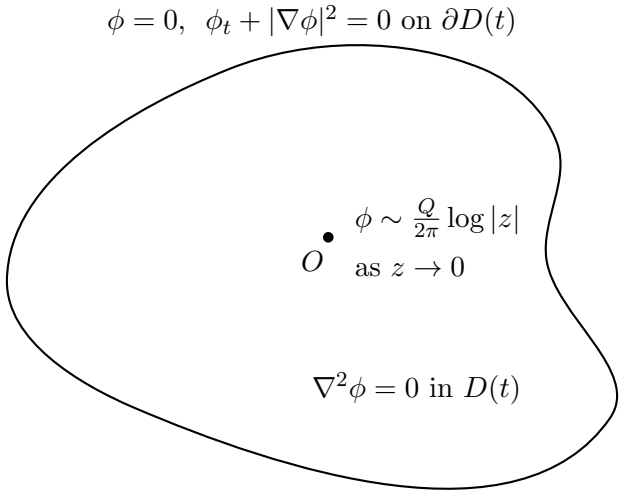

Figure 3.15: Canonical injection/suction free boundary problem.

As ϕ is a velocity potential we have a complex potential $w(z,t) = \phi + \mathrm{i}\psi$, which is a holomorphic function of z inside $D(t)$ except for a singularity at $z = 0$, with

$$w(z,t) \sim \frac{Q}{2\pi} \log z \quad \text{as } z \to 0. \tag{3.41}$$

Clearly there is a branch point at $z = 0$, which reflects the fact that the streamfunction ψ increases by Q on a circuit of O. The velocity, given by $u - \mathrm{i}v = \partial w/\partial z$ has a pole at $z = 0$ but is single-valued. The boundary conditions (3.39 imply that

$$\operatorname{Re} w = 0, \qquad \operatorname{Re}\left[\frac{\partial w}{\partial t}\right] + \left|\frac{\mathrm{d}w}{\mathrm{d}z}\right|^2 = 0 \quad \text{on } \partial D(t). \tag{3.42}$$

Now suppose that $D(t)$ is the image of the unit disc $|\zeta| < 1$ under a time-dependent conformal map $\zeta \mapsto z = F(\zeta, t)$, as shown schematically in Figure 3.16. By the Riemann Mapping Theorem, there are three real degrees of freedom in the resulting map, so we can choose also to map the origin to itself, so that $F(0,t) \equiv 0$.

We write the complex potential in the ζ-plane as

$$W(\zeta, t) = w\big(F(\zeta,t), t\big). \tag{3.43}$$

In the ζ-plane $W(\zeta,t)$ is a holomorphic function whose real part vanishes on $|\zeta| = 1$ and with a logarithmic singularity at $\zeta = 0$. We see that the appropriate function is

$$W(\zeta,t) = \frac{Q}{2\pi} \log\zeta. \tag{3.44}$$

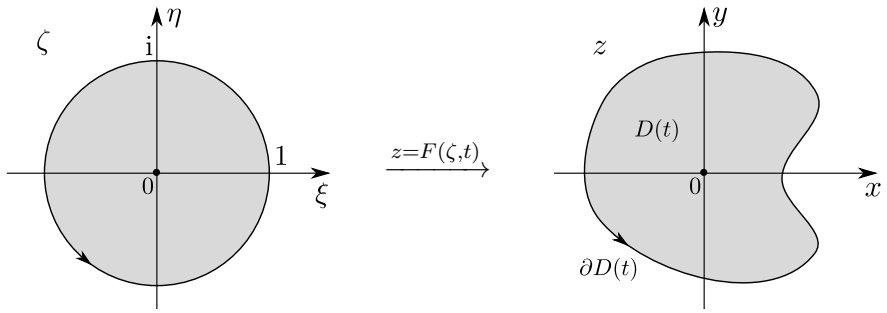

Figure 3.16: The fluid region $D(t)$ is the image of the unit disc $|\zeta| < 1$ under a time-dependent conformal map $z = F(\zeta, t)$.

It remains to impose the boundary condition (3.42). By differentiating (3.43) with respect to ζ and t we have

$$\frac{\partial W}{\partial \zeta} = \frac{\partial w}{\partial z}\frac{\partial F}{\partial \zeta}, \qquad \frac{\partial W}{\partial t} = \frac{\partial w}{\partial t} + \frac{\partial w}{\partial z}\frac{\partial F}{\partial t}, \tag{3.45}$$

and hence

$$\frac{\partial w}{\partial t} = \frac{\partial W}{\partial t} - \frac{\partial W}{\partial \zeta}\frac{\partial F}{\partial t}\bigg/\frac{\partial F}{\partial \zeta} \tag{3.46}$$

Therefore the boundary condition (3.42) is equivalent to

$$\mathrm{Re}\left[\frac{\partial W}{\partial t} - \frac{\partial W}{\partial \zeta}\frac{\partial F}{\partial t}\bigg/\frac{\partial F}{\partial \zeta}\right] + \left|\frac{\partial W}{\partial \zeta}\right|^2 \bigg/ \left|\frac{\partial F}{\partial \zeta}\right|^2 . \tag{3.47}$$

Now we just substitute for $W(\zeta, t)$ from (3.44), assuming that Q is constant, so that $\partial W/\partial t = 0$:

$$\mathrm{Re}\left[-\frac{Q}{2\pi\zeta}\,\frac{\partial F}{\partial t}\bigg/\frac{\partial F}{\partial \zeta}\right] + \frac{Q^2}{4\pi^2|\zeta|^2}\bigg/\left|\frac{\partial F}{\partial \zeta}\right|^2 = 0. \tag{3.48}$$

On the free boundary $|\zeta| = 1$ this tidies up to

$$\mathrm{Re}\left[\zeta\,\frac{\partial F}{\partial \zeta}\,\overline{\frac{\partial F}{\partial t}}\right] = \frac{Q}{2\pi}, \tag{3.49}$$

which is known as the *Polubarinova-Galin equation*.

The initial shape of the fluid domain $D(0)$ in principle determines $F(\zeta, 0)$. If we can solve equation (3.49) for $F(\zeta, t)$, then the shape of the fluid domain $D(t)$ for $t > 0$ is given by the image of the unit disc under the map $z = F(\zeta, t)$. There is no general method to solve equation (3.49), but a large number of exact solutions do exist, as the following Theorem (proved on the problem sheet) shows.

Theorem. If $F(\zeta, 0)$ is a polynomial of degree n, conformal and one-to-one for $|\zeta| < 1$, then $F(\zeta, t)$ remains a polynomial of degree n for $t > 0$; moreover the (time-dependent) coefficients of this polynomial satisfy a set of $n + 1$ ODEs.

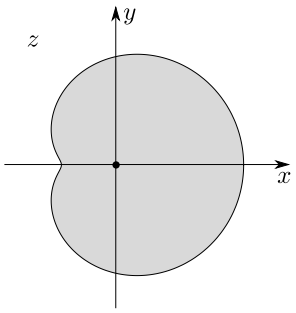

$$\begin{aligned} x &= a_{10}\cos\theta + a_{20}\cos 2\theta, \\ y &= a_{10}\sin\theta + a_{20}\sin 2\theta. \end{aligned}$$

Figure 3.17: A limaçon.

Example. Suppose $F(\zeta, 0) = a_{10}\zeta + a_{20}\zeta^2$, where a_{10}, a_{20} are real and positive, and $a_{10} > 2a_{20}$ (so that $F' \neq 0$ on the unit disc). Find the evolution under a source/sink at the origin.

Solution. The initial shape is called a *limaçon*, as illustrated in Figure 3.17.

We try

$$F(\zeta, t) = a_1(t)\zeta + a_2(t)\zeta^2, \tag{3.50}$$

where a_1, a_2 are real. Then substitution into the evolution equation (3.49) leads to

$$\mathrm{Re}\left[\zeta(a_1 + 2a_2\zeta)(\dot{a}_1\overline{\zeta} + \dot{a}_2(t)\overline{\zeta}^2)\right] = \frac{Q}{2\pi} \quad \text{on } |\zeta| = 1. \tag{3.51}$$

Since $\zeta\overline{\zeta} = 1$ this is equivalent to

$$\mathrm{Re}\left[a_1\dot{a}_1 + 2a_2\dot{a}_2 + 2a_2\dot{a}_1\zeta + a_1\dot{a}_2\overline{\zeta}\right] = \frac{Q}{2\pi}, \tag{3.52}$$

which must be true for all $|\zeta| = 1$, and hence we obtain two ODEs for the coefficients a_1 and a_2:

$$a_1\dot{a}_1 + 2a_2\dot{a}_2 = \frac{Q}{2\pi}, \qquad\qquad 2a_2\dot{a}_1 + a_1\dot{a}_2 = 0. \tag{3.53}$$

The first equation (3.53a) is an exact differential which we can integrate directly to give

$$\frac{1}{2}\left(a_1^2 + 2a_2^2\right) = \frac{Qt}{2\pi} + \frac{1}{2}\left(a_{10}^2 + 2a_{20}^2\right), \tag{3.54}$$

which represents net mass conservation. Multiplying (3.53b) by a_1 turns that into an exact differential, which we can integrate to give

$$a_1^2 a_2 = a_{10}^2 a_{20}. \tag{3.55}$$

Equations (3.54) and (3.55) determine $a_1(t)$ and $a_2(t)$ for $t > 0$. To get explicit formulae involves messy solution of a cubic. However, we can deduce the qualitative behaviour by eliminating $\dot{a}_2$ from (3.53) to get

$$a_1\dot{a}_1\left(1 - \frac{4a_2^2}{a_1^2}\right) = \frac{Q}{2\pi}. \tag{3.56}$$

First consider the case of injection, with $Q > 0$. Since we assumed that $a_1 > 2a_2$ initially, $\dot{a}_1 > 0$ initially. But (3.55) implies that, if a_1 increases, then a_2 decreases so that $a_1 > 2a_2$ always. Thus when $Q > 0$, a_1 increases with t while a_2 decreases, and $D(t)$ approaches a large circle. However, if $Q < 0$ (suction), then a_1 decreases and a_2 increases, until we get to a time when $a_1 = 2a_2$ and the map ceases to be conformal at $\zeta = -1$. At this point there is a *cusp* on the boundary (which is then a *cardioid*), and the solution ceases to exist. The evolution for positive and negative values of Q is shown in Figure 3.18.

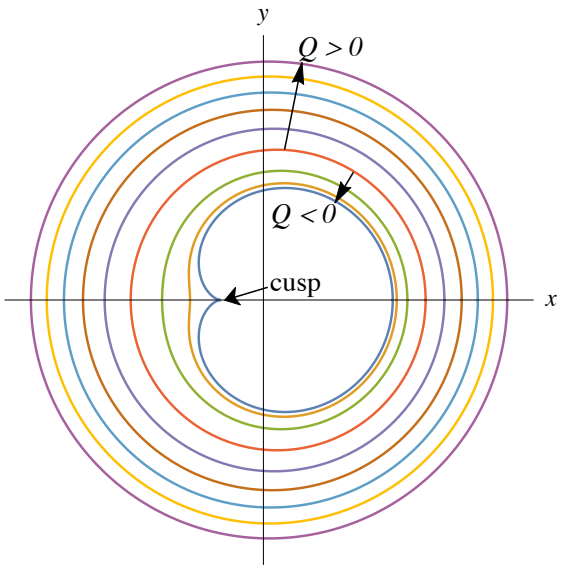

Figure 3.18: A limaçon evolving under Hele-Shaw flow due to a source/sink at the origin.

This example shows that for the case of suction, with $Q < 0$, the free surface may develop a cusp in finite time. In fact the situation is much worse than this. The suction problem is *ill posed*, in that an arbitrarily small perturbation to the initial boundary $\partial D(0)$ may lead to an arbitrarily large change in the boundary $\partial D(t)$ after an arbitrarily small time t. In reality, such pathalogical behaviour is prevented by physical effects not included in our model, for example surface tension.

4 Plemelj formulae and applications

4.1 Introduction

The problem of determining a holomorphic function $w(z)$ in terms of its values on a curve Γ is equivalent to solving a Cauchy problem for Laplace's equation and therefore *ill-posed*: the solution may not exist or may not be unique or it may not depend continuously on the boundary values.

Example. If $w(z)$ is holomorphic in $y > 0$ and

$$w(x) = \frac{\delta^2 \epsilon}{\delta^2 + x^2} \quad \text{for } y = 0, \ -\infty < x < \infty, \tag{4.1}$$

then

$$w(z) = \frac{\delta^2 \epsilon}{\delta^2 + z^2}. \tag{4.2}$$

Thus $|w| \leq \epsilon$ on $y = 0$, and $w \to \infty$ as $z \to \mathrm{i}\delta$. Since ϵ and δ may be arbitrarily small, we see that, however small w is on $y = 0$, it may become arbitrarily large an arbitrarily small distance from $y = 0$.

This example illustrates that trying to specify $w(z)$ on a given curve is ill posed. However, well-posed problems may be formulated in which, for example, $\operatorname{Re} w$ or $\operatorname{Im} w$ are specified on Γ or the jump in w across Γ is prescribed. We will show how a wide class of such problems may be tackled using the so-called *Plemelj formulae*.

4.2 Plemelj formulae

Recall that if w is holomorphic inside and on the closed contour Γ and z is a point inside Γ, then Cauchy's integral formula states that

$$w(z) = \frac{1}{2\pi \mathrm{i}} \oint_\Gamma \frac{w(\zeta)\,\mathrm{d}\zeta}{\zeta - z}. \tag{4.3}$$

This relates the values of w inside the contour to the values of w on the contour.

Let us consider more generally the *Cauchy integral*

$$w(z) = \frac{1}{2\pi \mathrm{i}} \int_\Gamma \frac{f(\zeta)\,\mathrm{d}\zeta}{\zeta - z}, \tag{4.4}$$

where f is a given function on the contour Γ, which may now be closed or open. If Γ is open, it is convenient in the subsequent analysis to adopt the convention that it does not contain its endpoints, a, $b \in \mathbb{C}$ say. Thus, an open contour may be parametrized by

$$\Gamma = \{\gamma(t) \in \mathbb{C} : t_0 < t < t_1\}, \tag{4.5}$$

where $a = \gamma(t_0) \neq \gamma(t_1) = b$ and $t_0 < t_1$ are real constants. We then define

$$\overline{\Gamma} = \{\gamma(t) \in \mathbb{C} : t_0 \leq t \leq t_1\} \tag{4.6}$$

to be the (topological) *closure* of Γ, i.e. $\overline{\Gamma}$ is the union of Γ and its endpoints. (If Γ is a closed contour, then $\overline{\Gamma} = \Gamma$ because Γ is (topologically) closed.)

If f is sufficiently smooth (e.g. continuous) on $\overline{\Gamma}$, then the function $w(z)$ defined by the Cauchy integral (4.4) is holomorphic on $\mathbb{C} \setminus \overline{\Gamma}$ (its derivatives may be found by differentiating under the integral sign). Now we pose the question: what is the limiting value of $w(z)$ as z approaches Γ? It turns out that the answer depends on which side of Γ is approached by z.

Suppose $t \in \Gamma$ is any point at which Γ is smooth and that f is holomorphic in a neighbourhood of t and continuous on Γ. Let us label the left-hand side of Γ (as Γ is traversed in the direction of integration) as "+", and the right-hand side as "−". Let z approach $t \in \Gamma$ from the positive side as illustrated in Figure 4.1(a). We deform Γ near t by replacing

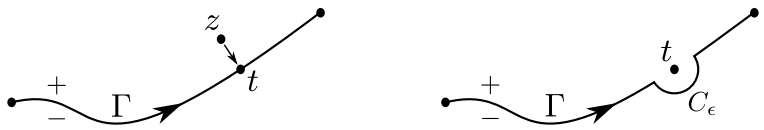

(a) Original contour (b) Deformed contour

Figure 4.1: Deformed integration contour for $w_+(z)$.

$\gamma_\epsilon = \Gamma \cap D(t;\epsilon) \subset \Gamma$ with a small semi-circle C_ϵ as illustrated in Figure 4.1(b), where ϵ is sufficiently small that f is holomorphic in the disc $D(t;2\epsilon) = \{z : |z-t| < 2\epsilon\}$ say. By the deformation theorem,

$$w_+(t) = \lim_{z\to t} \frac{1}{2\pi\mathrm{i}} \left(\int_{\Gamma\setminus\gamma_\epsilon} + \int_{C_\epsilon} \right) \frac{f(\zeta)}{\zeta - z}\,\mathrm{d}\zeta = \frac{1}{2\pi\mathrm{i}} \left(\int_{\Gamma\setminus\gamma_\epsilon} + \int_{C_\epsilon} \right) \frac{f(\zeta)}{\zeta - t}\,\mathrm{d}\zeta. \tag{4.7}$$

As $\epsilon \to 0$, the semi-circle gives a residue contribution

$$\frac{1}{2} \times 2\pi\mathrm{i} \times \frac{f(t)}{2\pi\mathrm{i}} = \frac{1}{2} f(t),$$

where the factor of $1/2$ arises because we are only integrating over a semi-circle. Hence,

$$w_+(t) = \lim_{\epsilon\to 0} \frac{1}{2\pi\mathrm{i}} \left(\int_{\Gamma\setminus\gamma_\epsilon} + \int_{C_\epsilon} \right) \frac{f(\zeta)}{\zeta - t}\,\mathrm{d}\zeta = \frac{1}{2\pi\mathrm{i}} \int\!\!\!\!\!\!-_{\Gamma} \frac{f(\zeta)}{\zeta - t}\,\mathrm{d}\zeta + \frac{1}{2} f(t), \tag{4.8}$$

where we define the *Principal Value integral* as

$$\int\!\!\!\!\!\!-_{\Gamma} \frac{f(\zeta)}{\zeta - t}\,\mathrm{d}\zeta = \lim_{\epsilon\to 0} \int_{\Gamma\setminus\gamma_\epsilon} \frac{f(\zeta)}{\zeta - t}\,\mathrm{d}\zeta. \tag{4.9}$$

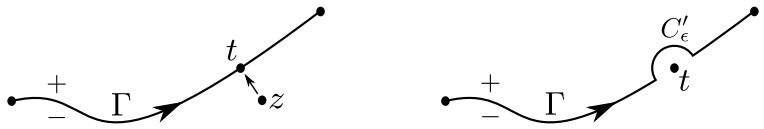

(a) Original contour (b) Deformed contour

Figure 4.2: Deformed integration contour for $w_-(z)$.

This limit always exists because the log singularities from the endpoints cancel as $\epsilon \to 0$ when f is continuous on Γ.

If we let $z \to t \in \Gamma$ from the minus side as illustrated in Figure 4.2(a), then we must deform Γ near $\zeta = t$ by replacing $\gamma_\epsilon \subset \Gamma$ with a small semi-circle C'_ϵ as illustrated in Figure 4.2(b). Again by the deformation theorem

$$w_-(t) = \lim_{\epsilon\to 0} \frac{1}{2\pi\mathrm{i}} \left(\int_{\Gamma\setminus\gamma_\epsilon} + \int_{C'_\epsilon} \right) \frac{f(\zeta)}{\zeta - t}\,\mathrm{d}\zeta = \frac{1}{2\pi\mathrm{i}} \int_\Gamma \frac{f(\zeta)}{\zeta - t}\,\mathrm{d}\zeta - \frac{1}{2} f(t). \tag{4.10}$$

In this case we are integrating in the opposite direction around the semi-circle, so that the residue contribution is $-f(t)/2$.

Equations (4.8) and (4.10) are known as the **Plemelj formulae**. In deriving them, we have assumed that Γ is a smooth contour and that f is continuous on $\overline{\Gamma}$. These conditions may be relaxed (see e.g. Ablowitz & Fokas), but we will persist with these assumptions henceforth. It follows that $w(z)$ is holomorphic and that $w(z) = O(1/z)$ as $z \to \infty$.

The contour deformation approach shown in Figures 4.1 and 4.2 clearly does not work if $t = t_e$ ($= a$ or b) is an end-point of Γ. The local behaviour as $z \to t_e$ depends on the local behaviour of $f(\zeta)$. The following results may be derived using perturbation methods or quoted from Ablowitz & Fokas.

As $z \to t_e$ with $z \in \mathbb{C} \setminus \overline{\Gamma}$:

if $f(\zeta) \to 0$ as $\zeta \to t_e$, then $w(z) = O(1)$; (4.11a)

if $f(\zeta) = O(1)$ as $\zeta \to t_e$, then $w(z) = O\big(\log(z - t_e)\big)$; (4.11b)

if $f(\zeta) = O\big((\zeta - t_e)^{-\alpha}\big)$ as $\zeta \to t_e$, with $\alpha \in (0, 1)$, then $w(z) = O\big((z - t_e)^{-\alpha}\big)$. (4.11c)

4.3 Solving problems with the Plemelj formulae

Problem 1

Find a function $w(z)$ holomorphic on $\mathbb{C} \setminus \overline{\Gamma}$ such that the limiting values of $w(z)$ as $z \to t \in \Gamma$ from either side satisfy

$$w_+(t) - w_-(t) = G(t), \tag{4.12}$$

where G is continuous on $\overline{\Gamma}$.

Solution. We seek a solution for w as a Cauchy integral

$$w(z) = \frac{1}{2\pi\mathrm{i}} \int_\Gamma \frac{f(\zeta)\,\mathrm{d}\zeta}{\zeta - z}, \tag{4.13}$$

where our aim is to use the jump condition (4.12) to determine the density function f. By subtracting the Plemelj formulae (4.10) and (4.8) we find that

$$w_+(t) - w_-(t) = f(t) \tag{4.14}$$

on Γ. Hence, we read off $f = G$, and a solution is given by

$$w(z) = \frac{1}{2\pi \mathrm{i}} \int_\Gamma \frac{G(\zeta)\,\mathrm{d}\zeta}{\zeta - z}. \tag{4.15}$$

This shows that the Plemelj formulae allow us easily to find *a* solution $w(z)$ that is holomorphic on $\mathbb{C} \setminus \overline{\Gamma}$ and satisfies the jump condition (4.12). However, the solution (4.15) is not unique. The homogeneous problem with $G = 0$ consists of finding a function that is holomorphic on $\mathbb{C} \setminus \overline{\Gamma}$ and continuous across Γ, which is satisfied by *any* function $w(z) = h(z)$ that is holomorphic on $\mathbb{C}\setminus\{a, b\}$. Morera's Theorem may be used to prove that *all* solutions of the homogeneous problem must be of this form. Therefore the general solution of Problem 1 is

$$w(z) = \frac{1}{2\pi \mathrm{i}} \int_\Gamma \frac{G(\zeta)\,\mathrm{d}\zeta}{\zeta - z} + h(z), \tag{4.16}$$

where $h(z)$ is an arbitrary function of z that is holomorphic on $\mathbb{C}\setminus\{a, b\}$.

To pin down h, it is necessary to prescribe the behaviour of w at a, b and ∞. For example, suppose we impose the additional conditions:

(I) w is finite or has a logarithmic singularity at each of the endpoints of Γ;

(II) there exists $n \in \mathbb{N}$ such that $w(z) = O(z^n)$ as $|z| \to \infty$.

Then, (I), the quotable results (4.11) and Laurent's Theorem imply that h can only have removable singularities at a and b, so that h is in fact entire. Hence, by (II) and the corollary to Liouville's theorem, $h(z) = p_n(z)$, an arbitrary polynomial of degree n.

Problem 2

Consider the particular case where Γ is a line segment on the real axis: $\Gamma = \{x : 0 < x < c\}$ for some $c > 0$. Suppose we are given $\operatorname{Im} w_\pm(x) = g_\pm(x)$ on Γ, with w holomorphic on $\mathbb{C} \setminus \overline{\Gamma}$. Find w when (1) $g_+(x) = -g_-(x) = g(x)$ and (2) $g_+(x) = g_-(x) = g(x)$, where $g(x)$ is continuous on $\overline{\Gamma}$.

Remark. If $w(z) = u(x, y) + \mathrm{i}v(x, y)$, then this problem is equivalent to the problem of finding v such that $\nabla^2 v = 0$ away from $\overline{\Gamma}$, and $v_\pm(x) = g_\pm(x)$ on Γ.

Solution. Seek a solution for w as a Cauchy integral of the form

$$w(z) = \frac{1}{2\pi \mathrm{i}} \int_0^c \frac{f(\xi)\,\mathrm{d}\xi}{\xi - z}, \tag{4.17}$$

which is holomorphic on $\mathbb{C} \setminus \overline{\Gamma}$, assuming f is sufficiently regular. The Plemelj formulae (4.8)–(4.10) become

$$w_\pm(x) = u_\pm(x) + \mathrm{i}g_\pm(x) = \pm\frac{1}{2} f(x) - \mathrm{i}F(x) \quad \text{on } \Gamma, \tag{4.18}$$

where we define

$$F(x) = \frac{1}{2\pi}\fint_0^c \frac{f(\xi)}{\xi - x}\mathrm{d}\xi. \tag{4.19}$$

Note that $F(x)$ is real on Γ if and only if $f(x)$ is real on Γ (because ξ, x are real on Γ).

Problem 2.1: If $g_+(x) = -g_-(x) = g(x)$, then (4.18) implies that

$$w_+(x) + w_-(x) = u_+(x) + u_-(x) = -2\mathrm{i}F(x) \qquad \text{on } \Gamma, \tag{4.20a}$$
$$w_+(x) - w_-(x) = u_+(x) - u_-(x) + 2\mathrm{i}g(x) = f(x) \qquad \text{on } \Gamma. \tag{4.20b}$$

By (4.20a), F must be pure imaginary, and hence f must be pure imaginary on Γ. Thus, by (4.20b), we have $u_+(x) - u_-(x) = 0$ and $f(x) = 2\mathrm{i}g(x)$ on Γ. It follows that a solution for w is given by

$$w(z) = \frac{1}{\pi}\int_0^c \frac{g(\xi)\,\mathrm{d}\xi}{\xi - z} + h(z), \tag{4.21}$$

where $h(z)$ is an arbitrary function of z that is holomorphic on $\mathbb{C}\setminus\overline{\Gamma}$ and real on Γ (thus a solution of the homogeneous problem in which $g = 0$).

Problem 2.2: If $g_+(x) = g_-(x) = g(x)$, then (4.18) becomes

$$w_+(x) + w_-(x) = u_+(x) + u_-(x) + 2\mathrm{i}g(x) = -2\mathrm{i}F(x) \qquad \text{on } \Gamma, \tag{4.22a}$$
$$w_+(x) - w_+(x) = u_+(x) - u_-(x) = f(x) \qquad \text{on } \Gamma. \tag{4.22b}$$

By (4.22b), f must be real, and hence F must likewise be real, on Γ; thus, by (4.22a), we have $u_+(x) + u_-(x) = 0$ and $F(x) = -g(x)$ on Γ. It follows that

$$w(z) = \frac{1}{2\pi\mathrm{i}}\int_0^c \frac{f(\xi)\,\mathrm{d}\xi}{\xi - z} \tag{4.23}$$

is a solution provided f satisfies the *Cauchy singular integral equation*

$$\frac{1}{\pi}\fint_0^c \frac{f(\xi)\,\mathrm{d}\xi}{\xi - x} = -2g(x) \qquad (0 < x < c), \tag{4.24}$$

which we need to invert to find f.

Remark: In Problem 2.1 the data gives $w_+ - w_-$ and hence f directly. In Problem 2.2 the data gives $w_+ + w_-$ leading to a Cauchy singular integral equation for f.

Solution. Suppose we can find an auxillary function $\tilde{w}(z)$ such that:

- $\tilde{w}(z)$ is holomorphic and non-zero on $\mathbb{C}\setminus\overline{\Gamma}$; (4.25a)
- $\tilde{w}(z)$ satisfies $\tilde{w}_+(x) = -\tilde{w}_-(x) \neq 0$ on Γ, (4.25b)

i.e. $\tilde{w}$ is a solution of the homogeneous problem (in which $g = 0$) that is non-zero on $\mathbb{C}\setminus\{a, b\}$.

Now we define

$$W(z) = \frac{w(z)}{\tilde{w}(z)}, \tag{4.26}$$

so that

$$\begin{aligned} W_+(x) - W_-(x) &= \frac{w_+(x)}{\tilde{w}_+(x)} - \frac{w_-(x)}{\tilde{w}_-(x)} \\ &= \frac{w_+(x)}{\tilde{w}_+(x)} - \frac{w_-(x)}{-\tilde{w}_+(x)} \\ &= \frac{w_+(x) + w_-(x)}{\tilde{w}_+(x)} \\ &= \frac{2\mathrm{i}g(x)}{\tilde{w}_+(x)} \quad \text{on } \Gamma. \end{aligned} \tag{4.27}$$

If $\tilde{w}_+$ is known, then $W_+ - W_-$ is known (because g is known). Therefore we have turned Problem 2.2 (in which $w_+ + w_-$ is given) into a version of Problem 1 (in which $W_+ - W_-$ is given). By Problem 1, equation (4.15), a solution for W is given by

$$W(z) = \frac{1}{2\pi\mathrm{i}} \int_0^c \frac{\tilde{f}(\xi)\,\mathrm{d}\xi}{\xi - z} + \tilde{H}(z), \tag{4.28}$$

where

$$\tilde{f}(x) = \frac{2\mathrm{i}g(x)}{\tilde{w}_+(x)} \quad \text{on } \Gamma, \tag{4.29}$$

and $\tilde{H}(z)$ is an arbitrary function holomorphic on $\mathbb{C}\setminus\{0, c\}$. Thus the solution of Problem 2.2 takes the form

$$w(z) = \tilde{w}(z)\left(\frac{1}{\pi}\int_0^c \frac{g(\xi)\,\mathrm{d}\xi}{\tilde{w}_+(\xi)(\xi - z)} + \tilde{H}(z)\right). \tag{4.30}$$

With W given by (4.28), the Plemelj formulae give

$$W_\pm(x) = \pm\frac{1}{2}\tilde{f}(x) + \frac{1}{2\pi\mathrm{i}}\int_0^c \frac{\tilde{f}(\xi)\,\mathrm{d}\xi}{\xi - x} + \tilde{H}(x) \qquad (0 < x < c), \tag{4.31}$$

so that

$$\tilde{f}(x) = W_+(x) - W_-(x) = \frac{2\mathrm{i}g(x)}{\tilde{w}_+(x)} \quad \text{on } \Gamma, \tag{4.32}$$

as required. Moreover,

$$\begin{aligned} \frac{1}{\pi\mathrm{i}}\!\!\int_0^c \frac{\tilde{f}(\xi)\,\mathrm{d}\xi}{\xi - x} + 2\tilde{H}(x) &= W_+(x) + W_-(x) \\ &= \frac{w_+(x)}{\tilde{w}_+(x)} + \frac{w_-(x)}{\tilde{w}_-(x)} \\ &= \frac{w_+(x) - w_-(x)}{\tilde{w}_+(x)} \\ &= \frac{f(x)}{\tilde{w}_+(x)} \quad \text{on } \Gamma, \end{aligned} \tag{4.33}$$

and, with $\tilde{f}$ given by (4.29), we deduce that

$$f(x) = \tilde{w}_+(x)\big(W_+(x) + W_-(x)\big) = 2\tilde{w}_+(x)\left(\frac{1}{\pi}\!\!\int_0^c \frac{g(\xi)\,\mathrm{d}\xi}{\tilde{w}_+(\xi)(\xi - x)} + \tilde{H}(x)\right) \tag{4.34}$$

satisfies the Cauchy singular integral equation (4.24).

Finding $\tilde{w}$

We have shown that the decomposition (4.26) allows us to transform Problem 2.2 into a version of Problem 1, and then solve it using the Plemelj formulae. As a bonus, (4.34) gives the solution $f(x)$ of the singular integral equation (4.24). It just remains to find an auxillary function $\tilde{w}(z)$ satisfying the properties (4.25), where $\Gamma = \{x + \mathrm{i}y : 0 < x < c,\, y = 0\}$ and $\overline{\Gamma} = \{x + \mathrm{i}y : 0 \leq x \leq c,\, y = 0\}$. We need to find a function whose value as Γ is approached from above is minus that as Γ is approached from below, as shown schematically in Figure 4.3.

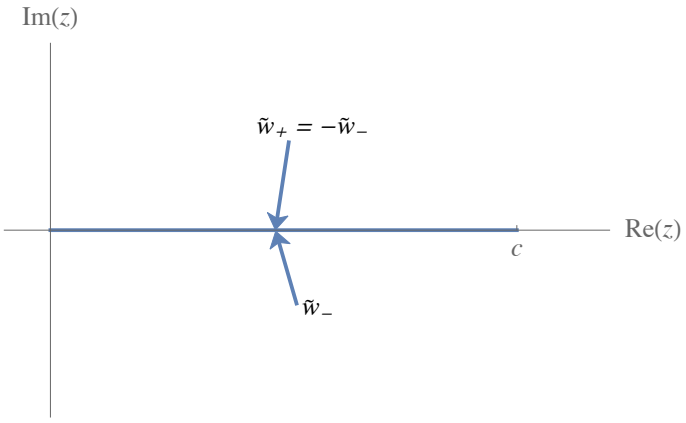

Figure 4.3: The jump conditions satisfied by the auxiliary function across Γ.

Example 1. When $c = \infty$, we can use $\tilde{w}(z) = z^{1/2}$, provided we take the branch cut along the positive real axis, i.e. $z^{1/2} = r^{1/2}\mathrm{e}^{\mathrm{i}\theta/2}$ for $z = r\mathrm{e}^{\mathrm{i}\theta}$, with $r > 0$ and $0 < \theta \leq 2\pi$. Then we will have $\tilde{w}_\pm(x) = \pm x^{1/2} \neq 0$ for $x > 0$, as required. We can obtain another valid solution by multiplying $\tilde{w}(z)$ by any function of z that is holomorphic and non-zero on $\mathbb{C} \setminus \{0\}$.

Example 2. When $0 < c < \infty$, we can use $\tilde{w}(z) = z^{1/2}(c-z)^{1/2}$, where we take the branch cut along Γ and then $\tilde{w}_\pm(x) = \pm x^{1/2}(c-x)^{1/2} \neq 0$ for $0 < x < c$. In this case, we can obtain another valid solution by multiplying $\tilde{w}(z)$ by any function of z that is holomorphic and non-zero on $\mathbb{C} \setminus \{0, c\}$.

In the above two examples, the auxiliary function $\tilde{w}(z)$ could plausibly have been found by inspection. However, we might wonder whether the functions so obtained are unique, and also how one could find $\tilde{w}$ more generally. We have $\tilde{w}_+/\tilde{w}_- = -1$ on Γ, so

$$\log \tilde{w}_+ - \log \tilde{w}_- = \log(-1) = (2m+1)\pi\mathrm{i} \quad \text{on } \Gamma, \tag{4.35}$$

where $m \in \mathbb{Z}$, corresponding to the infinite number of branches of the logarithm. Equation (4.35) is a version of Problem 1, and we read off from equations (4.12) and (4.16) the solution

$$\begin{aligned} \log \tilde{w}(z) &= \frac{1}{2\pi\mathrm{i}} \int_0^c \frac{(2m+1)\pi\mathrm{i}}{\xi - z}\, \mathrm{d}\xi + \tilde{h}(z) \\ &= \left(m + \frac{1}{2}\right) \big[\log(c-z) - \log z\big] + \tilde{h}(z), \end{aligned} \tag{4.36}$$

where $\tilde{h}(z)$ is an arbitrary function holomorphic on $\mathbb{C} \setminus \{0, c\}$. Therefore the general form for $\tilde{w}(z)$ is

$$\tilde{w}(z) = h^*(z) \left(\frac{c - z}{z} \right)^{m+1/2}, \tag{4.37}$$

where $h^*(z) = \mathrm{e}^{\tilde{h}(z)}$ is again an arbitrary function of z holomorphic and nonzero on $\mathbb{C} \setminus \{0, c\}$. The general solution (4.37) includes the particular form for $\tilde{w}$ found in Example 2 above, with $m = 0$ and $h^*(z) = z$.

Evidently the solution of Problem 2.2 is far from unique. There is a lot of freedom in the general form (4.37) for $\tilde{w}$, and also the arbitrary function $\tilde{H}(z)$ in (4.30) must be determined. We will now work through two concrete examples to show how a unique solution may be selected by prescribing the allowed behaviour of $w(z)$ at $z = 0$, $z = c$ and as $z \to \infty$.

4.4 Example: Fracture in solid mechanics

A famous problem in elasticity is to calculate the displacement field $\big(0, 0, \Phi(x, y)\big)$ in antiplane strain around a crack at $y = 0$, $0 < x < c$, as illustrated in Figure 4.4(a). The displacement Φ is such that:

- $\nabla^2 \Phi = 0$ except on the crack;
- $\lim_{y \downarrow \uparrow 0} \partial\Phi/\partial y = 0$ for $0 < x < c$ (zero traction on the crack surface);
- $|\nabla \Phi|$ has an inverse square-root singularity at $(0, 0)$ and at $(c, 0)$ (so that the displacement Φ is finite at the crack tips);
- $\partial\Phi/\partial y = T + O\left(r^{-2}\right)$ as $r^2 = x^2 + y^2 \to \infty$ (uniform shearing at large distances).

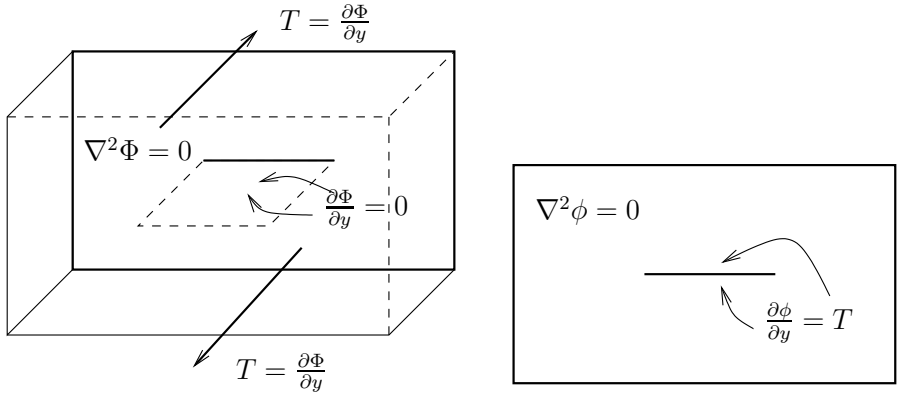

(a) (b)

Figure 4.4: (a) Antiplane strain around a crack. (b) The two-dimensional problem for $\phi(x, y)$.

Setting $\Phi = Ty - \phi(x, y)$ and $\phi_y = \operatorname{Im} w(z)$, we find that the corresponding properties of w are:

- $w(z)$ is holomorphic on $\mathbb{C} \setminus \overline{\Gamma}$;

- $\operatorname{Im} w_{\pm}(x) = T$ on $\Gamma = \{x + \mathrm{i}y : 0 < x < c,\, y = 0\}$;
- $w(z) = O\left(z^{-1/2}\right)$ as $z \to 0$ and $w(z) = O\left((z-c)^{-1/2}\right)$ as $z \to c$;
- $w(z) = O(z^{-2})$ as $z \to \infty$.

This is equivalent to Problem 2.2, with $g(x) = T =$ constant, so a solution is given by equation (4.30), namely

$$w(z) = \tilde{w}(z)\left(\frac{1}{\pi}\int_0^c \frac{g(\xi)\,\mathrm{d}\xi}{\tilde{w}_+(\xi)(\xi - z)} + \tilde{H}(z)\right), \tag{4.38}$$

where $\tilde{H}(z)$ is an arbitrary function of z holomorphic on $\mathbb{C}\backslash\{0, c\}$. We now make a specific choice for $\tilde{w}$, namely

$$\tilde{w}(z) = z^{-1/2}(c-z)^{-1/2}, \tag{4.39}$$

with the branch cut along Γ, so that $\tilde{w}_{\pm}(x) = \pm x^{-1/2}(c-x)^{-1/2}$ for $0 < x < c$, and equation (4.38) becomes

$$w(z) = \frac{1}{z^{1/2}(c-z)^{1/2}}\left(\frac{1}{\pi}\int_0^c \frac{\xi^{1/2}(c-\xi)^{1/2} g(\xi)}{(\xi - z)}\,\mathrm{d}\xi + \tilde{H}(z)\right). \tag{4.40}$$

Now we will use the prescribed properties of $w(z)$ to argue that $\tilde{H}(z)$ must in fact be zero.

- At the endpoints $z = 0$ and $z = c$ of Γ, the integral in (4.40) is finite (because of the choice we made for $\tilde{w}(z)$).
- Since $\tilde{H}(z)$ is holomorphic on $\mathbb{C}\backslash\{0, c\}$, it can only have *isolated* singularities at the end points.
- Since $w = O\left(z^{-1/2}\right)$ as $z \to 0$ and $w = O\left((c-z)^{-1/2}\right)$ as $z \to c$, it follows that $\tilde{H}(z)$ can only have *removable* singularities at $z = 0$ and $z = c$, and therefore $\tilde{H}(z)$ is *entire*.
- Finally, $w = O\left(z^{-2}\right)$ as $z \to \infty$ if and only if $\tilde{H}(z) = O\left(z^{-1}\right)$ as $z \to \infty$, and therefore $\tilde{H}(z) \equiv 0$ by Liouville's theorem.

Hence, the unique solution for $w(z)$ is given by

$$w(z) = \frac{T}{\pi z^{1/2}(c-z)^{1/2}}\int_0^c \frac{\xi^{1/2}(c-\xi)^{1/2}\,\mathrm{d}\xi}{(\xi - z)}. \tag{4.41}$$

The integral in equation (4.41) can be evaluated explicitly as follows. First note that

$$\int_0^c \frac{\xi^{1/2}(c-\xi)^{1/2}\,\mathrm{d}\xi}{(\xi - z)} = \frac{1}{2}\oint_C \frac{\zeta^{1/2}(c-\zeta)^{1/2}\,\mathrm{d}\zeta}{(\zeta - z)}, \tag{4.42}$$

where C is a small clockwise contour that encloses Γ, as shown in Figure 4.5(a). Now deform the contour C to infinity, as shown in Figure 4.5(b). There is a residue contribution from the pole at $\zeta = z$ of $\pi\mathrm{i}z^{1/2}(c-z)^{1/2}$. To evaluate the contribution from a large circle at infinity expand the integrand as

$$\frac{\zeta^{1/2}(c-\zeta)^{1/2}}{(\zeta - z)} \sim -\mathrm{i}\left(1 - \frac{c}{\zeta}\right)^{1/2}\left(1 - \frac{z}{\zeta}\right)^{-1} \sim -\mathrm{i}\left(1 + \frac{2z - c}{2\zeta} + \cdots\right) \tag{4.43}$$

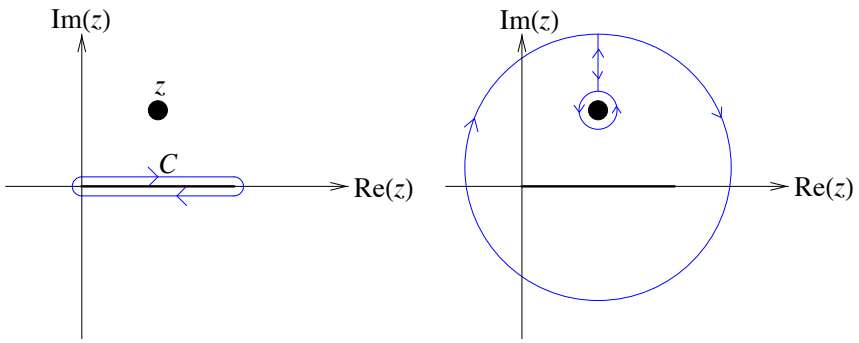

(a) (b)

Figure 4.5: Integration contours for the integral (4.41).

which integrates to $-\pi(z-c/2)$. Thus the explicit solution for $w(z)$ is

$$w = \frac{T}{\pi z^{1/2}(c-z)^{1/2}}\left(\pi \mathrm{i} z^{1/2}(c-z)^{1/2} - \pi\left(z-\frac{c}{2}\right)\right) = T\mathrm{i} - \frac{T(z-c/2)}{z^{1/2}(c-z)^{1/2}}. \tag{4.44}$$

We can easily verify that the solution (4.44) for $w(z)$ has all of the required properties. In principle we would have obtained exactly the same solution if we made a different choice of the auxiliary function $\tilde{w}(z)$: it would just have made the job of determining $\tilde{H}(z)$ slightly more difficult. In general, a judicious choice of $\tilde{w}(z)$ will make the whole solution procedure as straightforward as possible.

4.5 Example: Aerodynamics of a thin aerofoil

Here the physical model is the flow of a uniform stream of ideal fluid past a thin aerofoil with a sharp trailing edge and a small angle of attack, as illustrated in Figure 4.6(a). We denote

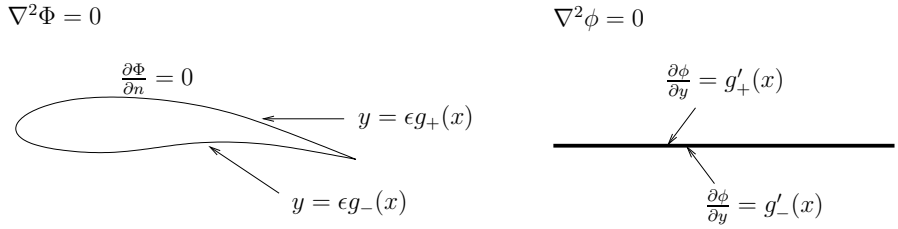

(a) (b)

Figure 4.6: Flow past a thin aerofoil. (a) The problem for the velocity potential $\Phi(x,y)$. (b) The linearised problem for the disturbance potential $\phi(x,y)$.

the boundary of the aerofoil by $y = \epsilon g_\pm(x)$ for $0 < x < c$, where $g_-(x) \le g_+(x)$ and $\epsilon \ll 1$. If $\Phi(x,y)$ is the velocity potential, then:

- $\nabla^2\Phi = 0$ in the fluid surrounding the aerofoil;

- the no-flux boundary condition states that $\partial\Phi/\partial n = 0$ on the boundary of the aerofoil;
- there is an *inverse square root* singularity in the velocity at the leading edge, so that $|\boldsymbol{\nabla}\Phi| = O\left(r^{-1/2}\right)$ as $r = \sqrt{x^2+y^2} \to 0$;
- the *Kutta condition* states that the velocity $\boldsymbol{\nabla}\Phi$ must be finite at the sharp trailing edge;
- the velocity is uniform at infinity, so that $\boldsymbol{\nabla}\Phi \sim (1,0) + O\left(r^{-1}\right)$ as $r \to \infty$.

In the limit of a thin aerofoil, $\epsilon \to 0$ and we can expand about the uniform flow, setting $\Phi(x,y) \sim x + \epsilon\phi(x,y)$. Since the outward normal to the upper surface of the aerofoil is proportional to $(-\epsilon g'_+, 1)$, the no-flux boundary condition on the upper surface implies

$$\begin{aligned} 0 &= (-\epsilon g'_+, 1)\cdot\nabla\Phi \quad \text{on } y = \epsilon g_+(x) \\ &= (-\epsilon g'_+, 1)\cdot\big(1 + \epsilon\phi_x(x,\epsilon g_+), \phi_y(x,\epsilon g_+)\big) \\ &\sim -\epsilon g'_+ + \epsilon\phi_y(x,0) + O(\epsilon^2) \end{aligned} \tag{4.45}$$

as $\epsilon \to 0$. A similar expansion holds for the no-flux boundary condition on the lower surface. Thus the boundary conditions which were originally imposed on the surface of the aerofoil may be linearised down onto the x-axis when ϵ is small.

The leading-order problem for the disturbance potential $\phi(x,y)$ is:

- $\nabla^2\phi = 0$ except on the line segment $\{(x,y) : 0 \le x \le c,\ y = 0\}$;
- $\dfrac{\partial\phi}{\partial y} = g'_\pm(x) \quad$ on $0 < x < c$, $y = 0_\pm$;
- $|\boldsymbol{\nabla}\phi| = O\left(r^{-1/2}\right)$ as $r \to 0$;
- $\boldsymbol{\nabla}\phi$ is finite as $(x,y) \to (c,0)$;
- $|\boldsymbol{\nabla}\phi| = O\left(r^{-1}\right)$ as $r \to \infty$.

We translate this into a Plemelj type problem by defining

$$w(z) = -\big(\phi_x(x,y) - \mathrm{i}\phi_y(x,y)\big) \tag{4.46}$$

(the unconventional minus sign is taken for convenience). Then $w(z)$ has the properties

- $w(z)$ is holomorphic on $\mathbb{C}\setminus\overline{\Gamma}$;
- $\operatorname{Im} w_\pm(x) = g'_\pm(x)$ on $\Gamma = \{x + \mathrm{i}y : 0 < x < c,\ y = 0\}$;
- $w(z) = O(z^{-1/2})$ as $z \to 0$ and $w(z) = O(1)$ as $z \to c$;
- $w(z) = O\left(z^{-1}\right)$ as $z \to \infty$.

	fracture	aerofoil
$z \to 0$	$w(z) = O\left(z^{-1/2}\right)$	$w(z) = O\left(z^{-1/2}\right)$
$z \to c$	$w(z) = O\left((z-c)^{-1/2}\right)$	$w(z) = O\left(1\right)$
$z \to \infty$	$w(z) = O\left(z^{-2}\right)$	$w(z) = O\left(z^{-1}\right)$

Table 1: Comparison between the prescribed behaviours of $w(z)$ in the fracture and aerofoil problems.

Figure 4.7: Schematic of a symmetric aerofoil (left); a zero-thickness aerofoil (right).

Remark: In Table 1 we summarise the conditions specified for $w(z)$ at $z = 0$, $z = c$ and as $z \to \infty$ in the fracture and aerofoil problems. Compared with the fracture problem, we have now *strengthened* the condition at $z = c$ but *weakened* the condition at infinity.

For a *symmetric* aerofoil, $g_+(x) = -g_-(x)$, so that $g'_+(x) = -g'_-(x)$ and we must solve an easy problem as in Problem 2.1. A zero-thickness aerofoil has $g_+(x) = g_-(x)$, as shown in Figure 4.7, so that $g'_+(x) = g'_-(x)$ and we must solve a harder problem as in Problem 2.2.

In the latter case, we let $g'_+(x) = g'_-(x) = g(x)$ and again choose $\tilde{w}(z) = z^{-1/2}(c-z)^{-1/2}$, so that we can use the same solution (4.40) as for the crack problem. As in the crack problem, $\tilde{H}(z)$ can only have isolated singularities at the endpoints of Γ and is therefore entire. However, now the weaker condition $w = O(z^{-1})$ as $z \to \infty$ implies that $\tilde{H}(z) = O(1)$ as $z \to \infty$, so $\tilde{H}(z)$ is constant by Liouville's theorem (in contrast to the crack problem). Finally, we ensure that w is finite as the trailing edge $z = c$ by setting

$$\tilde{H}(z) = \tilde{H}(c) = -\frac{1}{\pi}\int_0^c \frac{g(\xi)\xi^{1/2}(c-\xi)^{1/2}}{\xi - z}\,\mathrm{d}\xi\bigg|_{z=c}, \tag{4.47}$$

giving

$$\begin{aligned} w(z) &= \frac{1}{\pi z^{1/2}(c-z)^{1/2}}\int_0^c g(\xi)\xi^{1/2}(c-\xi)^{1/2}\left(\frac{1}{\xi - z} - \frac{1}{\xi - c}\right)\mathrm{d}\xi \\ &= \frac{(c-z)^{1/2}}{\pi z^{1/2}}\int_0^c \frac{g(\xi)\xi^{1/2}}{(c-\xi)^{1/2}(\xi - z)}\,\mathrm{d}\xi. \end{aligned} \tag{4.48}$$

It is an exercise in perturbation methods to verify that the solution (4.48) satisfies $w(z) = \mathrm{O}(1)$ as $z \to c$. Equation (4.48) could have been obtained more directly by choosing $\tilde{w}(z) = (c-z)^{1/2}/z^{1/2}$, thereby incorporating the specified behaviour of $w(z)$ near the end points.

4.6 General Hilbert problem

We have seen that when $w_+ - w_-$ is given on Γ we can solve immediately for f and therefore for w. When $w_+ + w_-$ is given on Γ, we find a singular integral equation for f, but we can

find w (and f) by introducing $\tilde{w}$ such that $\tilde{w}_+ = -\tilde{w}_- \neq 0$ on Γ. What about more general relations between w_+ and w_- on Γ?

The general so-called *Hilbert problem* is

$$a(z)w_+(z) + b(z)w_-(z) = c(z) \quad \text{on } \Gamma, \tag{4.49}$$

with a, $b \neq 0$ and c prescribed on Γ. Suppose we can find $\tilde{w}(z)$ holomorphic and non-zero away from Γ, with

$$a(z)\tilde{w}_+(z) = -b(z)\tilde{w}_-(z) \neq 0 \quad \text{on } \Gamma. \tag{4.50}$$

Then $W(z) = w(z)/\tilde{w}(z)$ satisfies

$$\begin{aligned} W_+(z) - W_-(z) &= \frac{w_+(z)}{\tilde{w}_+(z)} - \frac{w_-(z)}{\tilde{w}_-(z)} \\ &= \frac{w_+(z)}{\tilde{w}_+(z)} - \frac{w_-(z)}{-a(z)\tilde{w}_+(z)/b(z)} \\ &= \frac{a(z)w_+(z) + b(z)w_-(z)}{a(z)\tilde{w}_+(z)} \\ &= \frac{c(z)}{a(z)\tilde{w}_+(z)} \quad \text{on } \Gamma, \end{aligned} \tag{4.51}$$

giving

$$W(z) = \frac{1}{2\pi\mathrm{i}} \int_\Gamma \frac{c(\zeta)}{a(\zeta)\tilde{w}_+(\zeta)(\zeta - z)} \,\mathrm{d}\zeta + H(z), \tag{4.52}$$

where $H(z)$ is an arbitrary function of z that is holomorphic away from the endpoints of Γ.

To solve for $\tilde{w}(z)$ we again take logs. Since $\tilde{w}_+(z)/\tilde{w}_-(z) = -b(z)/a(z)$, we get

$$\log \tilde{w}_+(z) - \log \tilde{w}_-(z) = \log\left(-\frac{b(z)}{a(z)}\right) \quad \text{on } \Gamma. \tag{4.53}$$

We can therefore use the Plemelj formulae as before to solve for $\tilde{w}(z)$ and hence find $w(z)$.

The general linear Cauchy singular integral equation for f:

$$a(z)f(z) + b(z) \int_\Gamma \frac{f(\zeta)\,\mathrm{d}\zeta}{\zeta - z} = c(z), \tag{4.54}$$

can be rewritten as a Hilbert problem for

$$w(z) = \frac{1}{2\pi\mathrm{i}} \int_\Gamma \frac{f(z)}{\zeta - z} \mathrm{d}\zeta,$$

using the Plemelj formulae, and hence solved by following the above strategy.

5 Complex Fourier Transforms

5.1 Introduction

Below we summarise the main properties of the standard Fourier transform. One of the main restrictions on the Fourier transform is that it only applies to functions which decay sufficiently rapidly at infinity. Here we will show how this restriction may be lifted by extending the concept of the Fourier transform into the complex plane. We will then show how this generalised Fourier transform may be used to solve some linear differential equations.

Basic properties of the Fourier transform

Given an integrable function $f(x)$, we define the **Fourier transform** of f by

$$\mathcal{F}[f(x)] = \bar{f}(k) = \int_{-\infty}^{\infty} f(x)\mathrm{e}^{\mathrm{i}kx}\,\mathrm{d}x. \tag{5.1}$$

Given the transform $\bar{f}(k)$, then we can recover $f(x)$ using the **inverse Fourier transform**:

$$\frac{1}{2}\big(f(x_-) + f(x_+)\big) = \mathcal{F}^{-1}\left[\bar{f}(k)\right] = \frac{1}{2\pi}\fint_{-\infty}^{\infty} \bar{f}(k)\mathrm{e}^{-\mathrm{i}kx}\,\mathrm{d}k, \tag{5.2}$$

where the prinicipal value integral is defined by

$$\fint_{-\infty}^{\infty} = \lim_{R\to\infty}\int_{-R}^{R}. \tag{5.3}$$

If $f(x)$ is continuous, then the left-hand side of equation (5.2) is just $f(x)$. Moreover, the integrand on the right-hand side of equation (5.2) is integrable and the dash may be removed from the integral sign.

We will just list without proof some useful properties of the Fourier transform, assuming the required integrability where necessary. First, the **Fourier transform of a derivative** is given by

$$\mathcal{F}\left[f'(x)\right] = -\mathrm{i}k\bar{f}(k), \tag{5.4}$$

which is easily shown using integration by parts. Differentiation under the integral sign in (5.1) gives the **derivative of a Fourier transform**, namely

$$\frac{\mathrm{d}\bar{f}(k)}{\mathrm{d}k} = \mathrm{i}\mathcal{F}[xf(x)]. \tag{5.5}$$

Equation (5.4) shows that $\mathcal{F}$ will turn a linear differential equation for $f(x)$ into a linear algebraic equation for $\bar{f}(k)$. Once we have solved for $\bar{f}(k)$, in principle we can recover $f(x)$ from the inversion formula (5.2), typically using contour integration in the complex k-plane. In practice this is rarely necessary: one can look up very many Fourier transforms that often

arise, and the following is also useful. The **inverse Fourier transform of a product** is given by

$$\mathcal{F}^{-1}\left[\bar{f}(k)\bar{g}(k)\right] = (f \star g)(x), \tag{5.6}$$

where $f \star g$ denotes the **convolution** of f and g, defined by

$$(f \star g)(x) = \int_{-\infty}^{\infty} f(s)g(x-s)\,\mathrm{d}s. \tag{5.7}$$

Example: solving Laplace's equation by Fourier transform. Find $u(x,y)$ that satisfies Laplace's equation in the half-space $y > 0$, with the boundary condition $u(x,0) = u_0(x)$ on $y = 0$, and such that $u(x,y)$ is bounded as $y \to +\infty$.

Solution. We take the Fourier transform in x, i.e.

$$\bar{u}(k,y) = \int_{-\infty}^{\infty} u(x,y)\mathrm{e}^{\mathrm{i}kx}\,\mathrm{d}x. \tag{5.8}$$

The whole problem is transformed as follows:

$$\nabla^2 u = \frac{\partial^2 u}{\partial x^2} + \frac{\partial^2 u}{\partial y^2} = 0 \qquad \Rightarrow \qquad \frac{\partial^2 \bar{u}}{\partial y^2} - k^2\bar{u} = 0, \tag{5.9a}$$

$$u = u_0(x) \text{ at } y = 0 \qquad \Rightarrow \qquad \bar{u} = \bar{u}_0(k) \text{ at } y = 0, \tag{5.9b}$$

$$u \text{ bounded as } y \to \infty \qquad \Rightarrow \qquad \bar{u} \text{ bounded as } y \to \infty, \tag{5.9c}$$

where $\bar{u}_0(k)$ is the Fourier transform of $u_0(x)$.

The general solution of (5.9a) is

$$\bar{u}(k,y) = A(k)\mathrm{e}^{ky} + B(k)\mathrm{e}^{-ky}, \tag{5.10}$$

where A and B are arbitrary integration functions. We need to make sure that $\bar{u}$ is bounded as $y \to \infty$. Which of the two exponentials in (5.11) should be kept depends on k: if $k > 0$ then A must be zero, while if $k < 0$ then B must be zero. Both of these cases may be encompassed by setting

$$\bar{u}(k,y) = C(k)\mathrm{e}^{-|k|y}, \tag{5.11}$$

so that the decaying exponential is selected regardless of the sign of k. Finally we apply the boundary condition (5.9b) to get

$$\bar{u}(k,y) = \bar{u}_0(k)\mathrm{e}^{-|k|y}. \tag{5.12}$$

This shows how the Fourier transform converts a PDE for u to an ODE for $\bar{u}$ which is then easily solved. However, it remains to invert (5.12) to find u. Here we can use the convolution theorem (5.6) to get

$$u(x,y) = u_0(x) \star g(x,y) = \int_{-\infty}^{\infty} u_0(s)g(x-s,y)\,\mathrm{d}s, \tag{5.13}$$

where

$$g(x,y) = \mathcal{F}^{-1}\left[\mathrm{e}^{-|k|y}\right] = \frac{1}{2\pi}\int_{-\infty}^{\infty} \mathrm{e}^{-|k|y-\mathrm{i}kx}\,\mathrm{d}k = \frac{y}{\pi\,(x^2+y^2)}. \tag{5.14}$$

Thus we obtain the general solution

$$u(x,y) = \frac{y}{\pi}\int_{-\infty}^{\infty} \frac{u_0(s)}{(x-s)^2+y^2}\,\mathrm{d}s. \tag{5.15}$$

5.2 Complex Fourier transform

Our aim is to generalise the Fourier transform to a wider class of functions by allowing k to take complex values. For simplicity we will assume that $f(x)$ is continuous, although this assumption can be relaxed relatively easily. We also assume that f grows at most exponentially at infinity, that is $f(x) = O\left(\mathrm{e}^{c|x|}\right)$ as $x \to \pm\infty$ for some constant $c > 0$; this rules out $f(x) = \mathrm{e}^{x^2}$, for example.

To investigate the convergence of the Fourier integral (5.1) as $x \to \pm\infty$, we split up $f(x)$ by writing

$$f(x) = f_+(x) + f_-(x), \tag{5.16}$$

where

$$f_+(x) = 0 \quad \text{for } x < 0, \qquad\qquad f_-(x) = 0 \quad \text{for } x > 0. \tag{5.17}$$

From the definition of the Fourier transform,

$$\bar{f}_+(k) = \int_0^\infty f_+(x)\mathrm{e}^{\mathrm{i}kx}\,\mathrm{d}x = \int_0^\infty f_+(x)\mathrm{e}^{\mathrm{i}\,\mathrm{Re}(k)x}\mathrm{e}^{-\,\mathrm{Im}(k)x}\,\mathrm{d}x, \tag{5.18}$$

we see that

$$\left|\bar{f}_+(k)\right| \le \int_0^\infty |f(x)|\mathrm{e}^{-\,\mathrm{Im}(k)\,x}\,\mathrm{d}x, \tag{5.19}$$

and the integral converges provided $\mathrm{Im}\,k > c$. Thus $\bar{f}_+(k)$ exists and is holomorphic for $\mathrm{Im}\,k > c$, since its derivative

$$\frac{\mathrm{d}\bar{f}_+}{\mathrm{d}k} = \mathrm{i}\mathcal{F}\left[xf_+(x)\right] = \mathrm{i}\int_0^\infty xf_+(x)\mathrm{e}^{\mathrm{i}kx}\,\mathrm{d}x \tag{5.20}$$

likewise exists for $\mathrm{Im}\,k > c$.

Next we need to extend the Fourier inversion theorem to recover $f_+(x)$ from $\bar{f}_+(k)$. To this end, let $F_+(x) = \mathrm{e}^{-\alpha x}f_+(x)$, where $\alpha > c$, so that $\bar{F}_+(k) = \bar{f}_+(k + \mathrm{i}\alpha)$ exists and is holomorphic for $\mathrm{Im}\,k > c - \alpha$, in particular for $k \in \mathbb{R}$, since $\alpha > c$. Thus we can apply the Fourier Inversion Theorem (5.2), which gives

$$F_+(x) = \frac{1}{2\pi}\int_{-\infty}^{\infty} \bar{F}_+(k)\mathrm{e}^{-\mathrm{i}kx}\,\mathrm{d}k \tag{5.21a}$$

$$\Rightarrow \quad \mathrm{e}^{-\alpha x}f_+(x) = \frac{1}{2\pi}\int_{-\infty}^{\infty} \bar{f}_+(k+\mathrm{i}\alpha)\mathrm{e}^{-\mathrm{i}kx}\mathrm{d}k \tag{5.21b}$$

$$\Rightarrow \quad f_+(x) = \frac{1}{2\pi}\int_{-\infty}^{\infty} \bar{f}_+(k+\mathrm{i}\alpha)\mathrm{e}^{-\mathrm{i}(k+i\alpha)x}\mathrm{d}k. \tag{5.21c}$$

The final integral corresponds to integration along a horizontal contour in the complex k-plane, i.e.

$$f_+(x) = \frac{1}{2\pi}\int_{-\infty+\mathrm{i}\alpha}^{\infty+\mathrm{i}\alpha} \bar{f}_+(k)\mathrm{e}^{-\mathrm{i}kx}\,\mathrm{d}k, \tag{5.22}$$

where the integration contour is as shown in Figure 5.1.

Suppose $\bar{f}_+(k)$ can be continued below $\mathrm{Im}\,k = c$, so that it is holomorphic in some region $\Omega_+ \supset \{k : \mathrm{Im}\,k > c\}$ except for singularities at $k = a_1, a_2, \cdots$. By the deformation theorem,

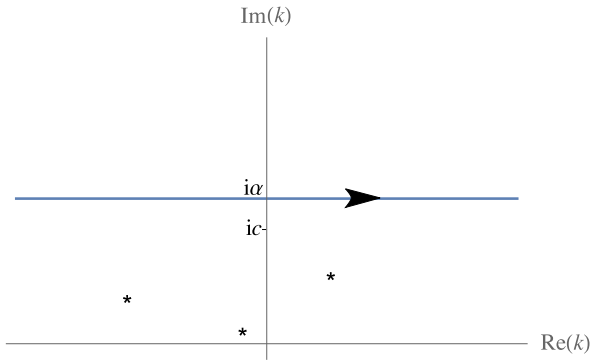

Figure 5.1: Inversion contour for complex Fourier transform $\bar{f}_+(k)$, where $f_+(x) = O\left(\mathrm{e}^{cx}\right)$ as $x \to \infty$.

the inversion contour $\Gamma_+ = \{x + i\alpha : -\infty < x < \infty\}$ may be deformed into Ω_+ provided it passes *above* all the singularities of $\bar{f}_+$, as shown in Figure 5.2(a). Since the singularities of $\bar{f}_+(k)$ are below the inversion contour, for $x < 0$ we can close the inversion contour at $+\mathrm{i}\infty$, as shown in Figure 5.2(b). This gives this expected result that $f_+(x) = 0$ for $x < 0$. For $x > 0$, we would need to close the contour in $\operatorname{Im} k < 0$, picking up the contributions from the singularities in $\bar{f}_+(k)$ and giving a nonzero value of $f_+(x)$.

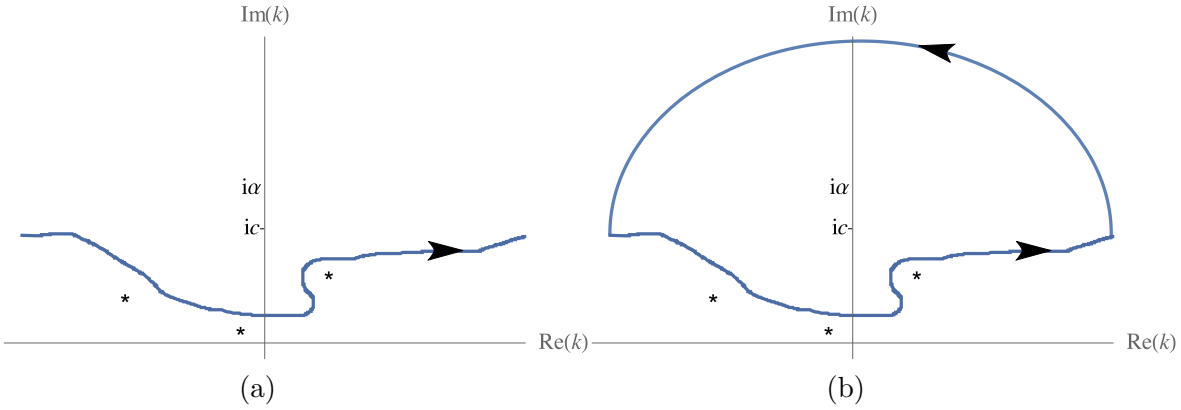

Figure 5.2: (a) An inversion contour that passes above the singularities ($\star$) in $\bar{f}_+(k)$. (b) Closing the contour at infinity when $x < 0$.

The same procedure works for $f_-(x)$ with everything upside down: $\bar{f}_-(k)$ exists and is holomorphic for $\operatorname{Im} k < -c$, while an application of the Fourier Inversion Theorem to $F_-(x) = \mathrm{e}^{\beta x} f_-(x)$ gives

$$f_-(x) = \frac{1}{2\pi} \int_{-\infty - \mathrm{i}\beta}^{\infty - \mathrm{i}\beta} \bar{f}_-(k) \mathrm{e}^{-\mathrm{i}kx} \, \mathrm{d}k \tag{5.23}$$

provided $-\beta < -c$. Suppose $\bar{f}_-(k)$ can be continued above $\operatorname{Im} k = -c$, so that it is holomorphic in some region $\Omega_- \supset \{k : \operatorname{Im} k < -c\}$ except for singularities at $k = b_1, b_2, \cdots$. By the deformation theorem, the inversion contour $\Gamma_- = \{x - i\beta : -\infty < x < \infty\}$ may be deformed into Ω_- provided it passes *underneath* the singularities b_j of $\bar{f}_-$.

If there is a non-empty *overlap region* $\Omega = \Omega_+ \cap \Omega_- \setminus (\{a_j\} \cup \{b_j\})$, then the Fourier

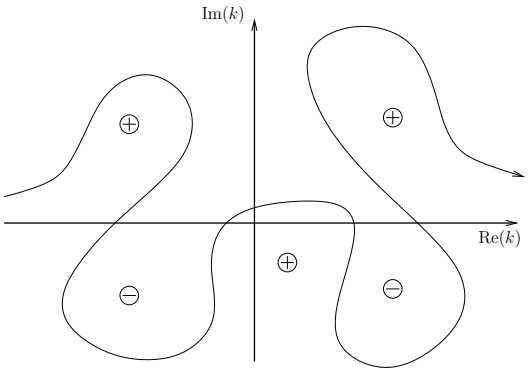

Figure 5.3: An inversion contour that passes above the singularities ($\oplus$) in $\bar{f}_+(k)$ and below the singularities ($\ominus$) in $\bar{f}_-(k)$.

transform of f is defined by

$$\bar{f}(k) = \bar{f}_+(k) + \bar{f}_-(k) \tag{5.24}$$

for $k \in \Omega$. Moreover, if Γ_+ and Γ_- can be deformed into the same contour $\Gamma \subset \Omega$, with Γ *above* the singularities of $\bar{f}_+(k)$ and *below* the singularities of $\bar{f}_-(k)$, as illustrated in figure 5.3, then

$$f(x) = \frac{1}{2\pi}\int_\Gamma \bar{f}(k)\mathrm{e}^{-\mathrm{i}kx}\,\mathrm{d}k. \tag{5.25}$$

Note that we need Γ to extend from $\operatorname{Re} k = -\infty$ to $\operatorname{Re} k = +\infty$ and $\{a_j\} \cap \{b_j\}$ to be empty, i.e. no singularities are shared by $\bar{f}_+(k)$ and $\bar{f}_-(k)$.

Example. Fourier transform of the Heaviside function The Heaviside function

$$\mathrm{H}(x) = \begin{cases} 0 & x < 0, \\ 1 & x > 0, \end{cases} \tag{5.26}$$

has Fourier transform

$$\bar{\mathrm{H}}(k) = \int_0^\infty \mathrm{e}^{\mathrm{i}kx}\,\mathrm{d}x = \left[\frac{\mathrm{e}^{\mathrm{i}kx}}{\mathrm{i}k}\right]_0^\infty = \frac{\mathrm{i}}{k} \tag{5.27}$$

provided $\operatorname{Im} k > 0$. We can analytically continue $\bar{\mathrm{H}}(k)$ into $\mathbb{C}\setminus\{0\}$ because i/k is holomorphic except for a simple pole at $k = 0$. When we invert, the inversion contour must pass *above* the pole at $k = 0$:

$$\mathrm{H}(x) = \frac{\mathrm{i}}{2\pi}\int_{-\infty+\mathrm{i}\alpha}^{\infty+\mathrm{i}\alpha} \frac{\mathrm{e}^{-\mathrm{i}kx}}{k}\,\mathrm{d}k, \qquad \text{where } \alpha > 0. \tag{5.28}$$

If $x < 0$ we can close the contour in the upper half plane to find by Cauchy's Theorem that $\mathrm{H}(x) = 0$ for $x < 0$. For $x > 0$ we need to close the contour in the lower half plane, and we pick up a residue contribution from the pole at the origin (note the minus sign since we are integrating clockwise round the pole) to find

$$\mathrm{H}(x) = -2\pi\mathrm{i} \times \left(\frac{\mathrm{i}}{2\pi}\right) = 1 \qquad \text{for } x > 0. \tag{5.29}$$

The inversion contours for $x > 0$ and $x < 0$ are illustrated in Figure 5.4.

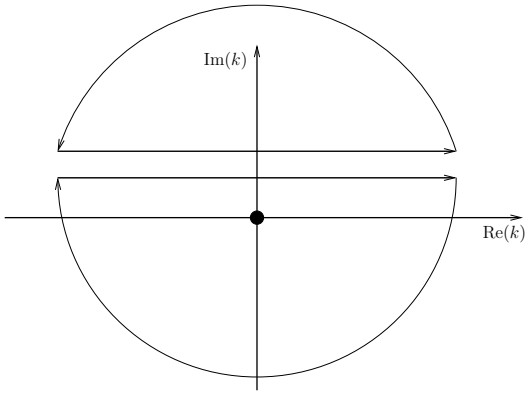

Figure 5.4: The inversion contours for the Heaviside function. For $x < 0$ we close in the upper half-plane; for $x > 0$ we close in the lower half-plane, picking up the residue from the pole at $k = 0$.

The Laplace transform

If we set $k = \mathrm{i}p$ (with p complex) and $\bar{f}_+(k) = \hat{f}_+(p)$, then the Fourier transform (5.18) takes the form

$$\bar{f}_+(k) = \hat{f}_+(p) = \int_0^\infty f_+(x) e^{-px}\,\mathrm{d}x, \tag{5.30}$$

while the inversion formula (5.22) is transformed to

$$f_+(x) = \frac{1}{2\pi\mathrm{i}} \int_{\alpha-\mathrm{i}\infty}^{\alpha+\mathrm{i}\infty} \hat{f}_+(p) e^{px}\,\mathrm{d}p. \tag{5.31}$$

Equation (5.30) defines the *Laplace transform* of a function $f_+(x) : [0, \infty) \mapsto \mathbb{R}$ such that $f_+(x) = O\left(\mathrm{e}^{cx}\right)$ as $x \to \infty$. Equation (5.31) is the Laplace transform inversion formula, where now α must be sufficiently large that the inversion contour lies to the *right* of any singularities of $\hat{f}(p)$, as illustrated in Figure 5.5. So we see that the Laplace transform is just a special case of the Fourier Transform if we allow complex values of k.

5.3 Complex Fourier transform with multifunctions

Example. Find a function $u(x, y)$ which satisfies Laplace's equation in the upper half-plane $y > 0$, which is bounded as $x^2 + y^2 \to \infty$ and which is equal to the Heaviside function on $y = 0$, that is $u(x, 0) = \mathrm{H}(x)$.

Solution. As we will see, it is straightforward to spot the appropriate harmonic function $u(x, y)$, but the aim of this example is to illustrate the solution procedure using the complex Fourier transform. The Fourier transform of $u(x, y)$ satisfies the problem

$$\frac{\partial^2 \bar{u}}{\partial y^2} - k^2 \bar{u} = 0 \qquad \text{in } y > 0, \tag{5.32a}$$

$$\bar{u} = \bar{\mathrm{H}}(k) = \frac{\mathrm{i}}{k} \qquad \text{at } y = 0, \tag{5.32b}$$

$$|\bar{u}| < \infty \qquad \text{as } y \to \infty. \tag{5.32c}$$

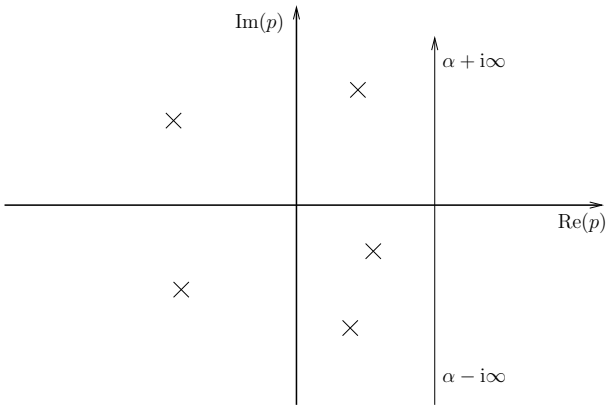

Figure 5.5: The Laplace transform inversion contour passes to the right of all singularities in $\hat{f}_+(p)$.

We recall that the Fourier transform $\bar{\mathrm{H}}(k)$ is defined for $\operatorname{Im} k > 0$ and can be analytically extended onto $\mathbb{C} \setminus \{0\}$.

As we found in equation (5.11), the general solution to (5.32a) which does not grow exponentially as $y \to \infty$ is $C(k)\mathrm{e}^{-|k|y}$ *if* k *is real*. When $k \in \mathbb{C}$, this approach does not work, since $|k|$ is not a holomorphic function of k so that none of the tools of complex analysis (e.g. Cauchy's theorems) can be used for the Fourier inversion.

To avoid this difficulty, we approximate k by a function that *is* holomorphic in a neighbourhood of the real k-axis, namely

$$|k| \approx |k|_\epsilon = \left(k^2 + \epsilon^2\right)^{1/2}, \tag{5.33}$$

where $0 < \epsilon \ll 1$. The branch of this multifunction is chosen such that the branch cuts are along the imaginary k-axis on the intervals $(-\mathrm{i}\infty, -\mathrm{i}\epsilon]$ and $[\mathrm{i}\epsilon, \mathrm{i}\infty)$, as shown in Figure 5.6, and $\left(k^2 + \epsilon^2\right)^{1/2} = \sqrt{k^2 + \epsilon^2} > 0$ when k is real. Then $|k|_\epsilon$ defines a function that is holomorphic on the cut complex plane, and $|k|_\epsilon \to |k|$ as $\epsilon \to 0$ when k is real.

Using this approximation, we write the solution for $\bar{u}$ as

$$\bar{u}(k, y) = \frac{\mathrm{i}}{k}\,\mathrm{e}^{-y\left(k^2+\epsilon^2\right)^{1/2}}. \tag{5.34}$$

Note that the solution (5.34) corresponds to solving the modified Helmholtz equation

$$\nabla^2 u = \epsilon^2 u \tag{5.35}$$

instead of Laplace's equation. The idea now is to invert (using contour integration) to find $u(x, y)$, and then let $\epsilon \to 0$. The inversion formula (5.22) gives

$$u(x, y) = \frac{\mathrm{i}}{2\pi} \int_\Gamma \mathrm{e}^{-y\left(k^2+\epsilon^2\right)^{1/2} - \mathrm{i}kx}\, \frac{\mathrm{d}k}{k}, \tag{5.36}$$

where the inversion contour Γ passes between the pole at $k = 0$ and the branch point at $k = \epsilon$, as shown in Figure 5.6. Now the contour used to evaluate $u(x, y)$ depends on the sign of x.

If x is negative, then to ensure that the exponential in (5.36) decays at infinity, we close the integration contour in the upper half-plane, as illustrated in Figure 5.7(a). This results

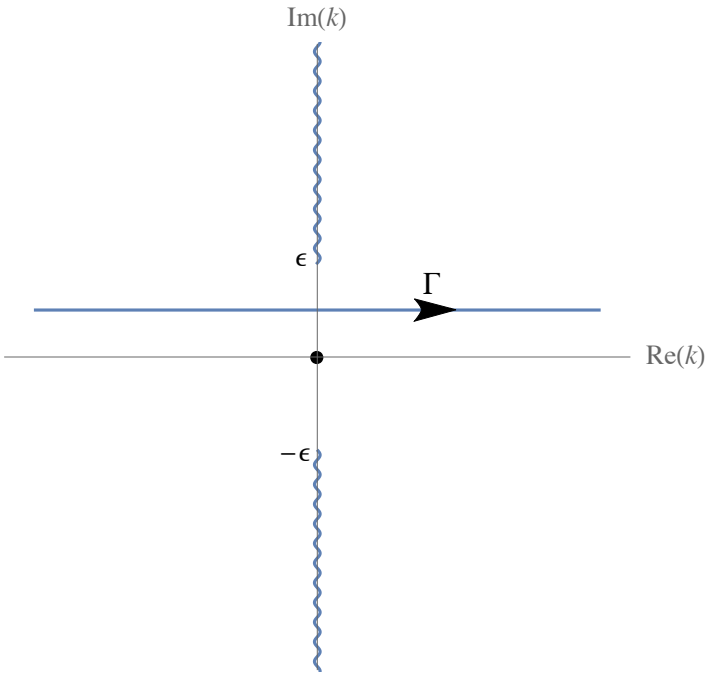

Figure 5.6: Inversion contour for (5.36) passing between the pole at $k = 0$ and the branch point at $k = \epsilon$. The branch cuts for the multifunction $\left(k^2 + \epsilon^2\right)^{1/2}$ are on the intervals $(-\mathrm{i}\infty, -\mathrm{i}\epsilon]$ and $[\mathrm{i}\epsilon, \mathrm{i}\infty)$ along the imaginary k-axis.

in two integrals along either side of the branch cut, which may be parameterised using $k = \mathrm{i}t$ with $t \in (\epsilon, \infty)$ and $\left(k^2 + \epsilon^2\right)^{1/2} = \pm\mathrm{i}\sqrt{t^2 - \epsilon^2}$ on $k = \mathrm{i}t \pm 0$. The resulting integrals may then be combined to give

$$u(x,y) = \frac{1}{\pi}\int_\epsilon^\infty \sin\left(y\sqrt{t^2-\epsilon^2}\right)\mathrm{e}^{tx}\,\frac{\mathrm{d}t}{t} \qquad \text{for } x < 0. \tag{5.37}$$

Letting $\epsilon \to 0$, we find

$$u(x,y) = \frac{1}{\pi}\int_0^\infty \sin(yt)\,\mathrm{e}^{tx}\,\frac{\mathrm{d}t}{t} = \frac{1}{\pi}\int_0^\infty \sin(r\sin\alpha)\,\mathrm{e}^{-r\cos\alpha}\,\frac{\mathrm{d}r}{r} \qquad \text{for } x < 0, \tag{5.38}$$

where $\sin\alpha = y/\sqrt{x^2+y^2}$ and $\cos\alpha = -x/\sqrt{x^2+y^2}$. By applying Cauchy's Theorem to the function e^{-z}/z on the closed contour sketched in Figure 5.8, we obtain

$$\lim_{\epsilon\to 0}\left\{\int_\epsilon^\infty \frac{\mathrm{e}^{-x}\,\mathrm{d}x}{x} - \int_\epsilon^\infty \mathrm{e}^{-r\cos\alpha}\big[\cos(r\sin\alpha) - \mathrm{i}\sin(r\sin\alpha)\big]\,\frac{\mathrm{d}r}{r} - \mathrm{i}\alpha\right\} = 0, \tag{5.39}$$

and the imaginary part gives

$$\int_0^\infty \mathrm{e}^{-r\cos\alpha}\sin(r\sin\alpha)\,\frac{\mathrm{d}r}{r} = \alpha. \tag{5.40}$$

Therefore the integral in (5.38) may be evaluated to give the solution

$$u(x,y) = \frac{1}{\pi}\,\tan^{-1}\left(\frac{y}{-x}\right) \qquad \text{for } x < 0. \tag{5.41}$$

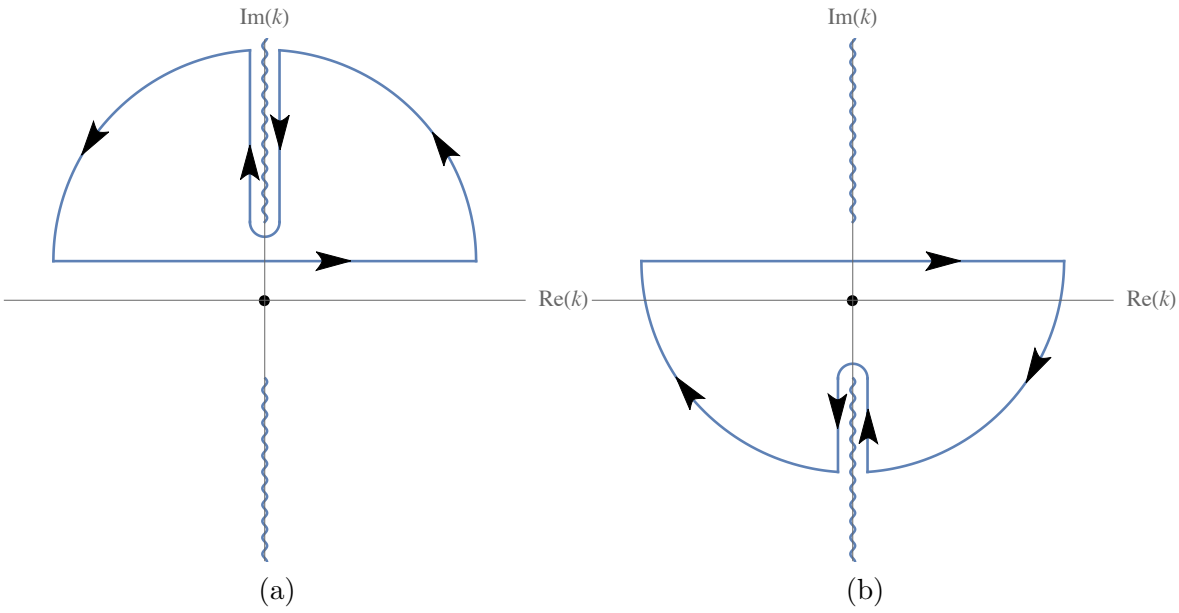

Figure 5.7: Inversion contours for (5.36). (a) If $x < 0$ the contour is closed in the upper half-plane. (b) If $x > 0$ the contour is closed in the lower half-plane, picking up the residue from the pole at $k = 0$.

If x is positive, then we evaluate (5.36) by closing the integration contour in the lower half-plane, as illustrated in Figure 5.7(b). This time we get two integrals along either side of the branch cut on the negative imaginary k-axis, as well as the residue from the pole at $k = 0$, resulting in

$$u(x, y) = 1 - \frac{1}{\pi} \int_0^\infty \sin(yt)\, \mathrm{e}^{-xt}\, \frac{\mathrm{d}t}{t} = 1 - \frac{1}{\pi} \tan^{-1}\left(\frac{y}{x}\right) \qquad \text{for } x > 0. \tag{5.42}$$

Finally, combining the solutions (5.41) and (5.42) in $x < 0$ and $x > 0$, we see that the solution is simply

$$u(x, y) = 1 - \frac{\theta}{\pi}, \tag{5.43}$$

where θ is the usual polar angle. As pointed out earlier, we might have spotted this simple solution of Laplace's equation straight away, either by using polar coordinates or by writing it as $1 - 1/\pi \operatorname{Im}(\log z)$.

5.4 Integral solutions of differential equations

Now we show how a class of linear ordinary differential equations may be solved by a generalised complex Fourier transform. We illustrate the general method using the simple first-order differential equation

$$\frac{\mathrm{d}y}{\mathrm{d}x} = xy. \tag{5.44}$$

Our aim is to represent the solution as a generalised Fourier integral

$$y(x) = \int_\Gamma g(\zeta) \mathrm{e}^{x\zeta}\, \mathrm{d}\zeta, \tag{5.45}$$

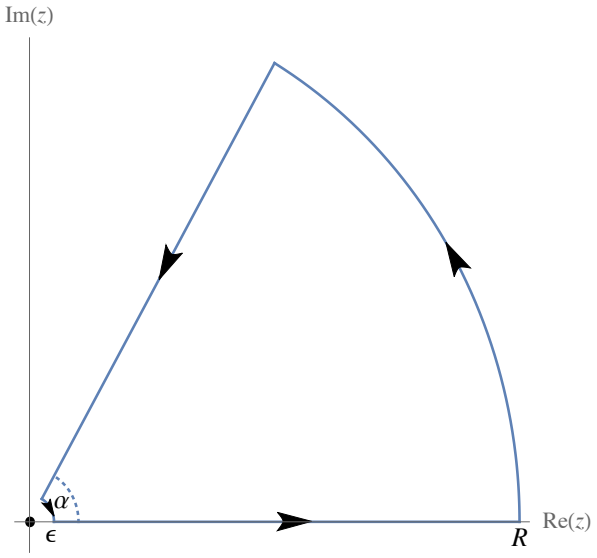

Figure 5.8: Closed contour for the integral of e^{-z}/z.

where both the function $g(\zeta)$ and the integration contour Γ are to be determined.

By differentiating under the integral sign and then integrating by parts, we get

$$\begin{aligned} 0 &= \frac{\mathrm{d}y}{\mathrm{d}x} - xy \\ &= \int_\Gamma \big(\zeta g(\zeta) - x g(\zeta)\big)\mathrm{e}^{x\zeta}\,\mathrm{d}\zeta \\ &= \Big[-g(\zeta)\mathrm{e}^{x\zeta}\Big]_\Gamma + \int_\Gamma \big(\zeta g(\zeta) + g'(\zeta)\big)\mathrm{e}^{x\zeta}\,\mathrm{d}\zeta. \end{aligned} \tag{5.46}$$

We require this equation to be satisfied for all x, and also the integration contour Γ to be independent of x. It follows that we will have a solution to the differential equation (5.44) only if

$$g'(\zeta) = -\zeta g(\zeta) \tag{5.47}$$

and the change in $g(\zeta)\mathrm{e}^{x\zeta}$ around Γ is zero. Integration of (5.47) gives

$$g(\zeta) = C\mathrm{e}^{-\zeta^2/2}, \tag{5.48}$$

for some constant C, and hence

$$y(x) = C\int_\Gamma \mathrm{e}^{x\zeta-\zeta^2/2}\,\mathrm{d}\zeta. \tag{5.49}$$

For the integral to exist, we need the integrand to decay as $|\zeta| \to \infty$, which is true provided $\mathrm{Re}\left[\zeta^2\right] > 0$, which occurs in two sectors $-\pi/4 < \arg\zeta < \pi/4$ and $3\pi/4 < \arg\zeta < 5\pi/4$. Thus the contour Γ must start and end in one of these "valleys". If Γ starts and ends in the same valley the integral (5.49) evaluates to zero by Cauchy's Theorem. Thus there is just one independent solution, corresponding to a contour Γ which starts in one valley and ends in the other, as shown in Figure 5.9. For example, we can simply take Γ along the real axis to

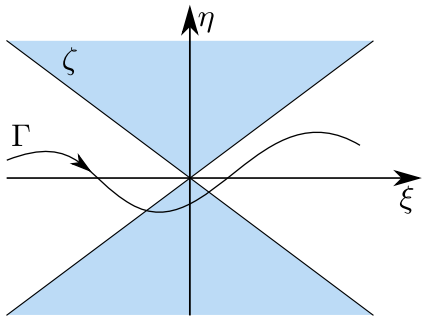

Figure 5.9: A possible integration contour Γ for equation (5.49).

obtain

$$y(x) = C\int_{-\infty}^{\infty} \mathrm{e}^{x\xi-\zeta^2/2}\,\mathrm{d}\xi = Ce^{x^2/2}\int_{-\infty}^{\infty} \mathrm{e}^{-(x-\xi)^2/2}\,\mathrm{d}\xi = C\sqrt{2\pi}\,\mathrm{e}^{x^2/2}. \tag{5.50}$$

Of course we could easily have found the solution (5.50) directly from the first-order ODE (5.44). The method becomes more useful when applied to higher-order ODEs which are not directly solvable in terms of elementary functions. For example, consider **Airy's equation**

$$\frac{\mathrm{d}^2y}{\mathrm{d}x^2} + xy = 0. \tag{5.51}$$

We again seek a solution for $y(x)$ in the form of the generalised Fourier integral (5.45), and again differentiate under the integral and integrate by parts, this time arriving at

$$\Big[g(\zeta)\mathrm{e}^{x\zeta}\Big]_\Gamma + \int_\Gamma \left(\zeta^2 g(\zeta) - g'(\zeta)\right)\mathrm{e}^{x\zeta}\,\mathrm{d}\eta = 0. \tag{5.52}$$

Hence, Airy's equation (5.51) is satisfied only if

$$g'(\zeta) = \zeta^2 g(\zeta) \qquad \text{and} \qquad \Big[g(\zeta)\mathrm{e}^{x\zeta}\Big]_\Gamma = 0. \tag{5.53}$$

Thus, $g(\zeta) = Ce^{\zeta^3/3}$, where C is an arbitrary constant, and

$$y(x) = C\int_\Gamma \mathrm{e}^{x\zeta+\zeta^3/3}\,\mathrm{d}\zeta. \tag{5.54}$$

Now the integrand decays at infinity in three sectors: either $\pi/6 < \arg\zeta < \pi/2$, or $5\pi/6 < \arg\zeta < 7\pi/6$, or $-\pi/2 < \arg\zeta < -\pi/6$. Therefore, the integration contour Γ should start and end as $\zeta \to \infty$ in one of these sectors. Since the integrand in (5.54) is entire, the integral will be nonzero only if Γ begins and ends in two different sectors. Therefore there are three possibilities for Γ, as shown in Figure 5.10, leading to three distinct solutions for $y(x)$. However, by contour deformation we can write

$$\int_{\Gamma_1} \mathrm{e}^{x\zeta+\zeta^3/3}\,\mathrm{d}\zeta + \int_{\Gamma_2} \mathrm{e}^{x\zeta+\zeta^3/3}\,\mathrm{d}\zeta = \int_{\Gamma_3} \mathrm{e}^{x\zeta+\zeta^3/3}\,\mathrm{d}\zeta, \tag{5.55}$$

so there are only two independent solutions, as expected for the second-order linear ODE (5.51).

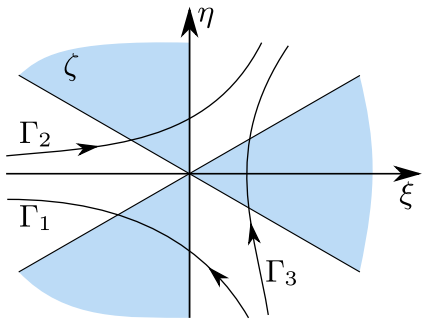

Figure 5.10: Three integration contours for Airy's equation.

This method is equivalent to formally taking a Fourier transform of the equation, and then choosing an inversion contour so that the resulting solution exists. Note that if there was a coefficient of x^2 in the ODE, then integration by parts would lead to a second-order ODE for $g(\zeta)$, which might be just as hard to solve as the original ODE for $y(x)$. The coefficient of x in the Airy equation (5.51) produced a first-order ODE (5.53) for $g(\zeta)$ and thus apparently a single integral solution (5.54). However, the freedom in the choice of the integration contour Γ gave us the required two independent solutions.

6 The Wiener-Hopf method

6.1 Example: an ODE problem

We will first illustrate the ideas underlying the Wiener–Hopf method by using it to solve a simple ODE problem, before moving onto more complicated integral equations and mixed-boundary-value problems. Suppose the complex-valued function $y(x)$ satisfies

$$\frac{\mathrm{d}^2y}{\mathrm{d}x^2} + b^2y = 0 \quad \text{for } x < 0, \qquad \frac{\mathrm{d}^2y}{\mathrm{d}x^2} + a^2y = 0 \quad \text{for } x > 0, \tag{6.1a}$$

with

$$y(0+) - y(0-) = 0, \qquad \frac{\mathrm{d}y}{\mathrm{d}x}(0+) - \frac{\mathrm{d}y}{\mathrm{d}x}(0-) = 1, \tag{6.1b}$$

and $y(x) \to 0$ as $|x| \to \infty$, where $a, b \in \mathbb{C}$ with $a \neq b$ and $\operatorname{Im} a > 0$ and $\operatorname{Im} b > 0$. The problem (6.1) may readily be solved via elementary methods; here we will show how to obtain the solution by taking a complex Fourier transform and using analytic continuation.

We begin by assuming that $y(x) = O\left(\mathrm{e}^{\alpha x}\right)$ as $x \to \infty$ and $y(x) = O\left(\mathrm{e}^{\beta x}\right)$ as $x \to -\infty$ for some real constants $\alpha < \beta$ whose existence we shall need to verify *a posteriori* (once we have found the solution). We then define the half-range functions

$$y_+(x) = \begin{cases} 0 & x < 0, \\ y(x) & x > 0, \end{cases} \qquad y_-(x) = \begin{cases} y(x) & x < 0, \\ 0 & x > 0, \end{cases} \tag{6.2}$$

so that

$$\bar{y}_+(k) = \int_0^\infty y(x)\mathrm{e}^{\mathrm{i}kx}\,\mathrm{d}x \tag{6.3}$$

is holomorphic in $\operatorname{Im} k > \alpha$, and

$$\bar{y}_-(k) = \int_{-\infty}^0 y(x)\mathrm{e}^{\mathrm{i}kx}\,\mathrm{d}x \tag{6.4}$$

is holomorphic in $\operatorname{Im} k < \beta$.

Integration by parts gives

$$\begin{aligned} 0 &= \int_0^\infty \left(y''(x) + a^2y(x)\right)\mathrm{e}^{\mathrm{i}kx}\,\mathrm{d}x \\ &= -y'(0+) + \mathrm{i}ky(0+) + \left(a^2 - k^2\right)\bar{y}_+(k), \end{aligned} \tag{6.5}$$

provided $\bar{y}_+(k)$ exists and $(y'(x) - \mathrm{i}ky(x))\mathrm{e}^{\mathrm{i}kx} \to 0$ as $x \to \infty$, which is the case for $\operatorname{Im} k > \alpha$. Similarly,

$$0 = y'(0-) - \mathrm{i}ky(0-) + (b^2 - k^2)\bar{y}_-(k) \tag{6.6}$$

provided $\operatorname{Im} k < \beta$. Using the jump conditions (6.1b) at $x = 0$ to eliminate the unknowns $y(0\pm)$ and $y'(0\pm)$ gives

$$\left(k^2 - a^2\right) \bar{y}_+(k) + \left(k^2 - b^2\right) \bar{y}_-(k) = -1, \tag{6.7}$$

for $\alpha < \operatorname{Im} k < \beta$. This is just one equation relating the two unknown functions $\bar{y}_-(k)$ and $\bar{y}_+(k)$. However, remarkably there is enough auxiliary information to determine both functions, using the *Wiener–Hopf method*.

Provided $k \neq a$ and $k \neq -b$, we can divide (6.7) through by $(k-a)(k+b)$ and rearrange to obtain

$$\left(\frac{k+a}{k+b}\right) \bar{y}_+(k) + \left(\frac{k-b}{k-a}\right) \bar{y}_-(k) = -\frac{1}{(k-a)(k+b)} = \frac{1}{a+b}\left(\frac{1}{k+b} - \frac{1}{k-a}\right) \tag{6.8}$$

so that

$$\left(\frac{k+a}{k+b}\right) \bar{y}_+(k) - \frac{1}{(a+b)(k+b)} = -\left(\frac{k-b}{k-a}\right) \bar{y}_-(k) - \frac{1}{(a+b)(k-a)}. \tag{6.9}$$

The left-hand side of (6.9) is holomorphic in $\operatorname{Im} k > \alpha_1 = \max(\alpha, -\operatorname{Im} b)$, while the right-hand side is holomorphic in $\operatorname{Im} k < \beta_1 = \min(\beta, \operatorname{Im} a)$. Since $\alpha < \beta$, by assumption, and $-\operatorname{Im} b < 0 < \operatorname{Im} a$, it follows that $\alpha_1 < \beta_1$ so that these half-planes intersect in the **overlap strip** $\alpha_1 < \operatorname{Im} k < \beta_1$. Hence, the left- and right-hand sides of (6.9) are equal on a dense set of points, and therefore the right-hand side is the analytic continuation of the left-hand side into the lower half-plane, so together they define an entire function, $E(k)$, that is

$$\left(\frac{k+a}{k+b}\right) \bar{y}_+(k) - \frac{1}{(a+b)(k+b)} = -\left(\frac{k-b}{k-a}\right) \bar{y}_-(k) - \frac{1}{(a+b)(k-a)} = E(k). \tag{6.10}$$

Since $\bar{y}_+(k) \to 0$ as $k \to \infty$ in $\operatorname{Im} k > \alpha_1$ and $\bar{y}_-(k) \to 0$ as $k \to \infty$ in $\operatorname{Im} k < \beta_1$, we deduce that $E(k) \to 0$ as $k \to \infty$ and hence by Liouville's theorem, $E(k) \equiv 0$. Thus we obtain unique solutions for *both* functions $\bar{y}_\pm(k)$, namely

$$\bar{y}_+(k) = \frac{1}{(a+b)(k+a)}, \qquad \bar{y}_-(k) = -\frac{1}{(a+b)(k-b)}, \tag{6.11}$$

which may easily be inverted, recalling that the inversion contour must pass *above* the pole $k = -a$ in $y_+(k)$ and *below* the pole $k = b$ in $y_-(k)$.

Thus we obtain the solution

$$y(x) = \begin{cases} \dfrac{\mathrm{e}^{-\mathrm{i}bx}}{\mathrm{i}(a+b)} & x < 0, \\ \dfrac{\mathrm{e}^{\mathrm{i}ax}}{\mathrm{i}(a+b)} & x > 0, \end{cases} \tag{6.12}$$

and we can confirm *a posteriori* our initial assumptions: $y(x) = O\left(\mathrm{e}^{\alpha x}\right)$ as $x \to \infty$ and $y(x) = O\left(\mathrm{e}^{\beta x}\right)$ as $x \to -\infty$, where $\alpha = -\operatorname{Im} a$ and $\beta = \operatorname{Im} b$, so that $\alpha < \beta$, as required.

6.2 The Wiener-Hopf method

The canonical Wiener–Hopf problem is to find functions $\bar{u}_+(k)$ holomorphic in $\operatorname{Im} k > \alpha$ and $\bar{v}_-(k)$ holomorphic in $\operatorname{Im} k < \beta$ such that

$$F(k)\bar{u}_+(k) + \bar{v}_-(k) = G(k) \quad \text{on } \Omega = \{k \in \mathbb{C} : \alpha < \operatorname{Im} k < \beta\}, \tag{6.13}$$

where $F(k)$, $G(k)$ are prescribed holomorphic functions and $F(k) \neq 0$ on Ω. Here, as in the example from §6.1, we use the subscript $_+$ to indicate a function that is holomorphic on some upper half-plane, and $_-$ to indicate a function holomorphic on a lower half-plane.

The general Wiener–Hopf method for solving this problem is as follows.

1. ***Product* decomposition of $F(k)$**
   Find $M_+(k)$ holomorphic in $\operatorname{Im} k > \alpha_1$ and $N_-(k)$ holomorphic in $\operatorname{Im} k < \beta_1$ such that $\alpha \leq \alpha_1 < \beta_1 \leq \beta$ and

   $$F(k) = \frac{M_+(k)}{N_-(k)} \quad \text{on } \Omega_1 = \{k \in \mathbb{C} : \alpha_1 < \operatorname{Im} k < \beta_1\} \subseteq \Omega. \tag{6.14}$$

   We can assume that $M_+(k) \neq 0$ and $N_-(k) \neq 0$ on Ω_1 by cancelling common factors. If we can find such functions $M_+(k)$ and $N_-(k)$, then we can transform (6.13) to

   $$M_+(k)\bar{u}_+(k) + N_-(k)\bar{v}_-(k) = N_-(k)G(k) \quad \text{on } \Omega_1. \tag{6.15}$$

2. ***Sum* decomposition of $N_-(k)G(k)$**
   Find $P_+(k)$ holomorphic in $\operatorname{Im} k > \alpha_2$ and $Q_-(k)$ holomorphic in $\operatorname{Im} k < \beta_2$ such that $\alpha_1 \leq \alpha_2 < \beta_2 \leq \beta_1$ and

   $$N_-(k)G(k) = P_+(k) + Q_-(k) \quad \text{on } \Omega_2 = \{k \in \mathbb{C} : \alpha_2 < \operatorname{Im} k < \beta_2\} \subseteq \Omega_1. \tag{6.16}$$

   Given the functions $P_+(k)$ and $Q_-(k)$, we can then transform (6.15) to

   $$M_+(k)\bar{u}_+(k) + N_-(k)\bar{v}_-(k) = P_+(k) + Q_-(k) \quad \text{on } \Omega_2. \tag{6.17}$$

3. **Analytic continuation**
   Define

   $$E(k) = M_+(k)\bar{u}_+(k) - P_+(k) = Q_-(k) - N_-(k)\bar{v}_-(k) \quad \text{on } \Omega_2. \tag{6.18}$$

   Since the two expressions for $E(k)$ are equal on a dense set of points Ω_2, we can combine them to analytically continue $E(k)$ outside Ω_2 as follows:

   $$E(k) = \begin{cases} M_+(k)\bar{u}_+(k) - P_+(k) & \operatorname{Im} k > \alpha_2, \\ Q_-(k) - N_-(k)\bar{v}_-(k) & \operatorname{Im} k < \beta_2. \end{cases} \tag{6.19}$$

   The resulting function $E(k)$ is therefore entire.

4. **Behaviour at infinity**
   Since $M_+(k)$, $P_+(k)$, $N_-(k)$, and $Q_-(k)$ are in principle known functions of k, we know their behaviour as $|k| \to \infty$.

   The behaviour of $\bar{u}_+(k)$ as $k \to \infty$ in $\operatorname{Im} k > \alpha_2$ and the behaviour of $\bar{v}_-(k)$ as $k \to \infty$ in $\operatorname{Im} k < \beta_2$ are in principle determined by the behaviours of $u_+(x)$ and $v_-(x)$ as $x \to 0_\pm$.

In general this step relies on asymptotic analysis of the relevant Fourier integrals, but in this course we will assume that the required behaviour is given.

Then we know the behaviour of $E(k)$ as $|k| \to \infty$, and we can then apply Liouville's theorem as follows.

- If $E(k) \to$ constant as $|k| \to \infty$, then $E(k)$ is entire and bounded, and therefore a constant by Liouville's theorem. In particular if $E(k) \to 0$ as $|k| \to \infty$, then $E(k) \equiv 0$.
- If $E(k) = O\left(k^n\right)$ as $|k| \to \infty$, where $n \in \mathbb{N}$, then $E(k)$ is a polynomial of degree n.

To solve the system for $n \geq 0$, we therefore need to determine $n+1$ coefficients from the boundary conditions. This means that in practice we want n to be as small as possible.

5. **Invert**
   To find $u_+(x)$ and $v_-(x)$, we need to apply Fourier inversion to

$$\bar{u}_+(k) = \frac{P_+(k) + E(k)}{M_+(k)} \qquad \text{and} \qquad \bar{v}_-(k) = \frac{Q_-(k) - E(k)}{N_-(k)}. \tag{6.20}$$

   In principle, analytic continuation allows the inversion contours to be deformed outside Ω_2 but they must still pass *above* the singularities in $P_+(k)$, $M_+(k)$, and *below* the singularities in $Q_-(k)$, $N_-(k)$.

Remarks

- Steps 1 and 2 in the Wiener–Hopf method are called **Wiener–Hopf decompositions** (product and sum, respectively). These are not unique, for example, the sum decomposition (6.16) would be unaffected if we add any entire function of k to $P_+(k)$ and subtract the same entire function from $Q_-(k)$. Our aim is to find the decomposition that makes analysing the behaviour at infinity (step 4) as straightforward as possible.
- In many applications we can spot the decompositions, though we will describe a constructive method below.

Wiener–Hopf decomposition

General method for sum decomposition

Suppose $G(z)$ is holomorphic in Ω where $\Omega = \{z \in \mathbb{C} : \alpha < \operatorname{Im} z < \beta\}$ and $G(z) \to 0$ as $z \to \infty$ in Ω. By Cauchy's integral formula we can write $G(z)$ as

$$G(z) = \frac{1}{2\pi \mathrm{i}} \int_\Gamma \frac{G(\zeta)}{\zeta - z} \, \mathrm{d}\zeta, \tag{6.21}$$

where $\Gamma \in \Omega$ is the contour illustrated in Figure 6.1, whose interior is the rectangular region $-R < \operatorname{Re} z < R$, $\alpha < \gamma_+ < \operatorname{Im} z < \gamma_- < \beta$. Since $G(\zeta) \to 0$ as $|\zeta| \to \infty$ in Ω, the contribution from the vertical sides tends to zero as $R \to \infty$, giving

$$G(z) = G_+(z) - G_-(z) \quad \text{for } \gamma_+ < \operatorname{Im} z < \gamma_-, \tag{6.22}$$

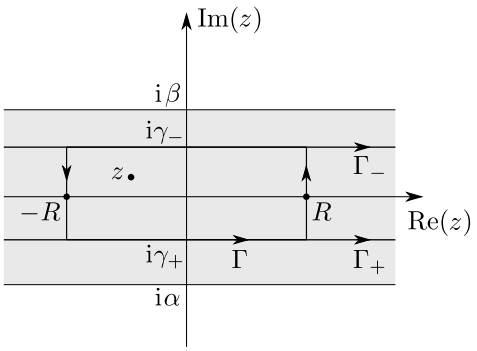

Figure 6.1: Integration contour for sum decomposition.

where

$$G_\pm(z) = \frac{1}{2\pi \mathrm{i}} \int_{\Gamma_\pm} \frac{G(\zeta)}{\zeta - z}\, \mathrm{d}\zeta \tag{6.23}$$

and $\Gamma_\pm = \{x + \mathrm{i}\gamma_\pm : -\infty < x < \infty\}$. Note that Γ_+ passes underneath z, while Γ_- passes above z. Since $G_\pm(z)$ is holomorphic everywhere except on $\Gamma_\pm$, we deduce that $G_+(z)$ is holomorphic in $\operatorname{Im} z > \gamma_+$ and $G_-(z)$ is holomorphic in $\operatorname{Im} z < \gamma_-$.

General method for product decomposition

Here the trick is to take logs to turn product decomposition into sum decomposition. Suppose $F(z)$ is holomorphic in Ω, that $F(z) \neq 0$ on Ω and that $F(z) \to 1$ as $z \to \infty$ in Ω, where Ω is again the strip $\{z \in \mathbb{C} : \alpha < \operatorname{Im} z < \beta\}$. Since $F(z)$ is non-zero, $\log F(z)$ is holomorphic on Ω and $\log F(z) \to 0$ as $z \to \infty$ in Ω. Hence, we can set $G(z) = \log F(z)$ in (6.22) to obtain

$$\log F(z) = G_+(z) - G_-(z) \quad \text{for } \gamma_+ < \operatorname{Im} z < \gamma_-. \tag{6.24}$$

Defining $F_\pm(z) = \mathrm{e}^{G_\pm(z)}$ on Ω, we deduce that

$$F(z) = \frac{\mathrm{e}^{G_+(z)}}{\mathrm{e}^{G_-(z)}} = \frac{F_+(z)}{F_-(z)} \quad \text{for } \gamma_+ < \operatorname{Im} z < \gamma_-, \tag{6.25}$$

where

$$F_\pm(z) = \exp\left(\frac{1}{2\pi \mathrm{i}} \int_{\Gamma_\pm} \frac{\log F(\zeta)}{\zeta - z}\, \mathrm{d}\zeta\right) \quad \text{for } \gamma_+ < \operatorname{Im} z < \gamma_-, \tag{6.26}$$

and $F_\pm(z)$ are holomorphic on $\operatorname{Im} z > \gamma_+$ and on $\operatorname{Im} z < \gamma_-$ respectively.

Example. Suppose we wish to find a product decomposition of

$$F(z) = \frac{z^2 - a^2}{z^2 - b^2} = \frac{(z-a)(z+a)}{(z-b)(z+b)} \tag{6.27}$$

where $a \neq b \in \mathbb{C}$, with $\operatorname{Im} a > 0$ and $\operatorname{Im} b > 0$. With the overlap region $-\gamma < \operatorname{Im} z < \gamma$, where $\gamma = \min(\operatorname{Im} a, \operatorname{Im} b)$, as shown in Figure 6.2, we find by inspection that

$$F(z) = \frac{F_+(z)}{F_-(z)}, \qquad \text{where} \quad F_+(z) = \frac{z+a}{z+b}, \qquad F_-(z) = \frac{z-b}{z-a}. \tag{6.28}$$

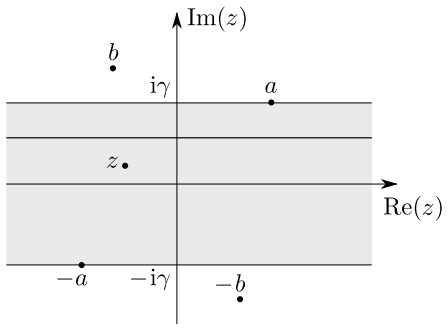

Figure 6.2: The overlap region $-\gamma < \operatorname{Im} z < \gamma$ for $F(z) = \left(z^2 - a^2\right) / \left(z^2 - b^2\right)$.

Thus $F_+(z)$ is holomorphic in $\operatorname{Im} z > -\gamma$ and $F_-(z)$ is holomorphic in $\operatorname{Im} z < \gamma$.

Clearly the factorisation (6.28) is not unique: We could for example multiply both $F_-(z)$ and $F_+(z)$ by any entire function. However, the decomposition (6.28) is the only one for which the overlap region includes $\operatorname{Im} z = 0$ and such that $F_\pm(z) \to 1$ as $z \to \infty$. If we multiplied through by a nontrivial entire function, for example a polynomial in z, the behaviour of $F_\pm(z)$ at infinity would be more complicated.

Now we show how the same decomposition may be found from the general formula (6.26). We write

$$\log F(z) = \big\{\log(z-a) - \log(z-b)\big\} + \big\{\log(z+a) - \log(z+b)\big\}, \tag{6.29}$$

and then consider each of the terms in turn. First consider

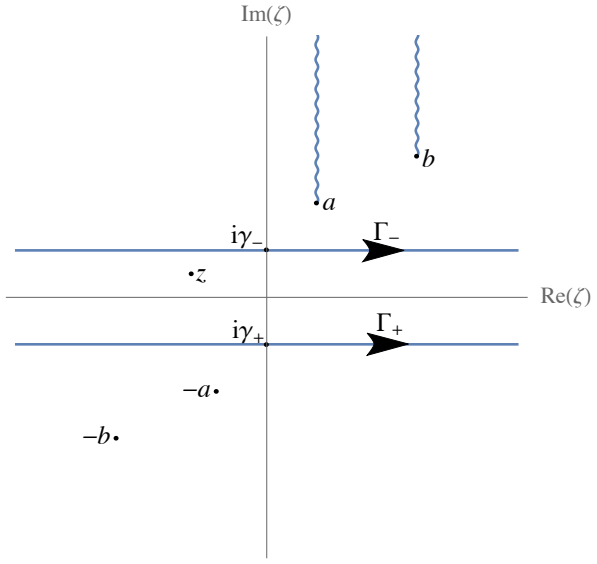

Figure 6.3: Integration contours for the integrals $I_\pm(z)$ defined in equation (6.30).

$$I_\pm(z) = \frac{1}{2\pi \mathrm{i}} \int_{-\infty+\mathrm{i}\gamma_\pm}^{\infty+\mathrm{i}\gamma_\pm} \frac{\log(\zeta-a) - \log(\zeta-b)}{\zeta - z}\,\mathrm{d}\zeta, \tag{6.30}$$

where $-\gamma < \gamma_+ < \operatorname{Im} z < \gamma_- < \gamma$. As shown in Figure 6.3, the integrand in (6.30) has singularities at $\zeta = a$, $\zeta = b$, but may be analytically continued into $\operatorname{Im}\zeta < \gamma_-$ except for the

pole at $\zeta = z$. By closing the contours $\Gamma_\pm$ at $-\mathrm{i}\infty$ and using Cauchy's Residue Theorem, we deduce that

$$I_+(z) = 0, \qquad I_-(z) = -\log(z-a) + \log(z-b), \tag{6.31}$$

where the minus sign comes from the clockwise orientation of the integration contour. Similarly, with

$$J_\pm(z) = \frac{1}{2\pi\mathrm{i}} \int_{-\infty+\mathrm{i}\gamma_\pm}^{\infty+\mathrm{i}\gamma_\pm} \frac{\log(\zeta+a) - \log(\zeta+b)}{\zeta - z}\,\mathrm{d}\zeta, \tag{6.32}$$

the branch points are at $\zeta = -a$, $-b$, and we can close the integration contours at $+\mathrm{i}\infty$ to get

$$J_+(z) = \log(z+a) - \log(z+b), \qquad J_-(z) = 0, \tag{6.33}$$

Combining (6.30) and (6.32), we get

$$\frac{1}{2\pi\mathrm{i}} \int_{\Gamma_+} \frac{\log F(\zeta)}{\zeta - z}\,\mathrm{d}\zeta = \log(z+a) - \log(z+b), \tag{6.34a}$$

$$\frac{1}{2\pi\mathrm{i}} \int_{\Gamma_-} \frac{\log F(\zeta)}{\zeta - z}\,\mathrm{d}\zeta = -\log(z-a) + \log(z-b), \tag{6.34b}$$

and therefore the general formula (6.26) produces

$$F_+(z) = \frac{z+a}{z+b}, \qquad F_-(z) = \frac{z-b}{z-a}, \tag{6.35}$$

in agreement with the previously spotted decomposition (6.28).

6.3 Wiener–Hopf applied to an integral equation

Problem. Find a smooth bounded function $f(x)$ such that

$$\int_0^\infty K(x-t) f(t)\,\mathrm{d}t = f(x) \quad \text{for } x \geq 0, \tag{6.36}$$

where $K(x) = \mathrm{e}^{-|x|}$ for $-\infty < x < \infty$.

Solution. If this were a full range integral equation ($-\infty < x < \infty$), then we could solve it easily by taking a Fourier transform. Our first step is thus to express (6.36) as a full-range integral equation. By defining

$$f_+(x) = \begin{cases} 0 & x < 0, \\ f(x) & x > 0, \end{cases} \qquad h_-(x) = \begin{cases} \displaystyle\int_0^\infty K(x-t) f(t)\,\mathrm{d}t & x < 0, \\ 0 & x > 0, \end{cases} \tag{6.37}$$

we can rewrite (6.36) as

$$\int_{-\infty}^\infty K(x-t) f_+(t)\,\mathrm{d}t = f_+(x) + h_-(x) \quad \text{for } -\infty < x < \infty. \tag{6.38}$$

Now we can take the Fourier transform of the full-range equation (6.38) and use the Convolution Theorem to get

$$\bar{K}(k)\,\bar{f}_+(k) = \bar{f}_+(k) + \bar{h}_-(k). \tag{6.39}$$

Since $f(x)$ is assumed to be bounded, $\bar{f}_+(k)$ is holomorphic in $\operatorname{Im} k > 0$. Since, for $x < 0$,

$$h_-(x) = \mathrm{e}^x \int_0^\infty \mathrm{e}^{-t} f(t)\,\mathrm{d}t = O\left(\mathrm{e}^x\right) \quad \text{as } x \to -\infty, \tag{6.40}$$

it follows that $\bar{h}_-(k)$ is holomorphic in $\operatorname{Im} k < 1$. Hence both $\bar{f}_+(k)$ and $\bar{h}_-(k)$ are holomorphic in the overlap strip $0 < \operatorname{Im} k < 1$, and the problem (6.39) may be solved by the Wiener–Hopf technique.

First we calculate

$$\bar{K}(k) = \int_{-\infty}^{\infty} \mathrm{e}^{-|x|+\mathrm{i}kx}\,\mathrm{d}x = \frac{2}{1+k^2}, \tag{6.41}$$

and substitute into (6.39) to get

$$\frac{1-k^2}{1+k^2}\,\bar{f}_+(k) = \bar{h}_-(k) \quad \text{for } 0 < \operatorname{Im} k < 1. \tag{6.42}$$

We factorise $\left(1-k^2\right) / \left(1+k^2\right)$ using

$$\frac{1-k^2}{1+k^2} = \frac{K_+(k)}{K_-(k)}, \qquad \text{where } K_+(k) = \frac{1-k^2}{k+\mathrm{i}}, \qquad K_-(k) = k-\mathrm{i}, \tag{6.43}$$

so that $K_+(k)$ is holomorphic in $\operatorname{Im} k > -1$ and $K_-(k)$ is entire. Hence,

$$\frac{1-k^2}{k+\mathrm{i}}\,\bar{f}_+(k) = (k-\mathrm{i})\bar{h}_-(k) = E(k) \text{ (say)} \quad \text{for } 0 < \operatorname{Im} k < 1, \tag{6.44}$$

with the left-hand side holomorphic in $\operatorname{Im} k > 0$ and the right-hand side holomorphic in $\operatorname{Im} k < 1$. Thus the right-hand side of (6.44) is the analytic continuation of the left-hand side of (6.44) into the lower half-plane, so together they define an entire function $E(k)$.

To pin down $E(k)$, we need to consider the behaviour of the functions in equation (6.44) as $k \to \infty$. It may be shown that, since $f(x)$ is assumed to be smooth and bounded on $(0, \infty)$, it follows that $\bar{f}_+(k)$ is $O\left(k^{-1}\right)$ as $k \to \infty$ in $\operatorname{Im} k > 0$. Similarly, assuming that $h_-(x)$ is smooth and bounded on $(-\infty, 0)$, it follows that $h_-(x) = O\left(k^{-1}\right)$ as $k \to \infty$ in $\operatorname{Im} k < 1$. The detailed asymptotic analysis required to prove these results is not required for this course: for completeness a simple derivation is given below.

Given that $\bar{f}_+(k)$ and $\bar{h}_-(k)$ are both $O\left(k^{-1}\right)$ as $k \to \infty$ in their respective half-planes, we deduce from equation (6.44) that $E(k) \to C$, a constant, as $k \to \infty$, and Liouville's theorem implies that that $E(k) \equiv C$. Hence we find

$$\bar{f}_+(k) = \frac{C(k+\mathrm{i})}{1-k^2}, \tag{6.45}$$

so the solution is given by

$$f_+(x) = \frac{C}{2\pi} \int_\Gamma \frac{(k+\mathrm{i})\mathrm{e}^{-\mathrm{i}kx}}{1-k^2}\,\mathrm{d}k, \tag{6.46}$$

where the inversion contour Γ lies in the strip $0 < \operatorname{Im} k < 1$ and thus passes *above* the poles of $\bar{f}_+(k)$ at $k = \pm 1$. By analytic continuation of $\bar{f}_+(k)$ into the lower half-plane, we can close the contour at $-\infty \mathrm{i}$ to obtain the solution

$$f(x) = f_+(x) = -2\pi\mathrm{i}\left(\operatorname{res}\left[\bar{f}_+(k)\mathrm{e}^{-\mathrm{i}kx}; -1\right] + \operatorname{res}\left[\bar{f}_+(k)\mathrm{e}^{-\mathrm{i}kx}; 1\right]\right) = \mathrm{i}C(\cos x + \sin x), \quad (6.47)$$

where C is an arbitrary constant.

Finally, we verify our claim about the asymptotic behaviour of $f_+(k)$ as $k \to \infty$. A simple approach is to assume that $f_+(x)$ is differentiable, with bounded derivative $f'_+(x)$, and then integrate by parts to get

$$\begin{aligned} \bar{f}_+(k) &= \int_0^\infty f_+(x)\mathrm{e}^{\mathrm{i}kx}\,\mathrm{d}x \\ &= \left[\frac{f_+(x)\mathrm{e}^{\mathrm{i}kx}}{\mathrm{i}k}\right]_0^\infty + \frac{\mathrm{i}}{k}\int_0^\infty f'_+(x)\mathrm{e}^{\mathrm{i}kx}\,\mathrm{d}x. \end{aligned} \quad (6.48)$$

In the first integrated term, the $x = \infty$ limit evaluates to zero provided $\operatorname{Im} k > 0$. In the second term, the integral is bounded, and indeed tends to zero as $k \to \infty$ with $\operatorname{Im} k > 0$ (this is an instance of the *Riemann–Lebesgue Lemma*). Therefore we have

$$\bar{f}_+(k) \sim \frac{\mathrm{i}f_+(0)}{k} + o\left(k^{-1}\right) \quad \text{as } k \to \infty \text{ with } \operatorname{Im} k > 0 \quad (6.49)$$

as required.

6.4 A mixed boundary value problem

The temperature $u(x, y)$ in an inviscid fluid flowing uniformly past a heated semi-infinite plate is governed by the partial differential equation

$$\nabla^2 u = \frac{\partial u}{\partial x} \quad \text{in } y > 0, \quad (6.50a)$$

with the boundary and far field conditions

$$u = 1 \quad \text{on } y = 0,\ x > 0, \qquad \frac{\partial u}{\partial y} = 0 \quad \text{on } y = 0,\ x < 0, \quad (6.50b)$$

$$u \to 0 \quad \text{as } |\boldsymbol{x}| \to \infty, \qquad u = 1 + O\left(|\boldsymbol{x}|^{1/2}\right) \quad \text{as } |\boldsymbol{x}| \to 0, \quad (6.50c)$$

where $\boldsymbol{x} = (x, y)$. Note that this is a *mixed boundary value problem* because the boundary conditions switch from Neumann (specified $\partial u/\partial y$) to Dirichlet (specified u) across $x = 0$. We know from Chapter 4 to expect square root type behaviour at the origin where the boundary condition switches.

Take the Fourier transform of the partial differential equation (6.50a) to give

$$\frac{\partial^2 \bar{u}}{\partial y^2} - (k^2 - \mathrm{i}k)\bar{u} = 0 \quad \text{in } y > 0. \quad (6.51)$$

Since we require $\bar{u}(k, y) \to 0$ as $y \to \infty$, the relevant solution is

$$\bar{u}(k, y) = A(k)\mathrm{e}^{-(k^2 - \mathrm{i}k)^{1/2} y}, \quad (6.52)$$

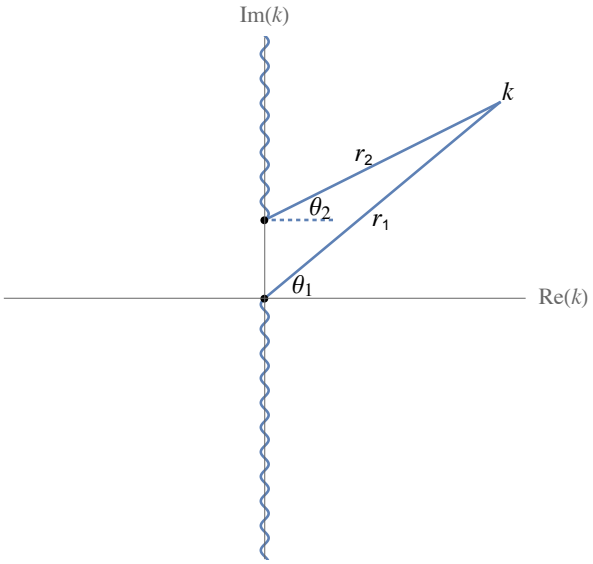

$$r_1 = |k| \in [0, \infty),$$

$$r_2 = |k - \mathrm{i}| \in [0, \infty),$$

$$\theta_1 = \arg k \in [-\pi/2, 3\pi/2),$$

$$\theta_2 = \arg(k - \mathrm{i}) \in [-3\pi/2, \pi/2).$$

Figure 6.4: The lengths r_1, r_2 and angles θ_1, θ_2 used to define the multifunction $\left(k^2 - \mathrm{i}k\right)^{1/2}$.

where $A(k)$ is an arbitrary integration function, and the branch of the square root is defined such that $\mathrm{Re}\left(k^2 - \mathrm{i}k\right)^{1/2} > 0$ on the inversion contour. Thus we place the branch cut along the imaginary k-axis from $-\infty\mathrm{i}$ to 0 and from i to $\infty\mathrm{i}$, as illustrated in Figure 6.4, and define

$$(k^2 - \mathrm{i}k)^{1/2} = \sqrt{r_1 r_2}\, \mathrm{e}^{\mathrm{i}(\theta_1 + \theta_2)/2}, \tag{6.53}$$

where the lengths $r_{1,2}$ and angles $\theta_{1,2}$ are as shown in Figure 6.4, so that $\mathrm{Re}(k^2 - \mathrm{i}k)^{1/2} > 0$ everywhere on the cut k-plane.

Now to take care of the mixed boundary conditions on $y = 0$, let

$$g_+(x) = \begin{cases} 0 & x < 0, \\ \dfrac{\partial u}{\partial y}(x, 0) & x > 0, \end{cases} \qquad f_-(x) = \begin{cases} u(x, 0) & x < 0, \\ 0 & x > 0, \end{cases} \tag{6.54}$$

so that (6.50b) may be restated as the full-range boundary conditions

$$u(x, 0) = f_-(x) + \mathrm{H}(x), \qquad \frac{\partial u}{\partial y}(x, 0) = g_+(x), \tag{6.55}$$

where $\mathrm{H}(x)$ is the Heaviside function.

We suppose that $g_+(x) = O\left(\mathrm{e}^{\alpha x}\right)$ as $x \to \infty$ and that $f_-(x) = O\left(\mathrm{e}^{\beta x}\right)$ as $x \to -\infty$ for some constants α, β such that $\alpha < \beta$. Then $\bar{g}_+(k)$ is holomorphic in $\mathrm{Im}\, k > \alpha$ and $\bar{f}_-(k)$ is holomorphic in $\mathrm{Im}\, k < \beta$, so that both functions are holomorphic in the overlap strip $\alpha < \mathrm{Im}\, k < \beta$. We also recall that $\bar{\mathrm{H}}(k) = \mathrm{i}/k$ for $\mathrm{Im}\, k > 0$, so that, provided $\beta > 0$, we can take the Fourier transform of the boundary conditions (6.55) to get

$$\bar{u}(k, 0) = \bar{f}_-(k) + \frac{\mathrm{i}}{k} \quad \text{for } 0 < \mathrm{Im}\, k < \beta, \qquad \frac{\partial \bar{u}}{\partial y}(k, 0) = \bar{g}_+(k) \quad \text{for } \mathrm{Im}\, k > \alpha. \tag{6.56}$$

Now we just substitute in the solution (6.52) for $\bar{u}$:

$$A(k) = \bar{f}_-(k) + \frac{\mathrm{i}}{k}, \qquad -A(k)(k^2 - \mathrm{i}k)^{1/2} = \bar{g}_+(k). \tag{6.57}$$

Elimination of $A(k)$ gives

$$\frac{1}{(k^2 - \mathrm{i}k)^{1/2}}\,\bar{g}_+(k) + \bar{f}_-(k) = -\frac{\mathrm{i}}{k}, \tag{6.58}$$

where $\bar{f}_-(k)$ is holomorphic in $\operatorname{Im} k < \beta$ and $\bar{g}_+(k)$ is holomorphic in $\operatorname{Im} k > \alpha$. Provided $0 \le \alpha < \beta \le 1$, we can apply the Wiener–Hopf method, as follows.

First we split $\left(k^2 - \mathrm{i}k\right)^{1/2}$ to separate the singularities at $k = 0$ and $k = 1$ by setting

$$\left(k^2 - \mathrm{i}k\right)^{1/2} = k^{1/2}\,(k - \mathrm{i})^{1/2}\,, \qquad k^{1/2} = \sqrt{r_1}\,\mathrm{e}^{\mathrm{i}\theta_1/2} \qquad (k - \mathrm{i})^{1/2} = \sqrt{r_2}\,\mathrm{e}^{\mathrm{i}\theta_2/2}, \tag{6.59}$$

where $r_{1,2}$ and $\theta_{1,2}$ are again as in Figure 6.4. Then (6.58) may be rearranged to

$$\frac{\bar{g}_+(k)}{k^{1/2}} + (k - \mathrm{i})^{1/2}\bar{f}_-(k) = -\mathrm{i}\frac{(k - \mathrm{i})^{1/2}}{k}, \tag{6.60}$$

where the first and second terms are holomorphic in $\operatorname{Im} k > \alpha$ and in $\operatorname{Im} k < \beta$ respectively.

The right-hand side of equation (6.60) has a pole at $k = 0$ and a branch point at $k = \mathrm{i}$. To split these, the trick is to separate out the principal part of the pole as follows:

$$\frac{(k - \mathrm{i})^{1/2}}{k} = \frac{(-\mathrm{i})^{1/2}}{k} + \frac{(k - \mathrm{i})^{1/2} - (-\mathrm{i})^{1/2}}{k}. \tag{6.61}$$

The second term on the right-hand side of (6.61) now has a removable singularity at $k = 0$ and therefore defines a holomorphic function in $\operatorname{Im} k < 1$. Here $(-\mathrm{i})^{1/2}$ is equal to $(k - \mathrm{i})^{1/2}$ evaluated at $k = 0$, namely $\mathrm{e}^{-\mathrm{i}\pi/4}$.

Hence, equation (6.60) may be rearranged to

$$\frac{\bar{g}_+(k)}{k^{1/2}} + \frac{\mathrm{e}^{\mathrm{i}\pi/4}}{k} = -(k - \mathrm{i})^{1/2}\bar{f}_-(k) - \frac{\mathrm{i}(k - \mathrm{i})^{1/2} - \mathrm{e}^{\mathrm{i}\pi/4}}{k} \quad \text{for } \alpha < \operatorname{Im} k < \beta, \tag{6.62}$$

with the left-hand side holomorphic in $\operatorname{Im} k > \alpha$ and the right-hand side holomorphic in $\operatorname{Im} k < \beta$. The right-hand side of (6.62) is the analytic continuation of the left-hand side of (6.62) into the lower half-plane, so together they define an entire function, $E(k)$ say.

To determine $E(k)$, we must consider the behaviours of the left- and right-hand sides of equation (6.62) as $k \to \infty$. Since $u(x, 0)$ is required to be bounded as $x \to 0$, it follows (as in the previous example) that $\bar{f}_-(k) = O\left(k^{-1}\right)$ as $k \to \infty$ with $\operatorname{Im} k < \beta$. However, since $u(x, y)$ has a square root behaviour as $(x, y) \to (0, 0)$, we expect $\partial u/\partial y$ to have an inverse square root singularity, that is

$$g_+(x) = O\left(x^{-1/2}\right) \quad \text{as } x \searrow 0. \tag{6.63}$$

It may be shown (for example using Laplace's method) that the corresponding asymptotic behaviour of the Fourier transform is

$$\bar{g}_+(k) = O\left(k^{-1/2}\right) \quad \text{as } k \to \infty \text{ with } \operatorname{Im} k > \alpha. \tag{6.64}$$

Hence, equation (6.62) implies that $E(k) \to 0$ as $k \to \infty$, and we deduce from Liouville's theorem that $E(k) \equiv 0$.

We then solve for $g_+(k)$ and $f_-(k)$:

$$g_+(k) = -\frac{\mathrm{e}^{\mathrm{i}\pi/4}}{k^{1/2}}, \qquad \bar{f}_-(k) = -\frac{\mathrm{i}}{k} + \frac{\mathrm{e}^{\mathrm{i}\pi/4}}{k(k-\mathrm{i})^{1/2}}, \tag{6.65}$$

and can now verify our assumptions *a posteriori*. Clearly $g_+(k)$ is holomorphic in $\operatorname{Im} k > 0$ and is order $k^{-1/2}$ as $k \to \infty$. Since the singularity at $k = 0$ is removable, $f_-(k)$ is holomorphic in $\operatorname{Im} k < 1$ and is order k^{-1} as $k \to \infty$. Thus the required overlap region does exist; the minimum admissible value of α is 0 and the maximum admissible value of β is 1.

To complete the solution, we substitute back into (6.57) to get

$$A(k) = \bar{f}_-(k) + \frac{\mathrm{i}}{k} = \frac{\mathrm{e}^{\mathrm{i}\pi/4}}{k(k-\mathrm{i})^{1/2}}, \tag{6.66}$$

and therefore

$$\bar{u}(k,y) = \frac{\mathrm{e}^{\mathrm{i}\pi/4}}{k(k-\mathrm{i})^{1/2}}\, \mathrm{e}^{\left(k^2-\mathrm{i}k\right)^{1/2} y}. \tag{6.67}$$

Hence the inversion formula gives

$$u(x,y) = \frac{\mathrm{e}^{\mathrm{i}\pi/4}}{2\pi} \int_\Gamma \frac{\mathrm{e}^{-\left(k^2-\mathrm{i}k\right)^{1/2} y - \mathrm{i}kx}}{k(k-\mathrm{i})^{1/2}}\, \mathrm{d}k, \tag{6.68}$$

where the contour Γ must pass between the singularities at $k = 0$ and at $k = \mathrm{i}$.

Remarkably, the integral (6.68) may be evaluated to obtain

$$u(x,y) = \operatorname{erfc}\left(\sqrt{\frac{\sqrt{x^2+y^2}-x}{2}}\right), \qquad \text{where } \operatorname{erfc}(t) = 1 - \frac{2}{\sqrt{\pi}} \int_0^t \mathrm{e}^{-\xi^2}\, \mathrm{d}\xi \tag{6.69}$$

is the complementary error function, One can readily verify that $u(x,y)$ satisfies the problem (6.50) and has the expected square root behaviour as $(x,y) \to (0,0)$.

The solution (6.69) may be expressed in the form

$$u(x,y) = \operatorname{erfc}\left(\operatorname{Im} z^{1/2}\right), \quad \text{where } z = x + \mathrm{i}y, \tag{6.70}$$

and in fact this solution may be obtained much more directly by first conformally mapping the problem using the map $z \mapsto \zeta = z^{1/2}$.